ELECTRICAL CHARACTERIZATION OF PHOTOVOLTAIC CELLS TO PREDICT CELL PERFORMANCE

By:
Alexander Eick

GRADUATION REPORT

Submitted to
Hanze University of Applied Sciences Groningen

in partial fulfilment of the requirements
for the degree of

Fulltime Honours Bachelor Advanced Sensor Applications

2015

ABSTRACT

ELECTRICAL CHARACTERIZATION OF PHOTOVOLTAIC CELLS TO PREDICT CELL PERFORMANCE

by
Alexander Eick

The predicted depletion of fossil fuel reservoirs, together with rising energy demands and an increasing environmental awareness make the production of energy from environmentally friendly and renewable sources necessary. One of those sources is solar power, from which energy can be harvested with photovoltaic panels.

The research presented here is aimed at modelling the output of photovoltaic modules using exclusively electrical parameters at standard test conditions (STC), usually provided by the manufacturer. This will enable power producers to predict their output accurately and effectively. Furthermore, it can help the industry to identify defects and shortcomings in newly developed solar cells and modules faster, thus reducing the development risks.

Presented results verify the proper operation of the proposed model. The validation process shows good results with Nash-Sutcliffe model efficiency coefficients above 0.95, for high and medium irradiance levels. At low irradiance levels the proposed model results in higher errors. However, further tests, with various other photovoltaic modules are needed to validate the proposed model completely.

DECLARATION

I hereby certify that this report constitutes my own product, that where the language of others is set forth, quotation marks so indicate, and that appropriate credit is given where I have used the language, ideas, expressions or writings of another.

I declare that the report describes original work that has not previously been presented for the award of any other degree of any institution.

Signed, 18/01/2015

……..

Alexander Eick

ACKNOWLEDGEMENTS

I would like to express my great appreciation to Prof. Dr. Davies William de Lima Monteiro for giving me the opportunity to conduct research in the field of renewable energy, specifically photovoltaics. He has provided me with excellent guidance and invaluable feedback. Furthermore, I am in debt to all the members of the Optronics and Microtechnology Laboratory, especially Poliana Henriques Bueno, André Luiz Costa de Carvalho and Diogo Ferraz Costa, of the photovoltaics group, for their continuous help and patience. They always had an open ear for my questions and assisted me with their vast knowledge.

My thanks are as well extended to Dr. Ronald A.J. van Elburg for his feedback on the deliverables and his guidance throughout the whole project.

I would like to show my appreciation to the staff of the Institute of Engineering, location Assen, for their support during my study and for preparing me for my graduation.

I wish to thank the Federal University of Minas Gerais (UFMG) and the Hanze University of Applied Sciences for offering me the possibility of graduating abroad.

Credit should also be given to my friends, who reviewed my thesis and provided me with feedback.

Finally, I am deeply thankful for the unconditional love and support of my family and my girlfriend, who encouraged me to pursue my dreams and who made me who I am.

Thank you all for your support and tolerance.

Alexander Eick

Table of Contents

LIST OF FIGURES

LIST OF TABLES

ABBREVIATIONS

AM1.5G Air Mass of 1.5

Air mass number that represents the solar spectrum at mid-latitudes, where the sun is at an angle to the earth´s surface, thus increasing the effective thickness of the atmosphere.

BRIC Acronym for Brazil, Russia, India, China

Group of countries which are at similar stages of their economic development. The acronym acknowledges the apparent shift in economic power away from the developed countries towards the developing nations.

CANCER Computer Analysis of Nonlinear Circuits, Excluding Radiation

General circuit analysis program that is especially suited to integrated-circuit simulation.

CCS Carbon capture and storage

A method of capturing carbon dioxide and depositing it at sites where it cannot enter the atmosphere.

CEMIG Companhia Energética de Minas Gerais

The state electrical energy-distribution company of Minas Gerais

CIGS Copper indium gallium selenide solar cells

A widely spread thin film solar cell made from the mentioned materials.

GCF Green Climate Fund

A foundation to provide easy access to funding for projects that will contribute to the achievement of the ultimate objective of the United Nations Framework Convention on Climate Change, i.e. stabilize greenhouse gas concentration in the atmosphere

LHS Left-hand side

The left-hand side of an equation with respect to the equal sign

NOCT Nominal Operating Cell Temperature

Cell temperature within the SRE

OECD Organization for Economic Co-operation and Development

Organization to provide a forum for governments and to promote policies to improve the economic and social well-being of the world population

OptMA Lab Optronics and Microtechnology Laboratory

A research laboratory at the electrical engineering department of UFMG under the supervision of Prof. Dr. Davies William de Lima Monteiro

PSPICE Personal Simulation Program with Integrated Circuit Emphasis

One of the first release of SPICE for personal computer

RHS Right-hand side

The right-hand side of an equation with respect to the equal sign

SPICE Simulation Program with Integrated Circuit Emphasis

A general purpose electronic simulation program with capabilities of nonlinear dc analysis, nonlinear transient analysis and small signal analysis

SRE Standard Reference Environment

Conditions under which the NOCT is determined:

- *Irradiance of 800 W/m^2*
- *Ambient temperature of 20°C*
- *Wind speed of 1 m/s*
- *Open-rack mounted cell (back side of the cell is open)*
- *Nil electrical load (open-circuit)*

STC Standard Test Conditions

Conditions under which electrical photovoltaic cell parameters are determined:

- *irradiance value of 1000 W/m^2*
- *Ambient temperature of 25°C*
- *Light spectrum of AM1.5G*

UFMG Universidade Federal de Minas Gerais

The Federal university of Minas Gerais in Belo Horizonte

UNITS

Unit	Description
°C	Degree Celsius
	Unit of temperature
A	Ampere
	Unit of current
A/°C	Ampere per degree Celsius
	Unit of a temperature coefficient
C	Coulomb
	Unit of electrical charge
EJ	Exajoule (10^{18}Joule)
	Unit of energy ($1J = 2.78*10^{-7}kWh$)
J/K	Joule per Kelvin
	Unit of heat capacity
K	Kelvin
	Unit of temperature
km^2	Square kilometre
	Unit of area
kWh	Kilowatt-hour
	Unit of energy ($1kWh = 3.6*10^6J$)
m/s	Meter per second
	Unit of speed
m^2	Square meter
	Unit of area
nm	Nanometer
	Unit of length, specifically wavelength

Unit	Description
TWh	Terawatt-hour
	Unit of energy
V	Volt
	Unit of voltage
V/°C	Volt per degree Celsius
	Unit of a temperature coefficient
W/m^2	Watt per square meter
	Unit of irradiance
W/m^{2}nm^1	Watt per square meter time nanometer
	Unit of irradiance per wavelength
Ω	Ohm
	Unit of resistance

PARAMETERS

Parameter	Unit	Description
AM	---	Air mass
E_c	---	Nash-Sutcliffe model efficiency coefficient of Castaner´s model towards the fitted model
E_p	---	Nash-Sutcliffe model efficiency coefficient of the proposed model towards the fitted model
FF	---	Fill factor
FF_0	---	ideal fill factor in absence of series resistance and with infinite shunt resistance
G	*W/m2*	Irradiance
I	*A*	Output current of a solar module
I_0	*A*	Diode saturation current
I_{01}	*A*	Diffusion-diode saturation current
I_{02}	*A*	Recombination-diode saturation current
I_C	*A*	Output current of a solar cell
I_{DR}	*A*	Combined diffusion and recombination current
I_m	*A*	Current at the maximum power point
I_{mr}	*A*	Current at the maximum power point at STC
I_{ph}	*A*	Photo-generated current of a solar module
I_{phC}	*A*	Photo-generated current of a solar cell
I_{sc}	*A*	Short-circuit current
I_{scr}	*A*	Short-circuit current at STC
k_B	*J/K*	Boltzmann constant ($1.38065*10^{-23}$)
$MADP_c$	*%*	Mean Absolute Deviation Percent of Castaner´s model towards the fitted model
$MADP_p$	*%*	Mean Absolute Deviation Percent of the proposed model towards the fitted model

Parameter	Unit	Description
n_1	---	Ideality factor of the diffusion-diode
n_2	---	Ideality factor of the recombination-diode
N_p	---	Number of solar cells in parallel connection
N_s	---	Number of solar cells in series connection
P_m	*W*	Power at the maximum power point
q	*C*	Electric charge ($1.60218*10^{-19}$)
R_s	*Ω*	Series resistance of a solar module
R_{sC}	*Ω*	Series resistance of a solar cell
R_{sh}	*Ω*	Shunt or parallel resistance of a solar module
R_{shC}	*Ω*	Shunt or parallel resistance of a solar cell
$RMSE_c$	*A*	Root mean square error of Castaner´s model towards the fitted model
$RMSE_{fit}$	*A*	Root mean square error of the fitted model towards the measured data
$RMSE_p$	*A*	Root mean square error of the proposed model towards the fitted model
T_a	*°C*	Ambient temperature
T_{mod}	*°C*	Temperature of the photovoltaic module/cell
V	*V*	Output voltage of a solar module
V_C	*V*	Output voltage of a solar cell
V_m	*V*	Voltage at the maximum power point
V_{mr}	*V*	Voltage at the maximum power point at STC
V_{oc}	*V*	Open-circuit voltage
V_{ocr}	*V*	Open-circuit voltage at STC
V_T	*V*	Thermal voltage
α_I	*A/°C*	Temperature coefficient of the short-circuit current

Parameter	Unit	Description
α_V	*V/°C*	Temperature coefficient of the open-circuit voltage
φ	°	Zenith angle (phi)

CHAPTER 1

RATIONALE

The state electrical energy-distribution company of Minas Gerais, CEMIG, is currently pursuing the goal of installing and operating multiple photovoltaic power plants in Minas Gerais, Brazil´s fourth largest state in regard to area and second largest in regard to population. To achieve that goal CEMIG is in the process of setting up a pilot plant in Sete Lagoas, a city close to the state capital of Belo Horizonte. The aim of the pilot plant is to collect data on the plant's output and efficiency for later power plants. Furthermore, the plant has a small research area where, in cooperation with the Optronics and Microelectronics Laboratory (OptMA Lab) of the department of electrical engineering at the Federal University of Minas Gerais, the best plant setup and the most effective solar cell type for the present conditions can be determined.

In the current time where a growing population means a growing need in energy, it is important that new resources are used to satisfy this need. In addition, increased awareness of pollution, especially the harm done by greenhouse gases (1, 2), stimulate the use of renewable and carbon-neutral energy resources. Brazil is already a forerunner in the use of renewable energy sources, especially hydroelectric power. However, this unilateral power production makes Brazil prone to natural disasters, like droughts (3, 4). Thus, Brazil is looking to diversify its power generation to reduce its dependence on the availability of hydropower.

Under the supervision of Professor Dr. Davies William de Lima Monteiro research into the modelling of solar cells and panels is performed. The project described in this report is based on a descriptive problem. It focuses on the accurate simulation of the solar cell output under non-ideal conditions. Especially the temperature dependence of solar cells (5-8) is to be taken into account. Many models are already available to simulate the output of a solar cell based on its physical parameters. However, more often than not those parameters are not available, since manufacturers rather keep their manufacturing process for themselves to strengthen their market position. Hence, it is necessary to develop an accurate model to predict the output of photovoltaic cells based on electrical characteristics measured under certain standard conditions. Physical parameters include the ideality factor, the dark saturation current and the material resistivity. To determine those parameters extensive experiments and calculations are needed, as well as high-priced equipment. On the other hand, electrical parameters, which include the open-circuit voltage, the short-circuit current and the voltage and current at the maximum power point under certain standard conditions, can be determined with affordable equipment, like a curve tracer.

A model, which can simulate solar cells based on their electrical characteristics, could as well be favourable for manufacturers of photovoltaic cells. When new cells are developed or the production recipes of available solar cells are improved, the manufacturer can simulate the behaviour of the new cell rapidly, after a prototype batch is produced, with easily measurable parameters. That could decrease the risk of developing faulty cells by recognizing production

errors earlier in the production process. From the modelled I-V curve, the manufacturers can predict the cell´s behaviour under various environmental conditions and identify shortcomings and their possible causes early in the production process.

It is desired to simulate the output of a photovoltaic cell accurately to determine the best suitable cell for power plants in Minas Gerais. The model should only use easily quantifiable electrical characteristics as inputs, to be able to simulate even little known and little-documented solar cells and modules. It should predict the solar cell output with an acceptable accuracy and under varying temperatures and irradiance values.

CHAPTER 2

SITUATIONAL & THEORETICAL ANALYSIS

This chapter will first analyse the current situation with a short outlook on the future of energy generation. Then the theory behind photovoltaic cells and how they can be modelled is shown. Furthermore are the stakeholders involved in this project described.

2.1 Energy future

The world population grows every year by about 1% (9), which, although declining, will increase the number of humans living on earth to 9.3 billion in the year 2050. Naturally, an increase in the population means an increase in energy needs as well. In 2013 the World Energy Council presented a study in which two different scenarios were characterized and analysed to describe the world and especially its energy needs in 2050 (10). The first scenario, called Jazz, assumes a consumer-focused world where the achievement of energy access, quality of supply and affordability while using the best available sources is a primary goal. Hence, multi-national companies and price-conscious consumers are the driving forces and the main part of the energy will be produced using fossil fuels (i.e. coal, oil and gas). The second scenario is called Symphony. In it, a voter consensus on environmental sustainability and energy security is assumed. Governments and their policies will be the driving forces in this scenario, where the use of fossil fuel for the energy generation will decline and renewable and environmentally friendly technologies will fill the gap.

Energy is classified as primary, secondary and final energy. Primary energy is the energy extracted from its sources while the physical or chemical characteristics are not changed (e.g. crude oil, coal, biomass, solar radiation) (11). On the contrary, there is secondary energy, which is the energy after transformation into electricity, fuel, heat or others. Secondary energy is always less than primary energy due to conversion losses (11). The energy consumed by the consumer is called final energy, which is even less than secondary energy due to transportation losses and others. Figure 2-1 describes the earlier mentioned relationship between the population and the primary energy need. The data shown until 2010 is real historic data obtained from (9) and (12) for the population and primary energy, respectively. The data after 2010 are predictions made by (10) in the symphony scenario. The data from this scenario was chosen since the world leaders are already trying to pave the way for a global consensus to support and promote renewable energy sources as well as to stabilize the greenhouse gas concentration in the earth´s atmosphere. One of the first steps in this direction was made with the Kyoto Protocol (13), an international agreement to reduce greenhouse gas emission. It entered into force in 2005, however, only 38 of the participating parties (to date 192 of which only 83 initially signed the protocol) committed to specific reduction targets between 2008 and 2012. In 2009 114 countries agreed on the Copenhagen accord, in it no specific greenhouse gas reduction targets are set, but the signatories recognize the critical impact of climate change and agreed, among others, on the following:

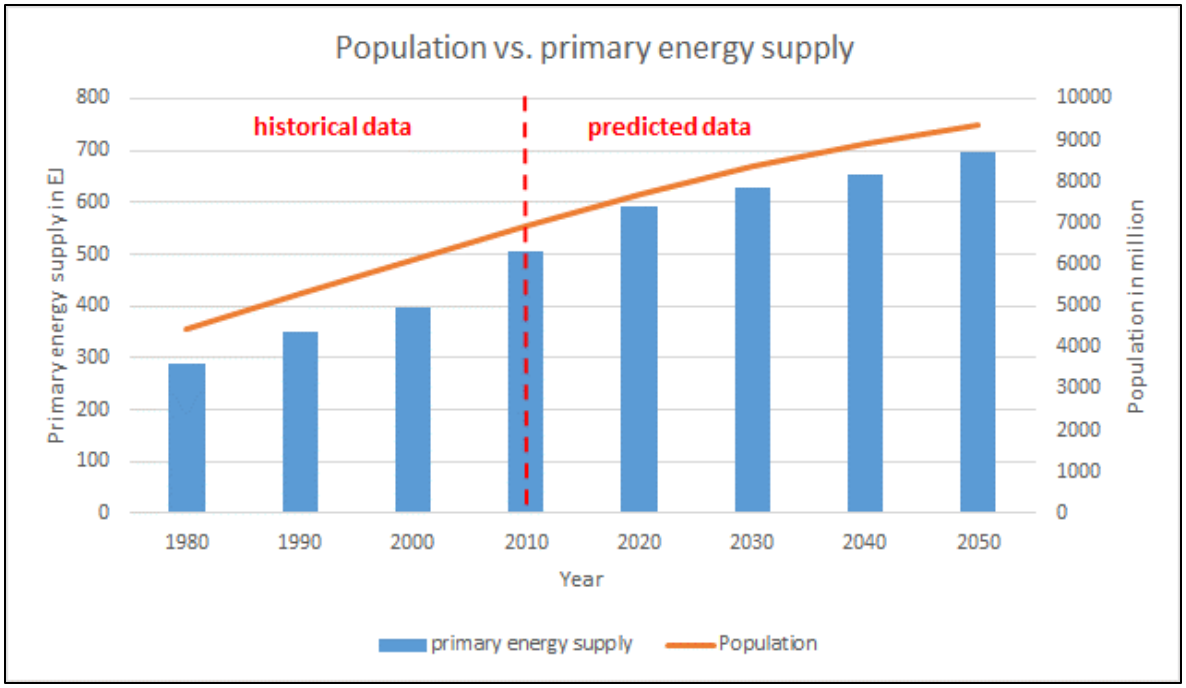

Figure 2-1 Primary energy supply in relation to the world population
It is apparent, that the primary energy needs rise with a growing population. The historic population data is extracted from (9), the historic data for the primary energy supply is from (12) and the predicted data is from the Symphony scenario of (10)

> *"2. We agree that deep cuts in global emissions are required according to science, and as documented by the IPCC Fourth Assessment Report with a view to reduce global emissions so as to hold the increase in global temperature below 2 degrees Celsius, and take action to meet this objective consistent with science and on the basis of equity. We should cooperate in achieving the peaking of global and national emissions as soon as possible, recognizing that the time frame for peaking will be longer in developing countries and bearing in mind that social and economic development and poverty eradication are the first and overriding priorities of developing countries and that a low-emission development strategy is indispensable to sustainable development."(2)*

In 2012 the Doha Amendment to the Kyoto Protocol (14) was adopted in which greenhouse gas reduction targets are set for the period between 2013 and 2020. However, until now only 22 parties accepted the amendment. At the latest climate conference in Lima (15) in December 2014 the initial funding of the Green Climate Fund (GCF) was achieved. The GCF´s target is to significantly contribute to the reduction in global emissions (16), i.e. the emission of greenhouse gases, e.g. carbon dioxide, methane, nitrous oxide and fluorinated gases. The largest part with 26% resulted from energy supply excluding transportation (17), hence mostly electricity generation. Therefore, it is not surprising that one of the three pillars to achieve deep reductions in the carbon dioxide emissions, the most common greenhouse gas (17), is the production of low-carbon electricity by replacing fossil fuel based generation with renewable

energy sources, nuclear power or fossil fuel based generation with carbon capture and storage (CCS) capabilities (1). This can as well be seen in Figure 2-2 where the predicted electricity mix in 2050 is shown according to the Symphony scenario. The generation of electricity from oil and coal will decline and renewable energy sources, i.e. solar, hydro and wind energy, will take their places together with coal, gas and biomass based generation with CCS. Of all the renewable energy sources, solar energy is predicted to grow the most, from 34TWh in 2010 to 7741TWh in 2050. That is attributed to the environmental concerns with other renewable energy sources. Hydropower requires usually a large intervention in the rivers ecosystem as well as a storage basin. The noise pollution associated with the generation of energy from wind is high as well as the visual pollution. Both of which are important aspects to consider, due to their sensitivity in the acceptance of local communities. Lastly, geothermal power production possesses the risk of toxic gas release and uses about a third of their produced energy for operations within the plant (18). Additional high initial investments make it an unattractive choice for energy suppliers (19).

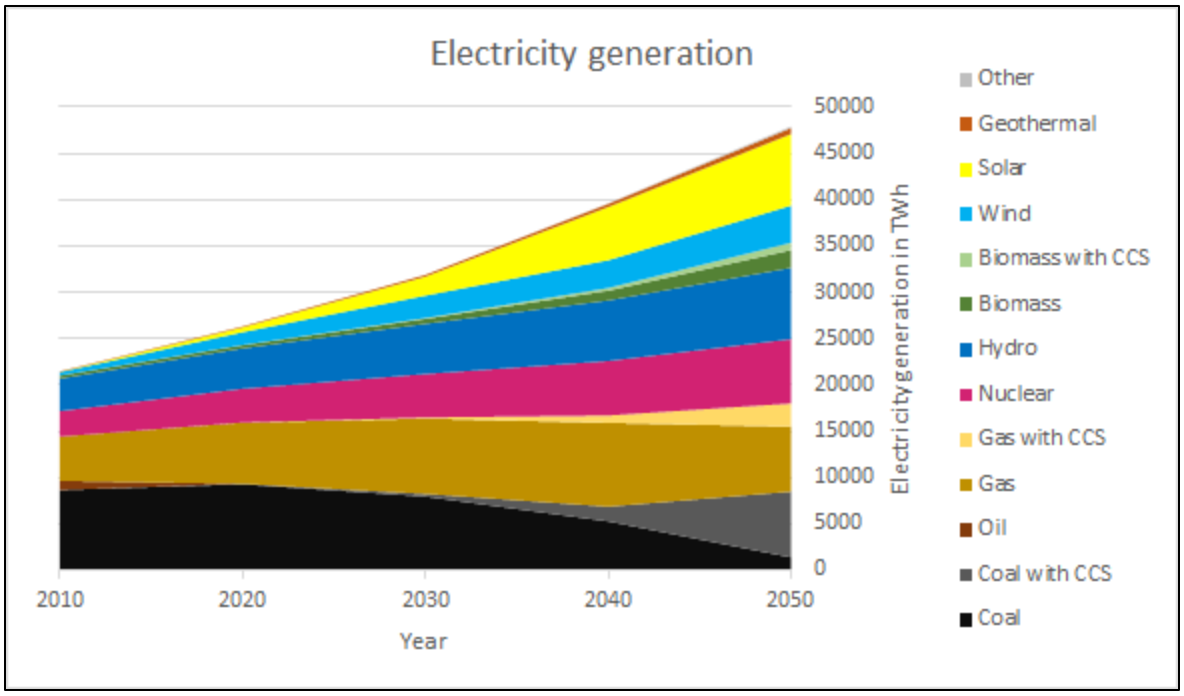

Figure 2-2 Predicted electricity generation between 2010 and 2050 by source
The use of fossil fuels without CCS will decrease in the future and renewable and low-carbon energy sources will take their places in the energy mix in 2050. The data is obtained from the Symphony scenario of (10)

2.1.1 Energy production in Brazil

The energy sector of Brazil is one of the least carbon intensive in the world (1, 20). With only 2.4 metric tons of carbon dioxide produced per person in 2011 (21) it is only second to India in a comparison of all OECD and BRIC countries. In 2013 more than 45% of its primary energy production came from renewable sources, e.g. hydro, wind or biomass, (Figure 2-3) and more than 70% of its electricity supply is from hydroelectric power plants (Figure 2-4). Therefore,

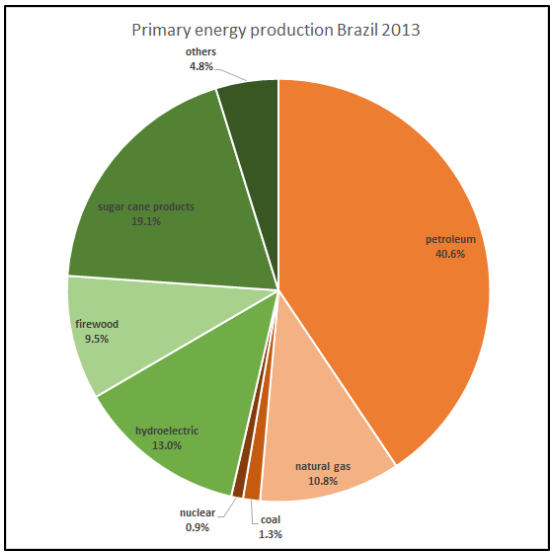

Figure 2-3 Primary energy production of Brazil in 2013
53.6% are produced using non-renewable sources, i.e. petroleum, natural gas, coal and nuclear power, and 46.4% are produced with renewable energy sources, i.e. sugar cane products, hydroelectric, firewood and other renewable sources. The data is adopted from (22).

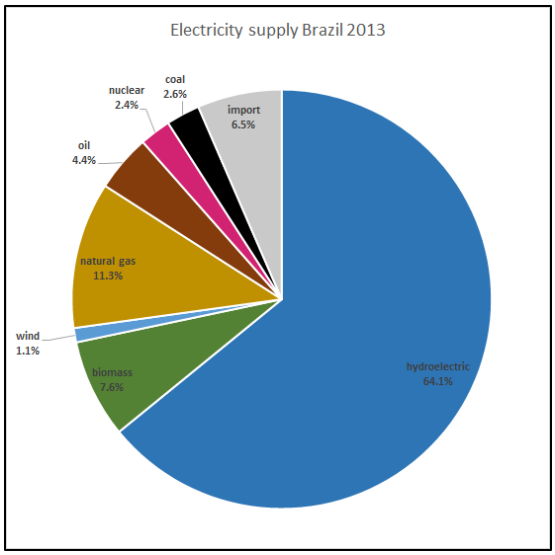

Figure 2-4 Electricity supply of Brazil in 2013
79.3% of the electricity is supplied by renewable sources, i.e. hydroelectric, biomass, wind and the imported electricity, which is mainly hydroelectric energy. Only a small amount of 20.7% is produced using non-renewable energy sources, i.e. natural gas, oil, coal and nuclear energy. The data is adopted from (23)

Brazil does not have to worry too much on cutting back on its greenhouse gas emissions. However, this rather unilateral electricity generation does have its pitfalls as well. Hydroelectric power is vulnerable to droughts, as it happened in 2001 (4) and again nearly in 2013 (3). Power shortages can severely damage the countries industry and scare away future investors. Hence, Brazil has to diversify its electricity generation capacities, to ensure coverage even in droughts, which might happen more often in the following years, due to the climate change (24). The generation of electricity from solar radiation will become a major player. Firstly, this is especially interesting for Brazil considering its high solar potential as seen in Figure 2-5. The highest level of irradiation is measured in a belt from the northeast to the southwest. Much lower levels occur in the Amazon region, in the north of Brazil, and in the coastal regions in

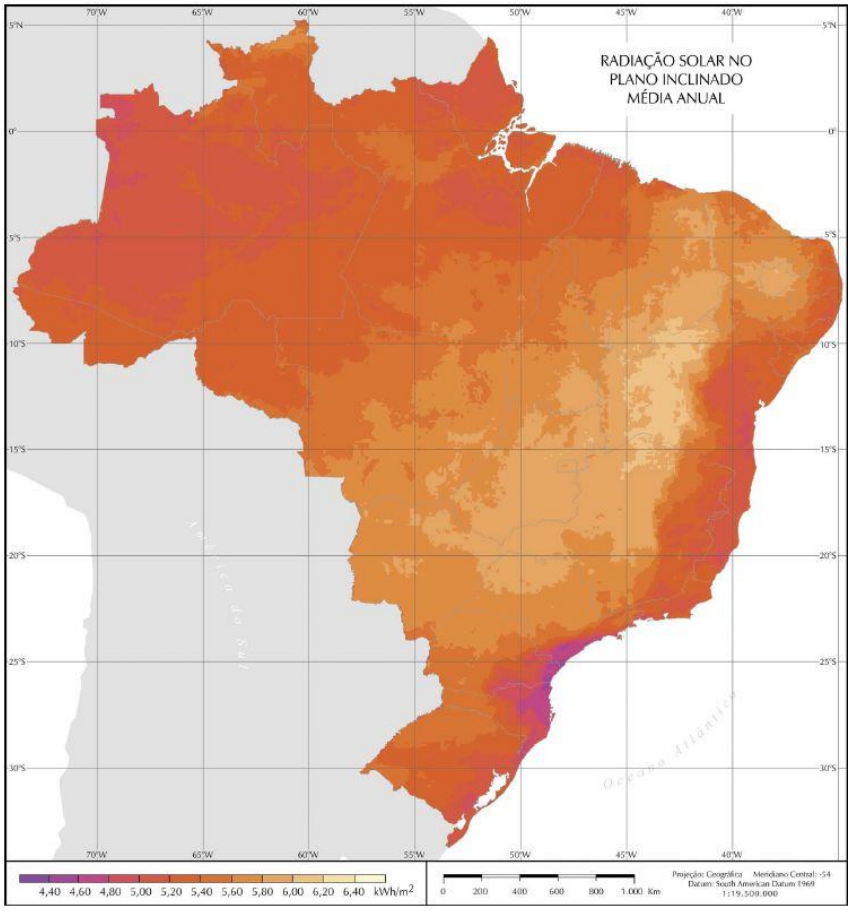

Figure 2-5 Annual average of daily inclined solar irradiation in Brazil (25) The irradiation is represented on a plane tilted in an angle equal to the latitude of the point on the map. Yellow and light red colours showing high irradiation, whereas dark red and purple show low irradiation.

the south of Brazil. The low levels in the Amazon region are due to its annual rain season, where clouds reflect much of the sunlight, hence diminishing the annual average solar irradiation levels. In 2011 Brazil could have covered all its electricity needs by covering a 2400km^2 area with an average annual solar irradiation of 1400kWh/m^2 with solar panels (26). Secondly, Brazil does not have a 100% electrification rate. Especially small villages in rural areas and the amazon region are not connected to the national power grid. With the use of solar energy systems, in combination with energy storage modules, the electrification of the whole country can be achieved.

2.2 Solar resources

The radiation received on the earth surface form the sun is dependent on many factors, e.g. location on earth, time, weather or season. The path length of the sunlight through earth´s atmosphere is referred to as air mass (AM), due to the fact that the light has to pass through this mass of air. Upon entering the Earth´s atmosphere sunlight is scattered, absorbed and reflected by the gasses and particles in it. These effects increase when clouds are present. When

the angle φ between the sun and the point directly overhead is known, the AM can be approximated by (27):

$$AM = \frac{1}{\cos\varphi} \qquad (2\text{-}1)$$

When φ=0° the air mass is AM1G and when φ=46.2° the air mass is AM1.5G, which is the standard spectrum of the sun used in photovoltaics. The spectrum of AM1.5G is shown in Figure 2-6. The spectrum depicts the spectral irradiance for each wavelength. The integral of the spectral irradiance over all wavelengths is the irradiance with its unit W/m^2. The dips at around 750, 950, 1150 and 1400 nm are due to light absorption of atmospherical gases, i.e. oxygen, water vapour and carbon dioxide.

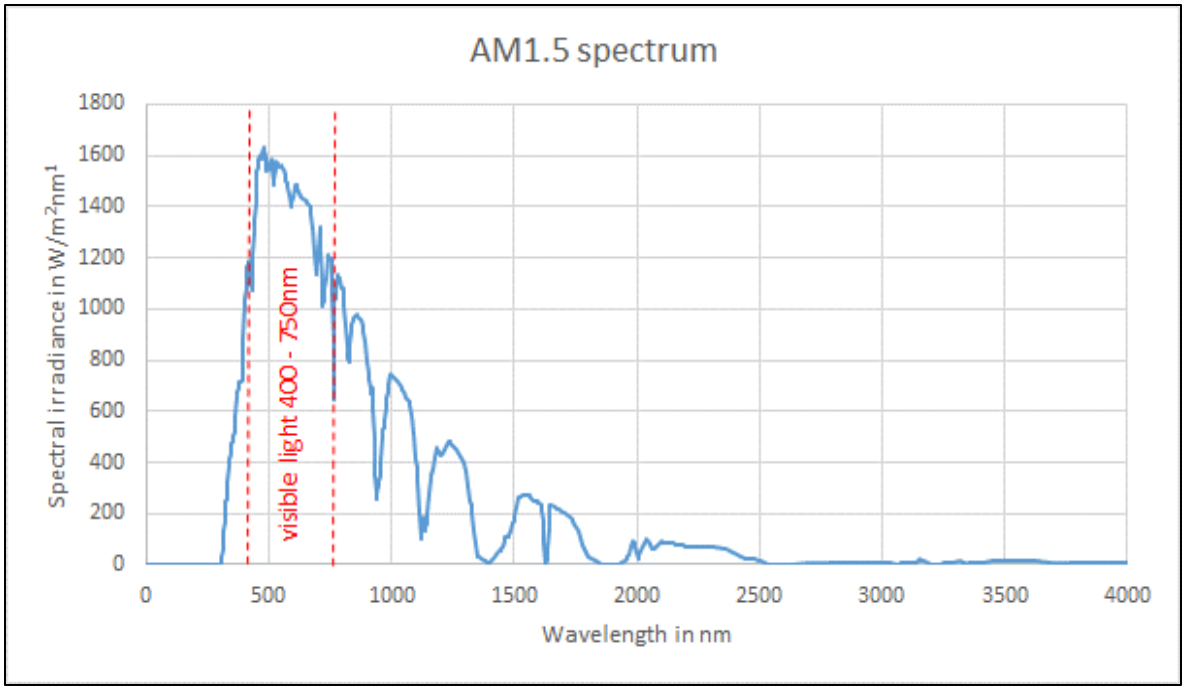

Figure 2-6 Spectrum of AM1.5G

2.3 Photovoltaics

Photovoltaic is the method to generate electricity from solar irradiation. Alexandre-Edmond Becquerel first observed the effect in 1839. He discovered that a photocurrent is produced, when silver chloride in an aqueous solution is connected with platinum electrodes. In 1906 photoconductivity was first observed in an organic compound, Anthracene (28). It was later used as photoreceptors in imaging systems. Scientific interest in the 1950s and 60s led to increased research into photoconductivity and related subjects, e.g. photovoltaics. This led to the development of the first inorganic solar cell at Bell Laboratories (29) in 1954. This marked the start for the commercial exploration of solar energy. Today many different solar cell structures exist. The most important ones are silicon, cadmium-telluride, CIGS and

multijunction solar cells. CIGS are made of copper, an alloy of indium and gallium and selenium, hence the name CIGS, from its chemical formula $CuInGaSe_2$. Multijunction solar cells are produced by stacking single junction cells, like the aforementioned ones on top of each other to achieve a better overall efficiency and a higher voltage output (30).

2.3.1 Operating principle

Many solar cells are made from silicon, a semiconductor material. The cell is a p-n junction in which current is generated through diffusion and drift of holes and electrons generated by absorbed photons. Silicon has 14 electrons of which four are situated on the outer shell of the Bohr-model (Figure 2-7). Those four valence electrons can be shared with other silicon atoms. Figure 2-8 shows schematically the structure of a simple silicon solar cell. It consists of 2 layers that exhibit different electrical properties, which are determined through doping with foreign atoms. The p-layer is much thicker than the n-layer and is produced through the replacement of some silicon atoms with a trivalent element, e.g. elements of the third group of the periodic table. Those elements only have three valence electrons on the outer shell, thus introducing a hole, which can be filled by neighbouring electrons leaving holes at their original positions. In the n-layer some silicon atoms are substituted with atoms of pentavalent elements at high

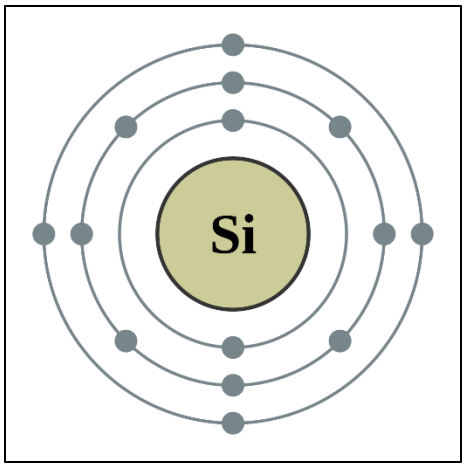

Figure 2-7 Bohr model of silicon (31) Silicon has 14 electrons, which are organized on three shells. 2 electrons on the first shell, eight on the second and four on the third and outermost shell.

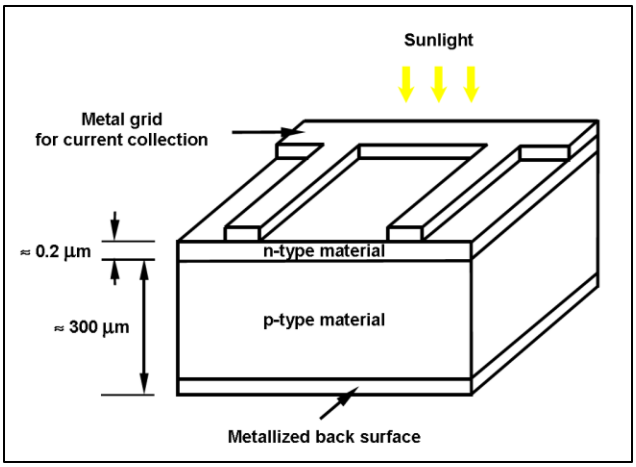

Figure 2-8 Schematic drawing of a silicon solar cell (32) Basic components are the p-layer, doped with trivalent elements, the n-layer, doped with pentavalent elements and a metal grid on the front and a complete metalized back for charge collection

temperatures. Such elements are phosphorus, arsenic and antimony. They have five valence electrons on the outer shell, hence introducing a surplus electron which can be ionized easily (33). The n-layer is called the donor layer and the p-layer the acceptor layer. The back of the cell, i.e. the acceptor layer side, is usually completely metalized for charge collection. On the contrary, on the front there is only a metal grid applied. The grid is sparse enough to allow light to pass through to the solar cell material and to collect charges.

The area where both layers intersect is called the p-n junction. Along it, free electrons from the donor layer will diffuse into the p-layer to combine with the holes. At the same time excess holes from the acceptor layer diffuse into the n-type material. This process leads to a negative charge build-up on the p-layer side of the junction and a positive charge build-up on the n-layer side of the junction. Therefore, an electric field is generated in the area around the p-n-junction, the so-called space-charge region or depletion region. This field prevents electrons and holes from farther away to diffuse in the opposing layer. Within the depletion region electrons and holes are still moving around, generating small currents which counteract each other. Thus an equilibrium is reached that results in a null net current. Figure 2-9 shows the effect of sunlight on the solar cell. When photons, with enough energy to split the bond between an electron and a silicon atom, hits the solar cell an electron-hole pair is generated. If that pair is generated in the p-layer of the cell the electron will meander around freely to recombine with a hole. However, due to the design of the cell it is likely that the free electron will encounter the junction before it can recombine with a hole. Within the field of the junction the electron is accelerated across the barrier into the donor layer. The minor amount of holes in the donor layer significantly reduces the chance of recombination with a hole. Furthermore is it not

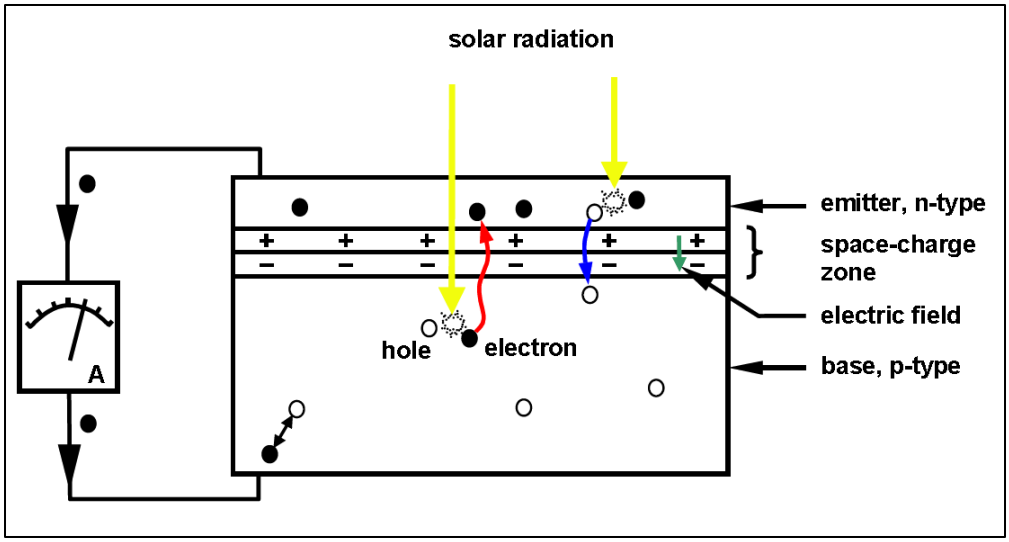

Figure 2-9 Schematic of the operating principle of a silicon solar cell (34)
Electrons formed in the p-layer and holes formed in the n-layer move across the p-n junction, which creates a light induced charge imbalance. The electrons then move through the external circuit form the n-layer to the p-layer generating a current.

possible for the electron to cross back into the p-layer, due to the electric field generated along the junction. If the electron-hole pair is created in the n-layer of the solar cell the free electron is rejected by the barrier, but the hole is filled by valence electrons from the p-layer, thus the hole moves over to the acceptor layer of the cell. When the n-layer and p-layer of the solar cell are now connected through an external circuit a current will flow. The electrons from the donor layer will move through the circuit into the acceptor layer, to reduce the light induced charge imbalance (35).

2.3.2 Photovoltaic characteristics

There are many parameters involved in the characterization of a solar cell however, the most important one are the short-circuit current (I_{sc}), open-circuit voltage (V_{oc}) and the maximum power point (P_m) which is described by its current (I_m) and voltage (V_m). All of those parameters are shown in Figure 2-10. I_{sc} is the maximum current the photovoltaic cell can produce, but the voltage is 0, hence the power is 0. V_{oc} is the maximum voltage the cell can produce, however the current is 0 at this point. P_m is the point where the cell delivers the maximum power. During operation, the system should operate at the voltage of the maximum power point, to ensure the highest possible efficiency for the solar cell.

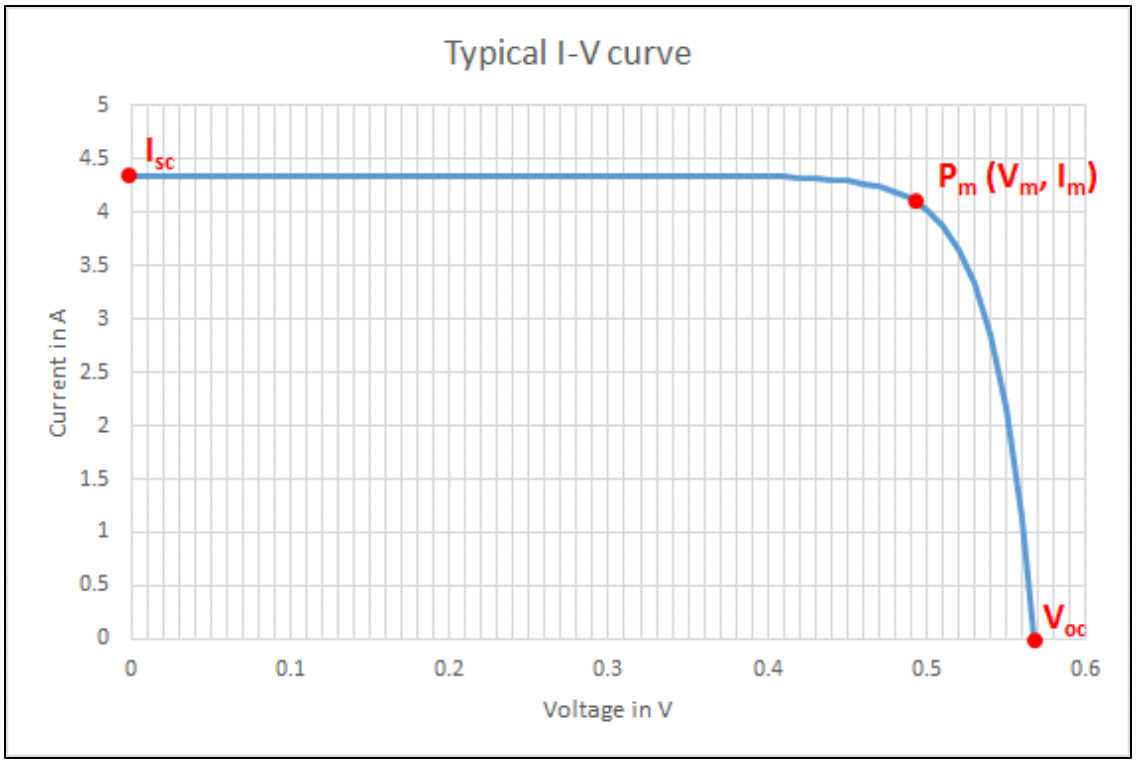

Figure 2-10 Typical I-V curve of a photovoltaic cell
With the most important parameters (I_{sc}, V_{oc}, P_m (V_m, I_m)) marked on the graph

These parameters are often given by the manufacturer under standard test conditions (STC). If that is not the case they can easily be determined using the proper equipment, e.g. a source meter. To quantify the quality of a photovoltaic cell another parameter is used, the fill factor (FF). It is defined as:

$$FF = \frac{P_m}{V_{oc} * I_{sc}} = \frac{V_m * I_m}{V_{oc} * I_{sc}} \qquad (2\text{-}2)$$

It basically describes how well the rectangle defined by V_m and I_m fills the rectangle defined by the open-circuit voltage and the short-circuit current. The closer the value is to unity, i.e. 1, the better is the performance of the photovoltaic cell.

2.3.2.1 Test conditions

To compare different photovoltaic cells, standard test conditions (STC) are specified. Parameters, like the open-circuit voltage and short-circuit current, measured under those conditions are often provided by the manufacturers or research institutions. The measurement conditions are (36):

- irradiance value of 1000 W/m^2
- Cell/Module temperature of 25°C
- Light spectrum of AM1.5G

Another set of specified test conditions is used to determine the nominal operating cell temperature (NOCT). NOCT is the operating temperature of the photovoltaic cell at specified conditions, i.e. the standard reference environment (SRE) (37):

- Irradiance of 800 W/m^2
- Ambient temperature of 20°C
- Wind speed of 1 m/s
- Open-rack mounted cell (back side of the cell is open)
- Nil electrical load (open-circuit)

With the NOCT the actual cell operating temperature for different ambient temperatures and irradiation values can be calculated with the following expression:

$$T_{mod} = T_a + \frac{NOCT - 20}{800} * G \qquad (2\text{-}3)$$

where T_{mod} and T_a are the cell operating temperature and ambient temperature respectively in °C, NOCT is the nominal operating temperature in °C and G is the solar irradiation in W/m^2. The 20 and 800 are the ambient temperature and Irradiance in SRE, respectively.

2.3.3 Factors influencing solar cell output

The ideal I-V curve of solar cells, as depicted in Figure 2-10, is only very rarely found under real operating conditions. Many factors influence the output of a photovoltaic cell. Those factors, among others, are the ambient temperature, the irradiance and the series resistance. The various effects can be seen in Figure 2-11.

2.3.3.1 Irradiance effects

Part (a) of Figure 2-11 shows the effect of changing irradiance on the I-V curve of a solar cell. As seen in chapter 2.3.2.1 above, the irradiance influences the operating temperature of the cell. However, this effect is not represented in Figure 2-11 (a), since the irradiance more importantly influences the amount of current generated. When less light arrives at the solar cell, then logically less electron-hole pairs are generated, where the electrons and holes are moved across the p-n junction, thus resulting in a lower charge imbalance and a lower current. From Figure 2-11 (a) it is apparent that the short-circuit current is directly proportional to the irradiance. In addition to the effects on I_{sc}, the irradiance affects the open-circuit voltage as well. However, V_{oc} is only logarithmically proportional to the irradiance. Summarizing, the

irradiance affects the short-circuit current greatly, but only small effects are observed on the open-circuit voltage.

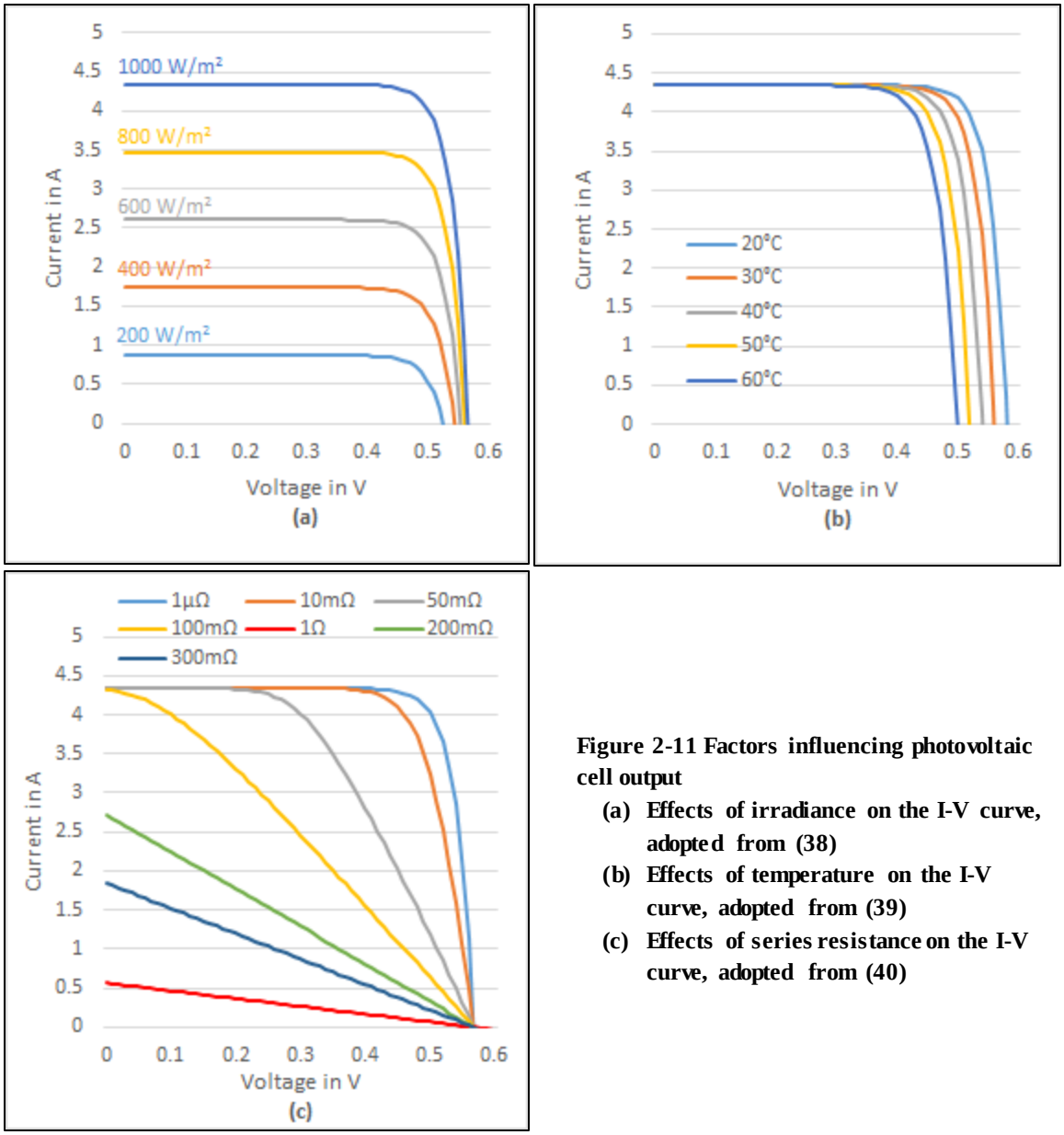

Figure 2-11 Factors influencing photovoltaic cell output

(a) Effects of irradiance on the I-V curve, adopted from (38)

(b) Effects of temperature on the I-V curve, adopted from (39)

(c) Effects of series resistance on the I-V curve, adopted from (40)

2.3.3.2 Temperature effects

A change in ambient temperature leads directly to a change in the operating temperature according to the NOCT equation, i.e. equation 2-3. With an increase in temperature the bandgap energy of the semiconductor decreases marginally, thus electron-hole pairs can be created with less photon energy. This results in an slight increase in the short-circuit current (27). Opposed to that, the open-circuit voltage is decreased significantly with increasing temperature. The decrease in bandgap energy results in a significant increase in the intrinsic carrier

concentration, since electrons can break away from their atoms more easily. This increase does in turn increases the dark saturation current which leads to the decrease in V_{oc} (8, 27). Figure 2-11 (b) shows this effect. The open-circuit voltage is decreasing significantly with increasing temperature, whereas the short-circuit current increases only slightly.

2.3.3.3 Series resistance effects

In solid states physics, specifically semiconductor physics, it is widely known how semiconductor diodes react on changes in temperature. A solar cell, made from semiconductor material, is effectively a p-n junction diode. Those diodes are researched extensively and four distinctive regions have been identified in the forward bias characteristics. When plotting the voltage-current characteristic on a semi-logarithmic scale, i.e. log(I) vs. V, the four regions can be identified easily (41). Figure 2-12 shows such a typical forward bias characteristic of a p-n junction diode. The dotted lines represent the slopes of the different parts of the curve. The blue part of curve is caused by the recombination of electrons and holes within the

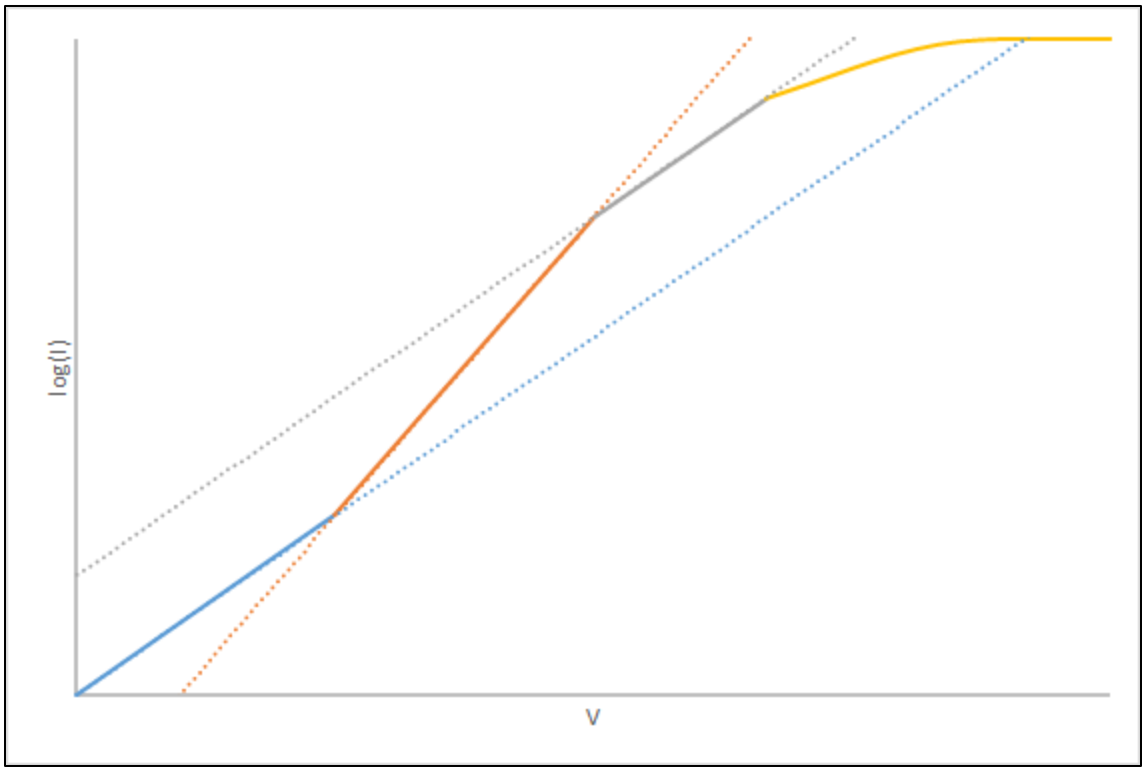

Figure 2-12 Typical forward bias characteristic of a p-n junction diode
Plotted on a semi-logarithmic scale with its four distinctive regions visible.

depletion region. The so created current does not benefit the diode, it therefore dampens the ideal characteristics in the low forward bias region where it dominates. The orange part of the curve resembles the ideal region of the diode. In it the diffusion current, the current generated when electrons move across the junction into the n-layer and holes diffuse into the p-layer, dominates. The deviation from the ideal curve in the grey part of Figure 2-12 is caused by high-

level injection. It has a slope much more similar to the first region. The last region, the yellow part of the curve, is the deterioration of the ideal curve due to series resistance of the diode. This series resistance is a combination of the resistivity of the semiconductor, the contact resistance between the semiconductor and the metal contacts and the resistance of the wiring.

However, in solar cells the last two regions are rarely exhibited. The open-circuit voltage usually occurs in the higher areas of the ideal region, i.e. the diffusion dominated region. Hence the series resistance as described above does not influence the solar cell output. The series resistance talked about in this report is a deterioration of the I-V characteristics in the ideal region, of the solar cell. The effect of dampening the curve as seen in Figure 2-11 (c) is described by an imaginary series resistance.

This series resistance is decreasing with increasing temperature and increasing irradiance. That can easily be seen when considering the simple diode equation:

$$\mathrm{I} = I_0 e^{\frac{q(V+IR_s)}{nk_BT}} \qquad (2\text{-}4)$$

where I is the current flowing through the diode, I_0 is the dark saturation current, q is the electric charge of electrons, k_B is the Boltzmann constant, n is the ideality factor of the diode, T is the absolute temperature in kelvin, R_s is the series resistance and V is the applied voltage across the diode terminals. If we rearranged equation 2-4 to:

$$ln\left[\frac{I}{I_0}\right] = \frac{q(V+IR_s)}{nk_BT} \qquad (2\text{-}5)$$

it is visible, that the aforementioned effect of the temperature on the dark saturation current together with the decrease of $\frac{q}{k_BT}$ lead to the described decrease in the series resistance. An increase in irradiance does cause an increase in I, which as well leads to a decrease in R_s. This is due to the dominance of the I on the RHS of equation 2-5 over the I on the LHS.

Figure 2-11 (c) shows that the short-circuit current is only effected by the series resistance, when it gets significantly large. Since manufacturers try to keep R_s as low as possible, that should not be the case for commercially available photovoltaic cells. Hence, the series resistance affects mostly the maximum power point and therefore the fill factor. An increase in R_s will lead to a decrease in the fill factor and vice versa; a decrease in the series resistance will lead to an increase in the fill factor.

2.4 PSPICE

SPICE stands for Simulation Program with Integrated Circuit Emphasis, which was first described in 1973 (42). It was developed by Laurence Nagel and Donald Pederson as a general purpose electronic simulation program based on the CANCER program (computer analysis of nonlinear circuits, excluding radiation). SPICE has the capabilities of nonlinear dc analysis, nonlinear transient analysis and small signal analysis. All analysis are based on matrix calculations of circuits nodes and loops containing mathematical models of electrical and electronic components (43). PSPICE, standing for personal SPICE was one of the first release

of SPICE for personal computer. The program analyses a circuit described in a text file or as a schematic. First a netlist is generated, on which the required analysis is run and the results are stored in an output file. These results are then displayed graphically or in a text editor.

2.4.1 OrCAD Capture

OrCAD Capture is one of the most widely used schematic design solutions according to its developers at Cadence Design Systems (44). It combines three main applications: Capture, in which a schematic of the electric circuit is drawn, PSPICE, which can simulate the circuits and analyse its behaviour and a PCB Editor, for the design of printed circuit boards. A free version of OrCAD is available for students and interested engineers. However, it has limitations regarding the number of nets and parts per design and the number of pins per created part. Designs which exceed those limits can be create and viewed, but they cannot be saved.

2.4.2 PSPICE A/D

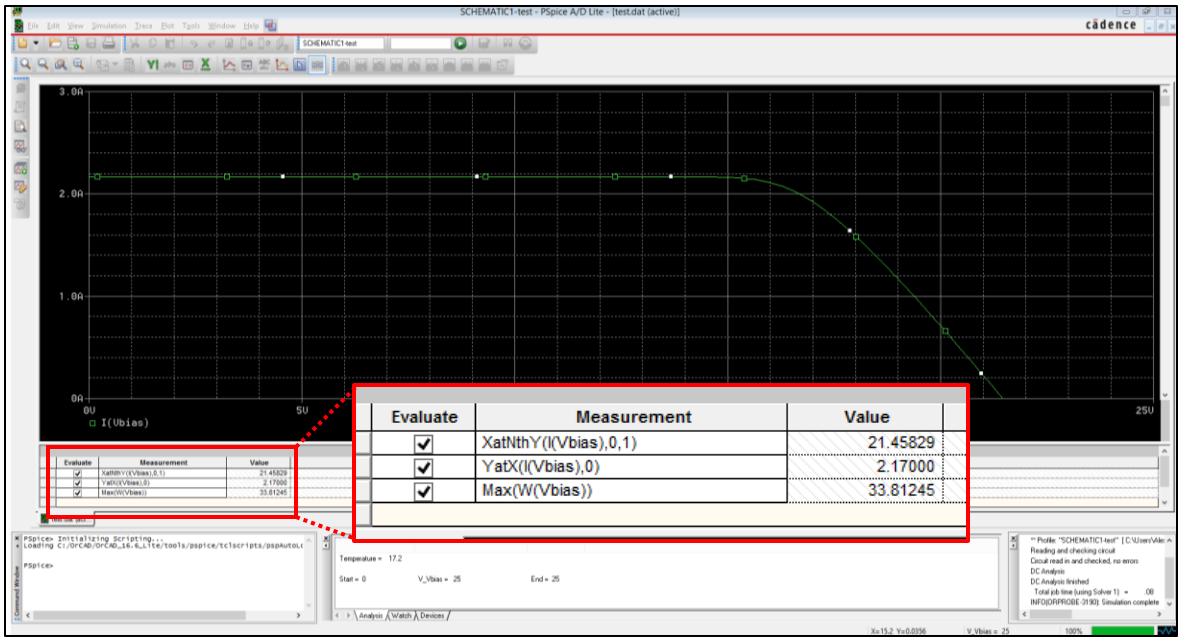

Figure 2-13 PSPICE A/D interface

PSPICE A/D is a SPICE-based simulator, which is able to simulate both analog and digital designs. It is fully integrated with OrCAD Capture, thus it easily simulates schematic circuits and performs various analysis on it, e.g. temperature analysis, DC or AC analysis or a Monte Carlo analysis. Once the circuit is simulated PSPICE A/D is able to evaluate many measurements on the active trace. Figure 2-13 shows the PSPICE A/D interface where an I-V curve is plotted and various measurements are evaluated, i.e. the open-circuit voltage, the short-circuit current and the maximum of the P-V curve.

2.4.3 PSPICE devices

PSPICE can model many common analog devices, e.g. capacitors, inductors, resistors and diodes. For resistor models (Figure 2-14(b)) at least the value of the resistance in Ohm has to be specified. Additionally, linear, quadratic or exponential temperature coefficients can be specified, to improve the model. The model for diodes (Figure 2-14(a)) is more complex than the resistor model. Parameters which can be defined by the user include saturation current, temperature coefficients, emission coefficient and parasitic resistance. All the model parameters have already set default values as specified in (45). Furthermore, PSPICE is able to simulate voltage-controlled voltage sources (Figure 2-14(c)) and voltage controlled current sources (Figure 2-14(d)), which are called e- and g-devices, respectively. These devices set the output voltage or current depending on the input and a specified gain. The gain can be linear or a more complex equation.

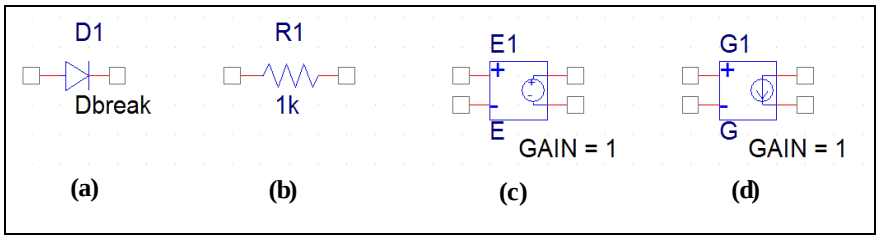

Figure 2-14 PSIPCE components in OrCAD Capture (46)

(a) Diode with the model specified (Dbreak)
(b) Resistor with its resistance value in Ohm
(c) Voltage-controlled voltage source (e-device)
(d) Voltage-controlled current source (g-device)

In PSPICE a specific library for analog behavioural modelling (ABM) is available as well. It reflects the structure of e- and g-devices where the differential input of some devices is set to ground (47).

2.5 Solar cell models

To predict the output of photovoltaic cells and to determine possible improvement factors it is important to simulate them. Multiple models have been developed for different purposes. A commonly used model is the single-diode model, which is used in several publications (48-55). As the name suggests it makes use of one diode in parallel with the current source. Another frequently used model, proposed by (56-61), among others, makes use of a second diode in parallel to the current source and is therefore called two-diode model. Although these two models are used by many authors other model have been developed, like the three-diode model proposed by (62). In the following the one- and two-diode model are presented in more detail.

2.5.1 Single-diode model

As mentioned earlier, this model represents a photovoltaic cell using a current source with a parallel diode (Figure 2-15). The current source simulates the photo generated current I_{phC} and

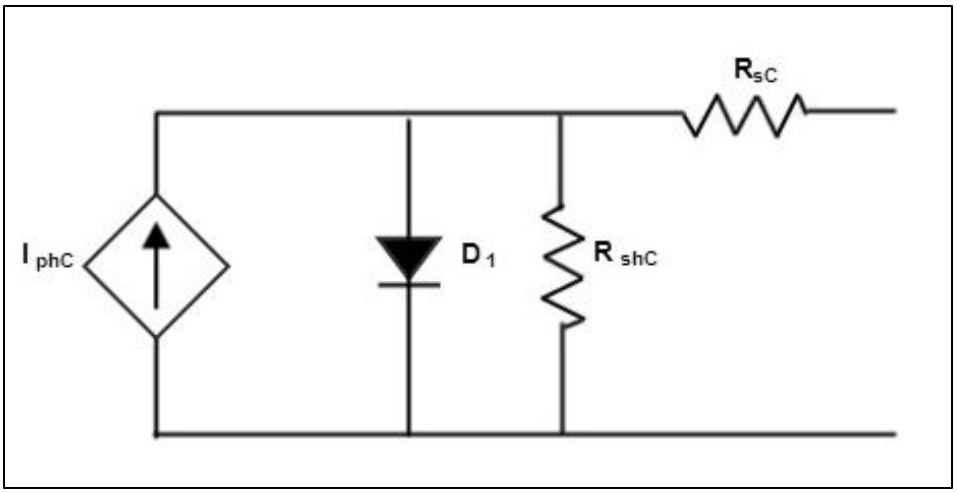

Figure 2-15 One-diode solar cell model
D_1 simulates the diffusion current which counteracts the photo generated current I_{phC}. R_{sC} and R_{shC} represent series and shunt resistive losses, respectively.

the diode D_1 the diffusion current which counteracts I_{phC}. The series resistance R_{sC} simulates the resistance encountered when the generated current travels through the semiconductor material, added by eventual contact resistance. The parallel or shunt resistance R_{shC} simulates a conductance in the depletion region due to atom vibrations as well as production impurities. The current flowing through this resistance is called the shunt current. It is the current that finds a way around the p-n junction, thus not generating any power for the solar cell (63). Generally, R_{sC} is very small, whereas R_{shC} is very large. Some authors ignore one or both variables to simplify their models.

The current output in this model is described as follows:

$$I_C = I_{phC} - I_0\left(e^{\frac{V_C + I_C R_{sC}}{nV_T}} - 1\right) - \left(\frac{V_C + I_C R_{sC}}{R_{shC}}\right) \qquad (2\text{-}6)$$

where I_{phC} is the photo generated current, I_0 and n are the saturation current and ideality factor of diode D_1 respectively, R_{sC} is the series resistance and R_{shC} is the shunt resistance. The C in the subscript indicates that those parameters are parameters of photovoltaic cells. When the model is to be used for a photovoltaic module a conversion of this formula according to Appendix A.1 has to be performed. V_T is the thermal voltage, which is calculated using Boltzmann´s constant k_B=1.38065*10^{-23} J/K, the absolute temperature T, in Kelvin, and the electric charge of electrons q=1.60218*10^{-19} C.

$$V_T = \frac{k_B T}{q} \qquad (2\text{-}7)$$

2.5.2 Two-diode model

The two-diode model adds another diode to the aforementioned model. This second diode simulates the recombination effects. They can occur at impurities in the crystal structure or at the surface of the material. When electrons recombine before they are being collected the current output of the solar cell suffers. Hence the recombination current counteracts the photo generated current, just as the diffusion current simulated by D_1. Figure 2-16 shows a general two-diode model. Some authors choose to neglect some parameters or combine others, to simplify their models and further calculations.

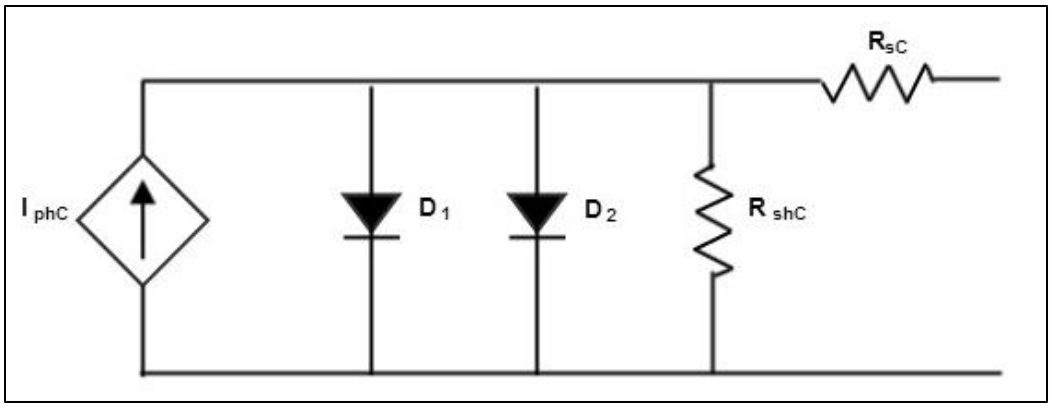

Figure 2-16 Two-diode solar cell model
D1 and D2 simulating the diffusion current and recombination current respectively, which counter act the generated photocurrent I_{phC}, R_{sC} represents the series resistive losses and R_{shC} the shunt resistive losses.

Similar to equation 2-6 for the single-diode model, the current output for the two-diode model is calculated. The two diodes are represented by the saturation currents I_{01} and I_{02} for diode D_1 and D_2 respectively. Both usually have different ideality factors n_1 and n_2 as well. Most often they are considered to be n_1=1 and n_2=2. In the equation the variables are defined as for the single-diode model

$$I_C = I_{phC} - I_{01}\left(e^{\frac{V_C + I_C R_{sC}}{n_1 V_T}} - 1\right) - I_{02}\left(e^{\frac{V_C + I_C R_{sC}}{n_2 V_T}} - 1\right) - \left(\frac{V_C + I_C R_{sC}}{R_{shC}}\right) \qquad (2\text{-}8)$$

2.6 Stakeholders

This project is initiated by CEMIG, the state electrical energy-distribution company of Minas Gerais, together with UFMG, Federal University of Minas Gerais. CEMIG is planning to develop multiple photovoltaic power plants in the Brazilian state of Minas Gerais in order to supply cheap and reliable energy to the population and the industry. The first of these plants is installed in Sete Lagoas, close to the states capital. CEMIG is interested in the modelling of photovoltaic cells and later systems to estimate the output of such a power plant. The research is carried out at the Optronics and Microtechnology Laboratory (OptMA Lab) of the department of electrical engineering at UFMG. The head of this lab, Dr. Davies William, is my supervisor for the here presented research. UFMG wants to position itself as the top photovoltaic research university in Brazil. Another stakeholder is Hanze University of Applied Sciences Groningen, although a secondary one. Represented by Mr. Ronald van Elburg and Mr. Bryan Williams as first and second graduation supervisor respectively. They will evaluate the research based on the here presented report and the final presentation.

CHAPTER 3

CONCEPTUAL MODEL

The general two-diode solar cell model requires that physical parameters, i.e. diffusion current, recombination current and shunt and series resistance, are known. But more often than not this is not the case. If solar cells have to be evaluated for new applications, the manufacturers provide relevant electrical data measured under STC or in the SRE. To obtain physical parameters from material databases is not always practical, since manufacturers might use materials, which are not yet listed in those databases, or they improved already known materials, thus altering their physical parameters. Therefore, it is of great value to model photovoltaic cells with only the available electrical parameters. The model described in detail in this chapter is able of doing so.

3.1 General concept

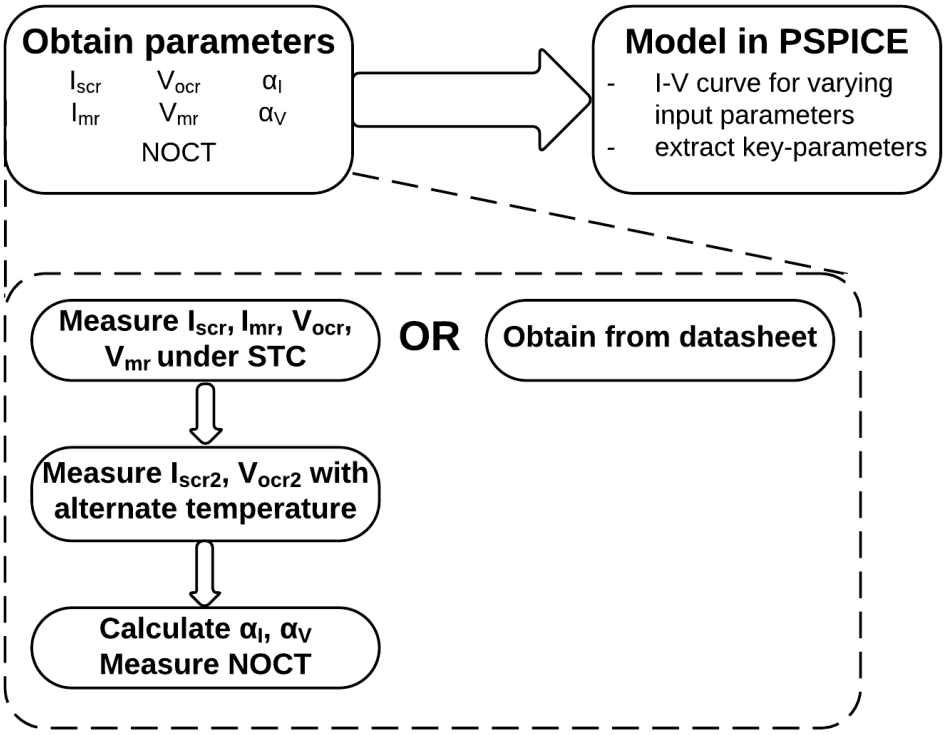

Figure 3-1 Flowchart of the general concept

The concept will largely focus on the accurate modelling of the solar cell, so that a good estimation on the power generation under changing conditions can be given. To be able to

model the photovoltaic cell in PSPICE certain parameters defining the cell have to be determined. Those electrical parameters are:

- short-circuit current (I_{scr})
- open-circuit voltage (V_{ocr})
- current at the maximum power-point (I_{mr})
- voltage at the maximum power-point (V_{mr})
- temperature coefficient of the short-circuit current (α_I)
- temperature coefficient of the open-circuit voltage (α_V)
- NOCT

where the first four are determined under standard test conditions, hence the subscript r for reference. If they are not provided from the manufacturer of the solar cell or if the solar cell is a new development, then the parameters have to be measured using suitable equipment. After determining the reference currents and voltages under STC the temperature coefficients are calculated. To do so the short-circuit current and open-circuit voltage are measured under conditions similar to STC where only the temperature is changed. From the difference between I_{scr} and V_{ocr} and the other set of short-circuit current and open-circuit voltage, change in the current and voltage per °C, thus the temperature coefficients are calculated. The last parameter, the NOCT, is determined within the standard reference environment. The parameters can then be inserted into the PSPICE model to predict the I-V curves with its maximum power-point under conditions different from the reference conditions. Furthermore, it is possible to load the temperature and irradiance data from one day into the model, which will then simulate the expected output during the whole day.

3.2 Proposed solar cell model

The proposed model is based on the model developed by Castaner (64), however its governing equations are based on the two-diode model instead of the single-diode model. Furthermore, the newly proposed model does incorporate the temperature dependence of the series resistance, which shall result in a more accurate prediction of the fill factor. The principal of purely using electrical parameters as inputs for the model is kept. That enables the quick evaluation of newly developed solar cells or modules for which physical parameters, e.g. ideality factor or diode saturation current, necessary for the two-diode model, are not yet available. The electrical parameters can easily be obtained from the manufacturer´s datasheet, experiments or published research articles. Hence, the proposed model can be valuable to the evaluation of newly designed photovoltaic cells and modules, as well as for cells/modules to which no extensive documentation is available, due to reasons of secrecy or negation.

Figure 3-2 shows a schematic of the proposed model. The actual model (red frame) consists of three voltage controlled current sources, i.e. Girrad, Gidiode and Gs, and a resistor Rsh in parallel to Girrad and Gidiode. This resistor represents the shunt resistance, which is assumed very large, i.e. 100GΩ. Girrad represents the photo-generated current I_{ph}. This current is counter acted by the currents through the recombination and diffusion diode. These currents are combined in the voltage controlled current source Gidiode. The series resistance is simulated by the last g-device (Gs), where the controlling and output nodes are the same. With

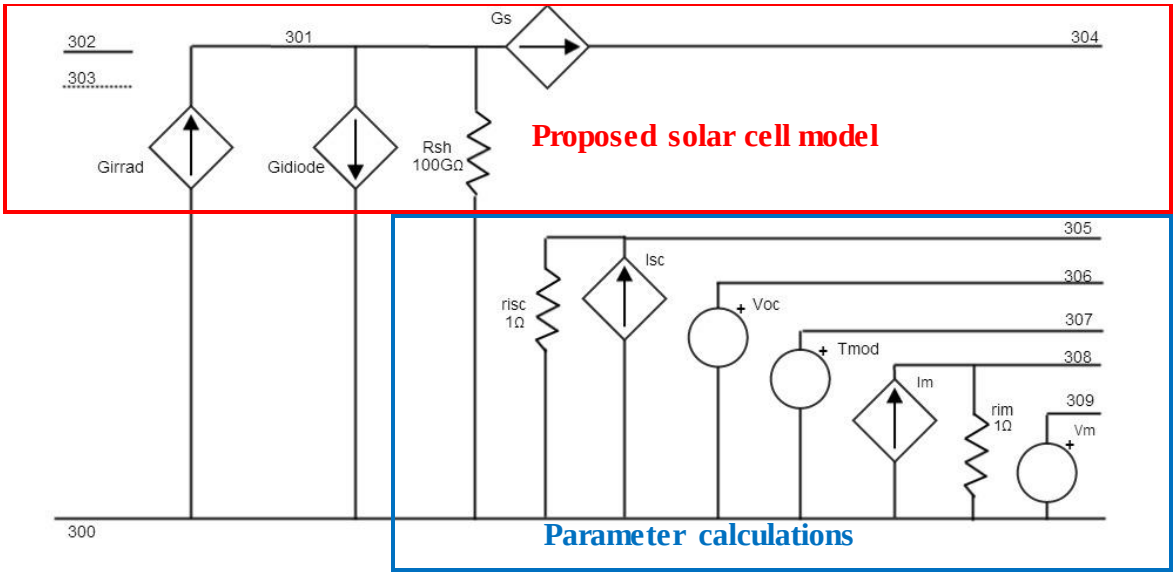

Figure 3-2 Schematic of the proposed solar cell model
The schematic is adapted from (62), it depicts the actual model (red frame) and voltage-controlled sources which calculate important cell parameters (blue frame) used in the model

it a conductance is simulated (65), which is the inverse of the resistance. Hence the voltage between the two controlling nodes divided by the resistance will generate the appropriate conductance to represent the desired series resistance. Node 302 is the input node for the irradiance, which is then used in many of the e- and g-devices to calculate the cell parameters and its overall output. The second input node, 303, is for the ambient temperature. If it is desired to simulate the output of a solar cell or module over the whole day, or week for that matter, than the irradiance and ambient temperature at previously specified times of the day can be input as a time series. The model then calculates the output of the cell or module at each time and a curve of the output vs the time is the result. If, however, the temperature effects on the cell are to be evaluated it is sufficient to use the PSPICE setting for the temperature. A series of temperatures can be set as well in these settings, but PSPICE will start for every temperature a new analysis. Hence, it is not sufficient if an output profile of the whole day is needed. At node 304 the output of the solar cell can be read.

The devices within the blue frame in Figure 3-2 calculate important photovoltaic cell parameters, which are used in the model and can be read out at the specified nodes. The devices Isc and Im calculate the short-circuit current I_{sc} at node 305 and the current at the maximum power point I_m at node 308, respectively. The resistors risc and rim are only to avoid floating nodes in the simulation, however their very small resistance values will not affect the simulation. At nodes 306 and 309 the open-circuit voltage and voltage at the maximum power point V_m are calculated by the e-devices Voc and Vm respectively. The e-device Tmod will calculate the cell operating temperature according to equation 2-3. Thus the voltage output at node 307 represents a temperature in °C.

As mentioned before, the here proposed model is based on the two-diode model described in chapter 2.5.2. It is adapted for the use with solar modules, where N_s and N_p are the number of photovoltaic cells in series and parallel, respectively. The conversion is shown in Appendix A.1. From this point on all parameters are thought of as photovoltaic module parameters. However, as a simplification, one can think of a solar cell as a module with N_s=N_p=1. Furthermore are the diode factors set according to Shockley´s diffusion theory (66) and the Sah-Noyce-Shockley diode equation (66), i.e. n_1=1 and n_2=2. Lastly it is assumed that the shunt resistance is very large, i.e. 100GΩ as seen in Figure 3-2. Hence, the last part on the RHS in equation **2-6** will be very small and can be neglected. Considering those assumptions the current output of the solar module is described by:

$$I = I_{ph} - N_p I_{01}\left(e^{\frac{V+IR_S}{N_S V_T}} - 1\right) - N_p I_{02}\left(e^{\frac{V+IR_S}{2N_S V_T}} - 1\right) \quad (3\text{-}1)$$

Based on this, the following equations describe the devices from Figure 3-2:

$$I_{sc} \cong I_{ph} = \frac{G}{1000} * [I_{scr} + \alpha_I(T_{cell} - 25)] \quad (3\text{-}2)$$

$$V_{oc} = V_{ocr} + \alpha_V(T_{cell} - 25) + N_S V_T \, ln\frac{I_{sc}}{I_{scr}} \quad (3\text{-}3)$$

$$I_{DR} = N_P I_0\left(e^{\left[\frac{V_{ph}}{N_S V_t}\right]} + e^{\left[\frac{V_{ph}}{2N_S V_t}\right]} - 2\right) \quad (3\text{-}4)$$

$$I_0 = \frac{I_{sc}}{N_P\left(e^{\left[\frac{V_{oc}}{N_S V_t}\right]} + e^{\left[\frac{V_{oc}}{2N_S V_t}\right]}\right)} \quad (3\text{-}5)$$

$$R_s = \frac{2.7V_{oc}\left\{1.1FF_0 - \sqrt{\left[1.21{FF_0}^2 + \frac{20}{27}\left(\frac{I_m V_m}{I_{sc} V_{oc}} - FF_0\right)\right]}\right\}}{I_{sc}} \quad (3\text{-}6)$$

$$FF_0 = \frac{\frac{V_{oc}}{N_S V_T} - \ln\left(\frac{V_{oc}}{N_S V_T} + 0.72\right)}{1 + \frac{V_{oc}}{N_S V_T}} \quad (3\text{-}7)$$

$$I_m = \frac{G}{1000} * [I_{mr} + \alpha_I(T_{cell} - 25)] \quad (3\text{-}8)$$

$$V_m = N_S V_T \, ln\left[\frac{I_{sc} - I_m}{I_{sc}}\left(e^{\left[\frac{V_{oc}}{N_S V_t}\right]} + e^{\left[\frac{V_{oc}}{2N_S V_t}\right]}\right)\right] - I_m R_s \quad (3\text{-}9)$$

The various parameters in the equations above are defined as follows:

- α_I temperature coefficient of the short-circuit current (A/°C)
- α_V temperature coefficient of the open-circuit voltage (V/°C)

- FF_0 fill factor for the ideal solar cell without resistive losses
- G irradiance (W/m^2)
- I_0 combined diode saturation current (A)
- I_{01} diffusion diode saturation current (A)
- I_{02} recombination diode saturation current (A)
- I_{DR} combined diffusion and recombination current (A)
- I_m current at the maximum power point (A)
- I_{mr} current at the maximum power point at STC (A)
- I_{ph} photo-generated current (A)
- I_{sc} short-circuit current (A)
- I_{scr} short-circuit current at STC (A)
- N_p number of photovoltaic cell connected in parallel
- N_s number of photovoltaic cell connected in series
- R_s series resistance (Ω)
- T_{cell} cell operating temperature (°C)
- V_{oc} open-circuit voltage (V)
- V_{ocr} open-circuit voltage at STC (V)
- V_m voltage at the maximum power point (V)
- V_{mr} voltage at the maximum power point at STC(V)
- V_{ph} voltage before the series resistance (photo-generated voltage) (V)
- V_T thermal voltage which is calculated using equation **2-5** (V)

Equation 3-2 is used to calculate the short-circuit current. I_{sc}, which is considered to be nearly equal to I_{ph}, the photo-generated current. The first part of the equation calculates I_{sc} at any irradiance value using I_{scr}, which is determined at AM1.5G and $1000W/m^2$ and G, the current irradiance, which is normalized towards the STC. The second part of the equation corrects for the temperature dependence of I_{sc} by multiplying the temperature coefficient of the short-circuit current with the difference between the current cell operating temperature and the cell operating temperature at STC, namely 25°C. This part is as well corrected for the irradiance normalized towards STC.

Equation 3-3 calculates the open-circuit voltage using V_{ocr}, which is corrected for its temperature dependence, with the second term on the RHS of the equation, and for the irradiance, with the third term on the RHS. The open-circuit voltage can be calculated by the following equation:

$$V_{oc} = N_S V_T \, ln\left[\frac{I_{sc}}{N_p I_0}\right] \qquad (3\text{-}10)$$

Which is derived from equation 3-1 under open-circuit conditions, i.e. $V=V_{oc}$ and $I=0$. Moreover is the temperature coefficient of the open-circuit voltage, as described in (64), determined by:

$$\alpha_V(T_{cell} - 25℃) = N_S V_T \, ln\left[\frac{I_{scr}}{N_p I_0}\right] - V_{ocr} \qquad (3\text{-}11)$$

Castaner et al. (64) added and subtracted V_{oc} on the RHS, substituted one of them with equation 3-10 and rearranged it to solve for V_{oc}, thus reaching equation 3-3. The complete derivation is shown in Appendix A.2.

The combined diffusion and recombination current is derived from the second and third term on the RHS of equation 3-1:

$$I_{DR} = N_p I_{01}\left(e^{\frac{V+IR_S}{N_S V_T}} - 1\right) - N_p I_{02}\left(e^{\frac{V+IR_S}{2N_S V_T}} - 1\right) \qquad (3\text{-}12)$$

where it is assumed that $I_{01} = I_{02} = I_0$ to simplify the calculation. That was first proposed and shown to be an accurate approximation by Ishaque et al. (57). To further simplify, we substitute the term $V+IR_s$ by V_{ph}, which represents the voltage before the series resistance, thus the voltage at node 301 in Figure 3-2. The described adjustments to equation 3-12 result in equation 3-4.

We can approximate I_0 by rearranging equation 3-1 to solve for I_{ph} under open-circuit conditions and substitute it into equation 3-1 under short-circuit conditions, i.e. V=0 and $I=I_{sc}$, which leads to:

$$I_{sc} = N_P I_0\left(e^{\left[\frac{V_{oc}}{N_S V_t}\right]} - e^{\left[\frac{I_{SC}R_S}{N_S V_t}\right]} + e^{\left[\frac{V_{oc}}{2N_S V_t}\right]} - e^{\left[\frac{I_{SC}R_S}{2N_S V_t}\right]} - 2 + 2\right) \qquad (3\text{-}13)$$

In the equation above we can neglect the terms $e^{\left[\frac{I_{SC}R_S}{N_S V_t}\right]}$ and $e^{\left[\frac{I_{SC}R_S}{2N_S V_t}\right]}$, because they are very small compared to $e^{\left[\frac{V_{OC}}{N_S V_t}\right]}$ and $e^{\left[\frac{V_{oc}}{2N_S V_t}\right]}$, due to the much larger magnitude of V_{oc} compared to $I_{sc}R_s$. Rearranging equation 3-13 will lead us to equation 3-5, which together with equation 3-4 is used to describe the g-device Gidiode.

Green (67) proposed an equation, which relates the fill factor, FF, to the ideal fill factor, FF_0:

$$FF = FF_0(1 - 1.1r_s) + \frac{{r_s}^2}{5.4} \qquad (3\text{-}14)$$

where $r_s = \frac{I_{sc}R_s}{V_{oc}}$. We can rearrange this quadratic equation in the form $0=ax^2+bx+c$ and solve it using MatLab (68). From the two solutions one will result in large R_s values of around 100Ω, which is highly unlikely as the series resistance for a photovoltaic module. The other solution, i.e. equation 3-6, yields results around 1Ω, an expected result for R_s. Green (69) also developed an equation to approximate FF_0, which we only have to adjust for our use for solar modules, thus resulting in equation 3-7. With these two equations the series resistance is determined. The voltage at the maximum power point needed to do so is assumed to be scale proportional to V_{oc} and approximated by equation 3-3, where V_{ocr} is replaced by V_{mr}, the voltage at the maximum power point at STC. Although scale proportionality is not always present, for the determination of the series resistance it is a valid assumption. The complete derivation is shown in Appendix A.3.

I_m is calculated similar to the short-circuit current, assuming that the temperature effects the current at maximum power point in the same way as it affects the short-circuit current. Hence α_I, the temperature coefficient of the short-circuit current is used to correct for the temperature dependence of I_m.

To approximate the voltage at the maximum power point we evaluate equation 3-1 at the maximum power point, i.e. I=I_m and V=V_m:

$$I_m = I_{ph} - N_p I_0 \left(e^{\frac{V_m + I_m R_s}{N_s V_T}} + e^{\frac{V_m + I_m R_s}{2 N_s V_T}} - 2 \right) \qquad (3\text{-}15)$$

due to the large magnitude, around 10^8 for single photovoltaic cells, of the first two terms in the bracket we can neglect the '-2'. We rearrange this equation and use the binomial theorem:

$$e^x + e^{\frac{x}{2}} = \left(e^{\frac{x}{2}} + \frac{1}{2} \right)^2 - \frac{1}{4} \qquad (3\text{-}16)$$

where we can again neglect the small constants $\frac{1}{2}$ and $\frac{1}{4}$, since they are much smaller than $e^{\frac{x}{2}}$, with $x = \frac{V_m + I_m R_s}{N_s V_T}$. We then arrive at:

$$\frac{V_m + I_m R_s}{N_s V_T} = ln \left[\frac{I_{ph} - I_m}{N_p I_0} \right] \qquad (3\text{-}17)$$

If we now substitute equation 3-5 into the above equation and assume the I_{ph}=I_{sc} we arrive at equation 3-9, which approximates V_m much more accurately than the assumption of scale proportionality. The complete derivation is shown in Appendix A.5

The OrCAD circuit schematic of the proposed model is shown in Figure 3-3. The actual model (Girrad, Gidiode, Gs, Rsh) is supported by e- and g-devices, which calculate I_{sc}, V_{oc}, I_m, V_m, T_{mod}, V_T, R_s, FF_0 and FF. The DC-voltage sources at the outputs of the g-devices Isc and Im are only to sense the current at those nodes. They are both set to 0V and thus don´t alter the results. This circuit is described by the following PSPICE netlist:

```
G_Girrad 0 301 VALUE {V(302,0)/1000*(Iscr+coef_Isc*(V(307)-
+  25))}
G_Gidiode 301 0 VALUE {(I(V_305)/(exp(V(306)/(Ns*V(Vt)))
+  +exp(V(306)/(Ns*2*V(Vt))))*(exp(V(301,0)/(Ns*V(Vt)))
+  +exp(V(301,0)/(2*Ns*V(Vt)))-2)}
G_Gs 301 304 VALUE {V(301, 304)/V(Rs)}
R_Rsh 0 301  100G TC=0,0
G_Isc 0 N21205 VALUE {V(302,
0)/1000*(Iscr+coef_Isc*(V(307)-
+  25))}
V_305 N21205 N21429 0Vdc
R_Risc N21429 0  1 TC=0,0
E_Voc 306 0 VALUE {Vocr+coef_Voc*(V(307)-
+  25)+Ns*V(Vt)*log(I(V_305)/Iscr)}
E_Tmod 307 0 VALUE {TEMP+V(302, 0)*(NOCT-20)/800}
```

```
G_Im 0 N21211 VALUE {V(302, 0)/1000*(Imr+coef_Isc*(V(307)-
+  25))}
V_308 N21211 N21449 0Vdc
R_Rim N21449 0  1 TC=0,0
E_Vm 309 0 VALUE {Ns*V(Vt)*log(((I(V_305)-
+  I(V_308))/I(V_305))*(exp(V(306)/(Ns*V(Vt)))+exp(V(306)/
+  (2*Ns*V(Vt)))))-I(V_308)*V(Rs)}
E_Vt VT 0 VALUE {0.025875*(V(307)+273.15)/300}
E_Rs RS 0 VALUE {(2.7*V(306)*(1.1*V(FF0)-
+  SQRT(1.21*V(FF0)**2+20*V(FF)/27-
20*V(FF0)/27)))/(I(V_305))}
E_FF0 FF0 0 VALUE {(V(306)/(Ns*V(Vt))-
+  log(V(306)/(Ns*V(Vt))+0.72))/(1+(V(306)/(Ns*V(Vt))))}
E_FF FF 0 VALUE {(I(V_308)*(Vmr+coef_Voc*(V(307)-
+  25)+Ns*V(Vt)*log(I(V_305)/Iscr)))/(V(306)*I(V_305))}
V_Vbias 304 0 0
V_Virrad 302 0 {Virrad}
.PARAM noct=45 np=2 vmr=17.7 ns=18 virrad=904 vocr=22.1
+  iscr=8.68 imr=7.91 coef_voc=-0.0796 coef_isc=5.2e-3
```

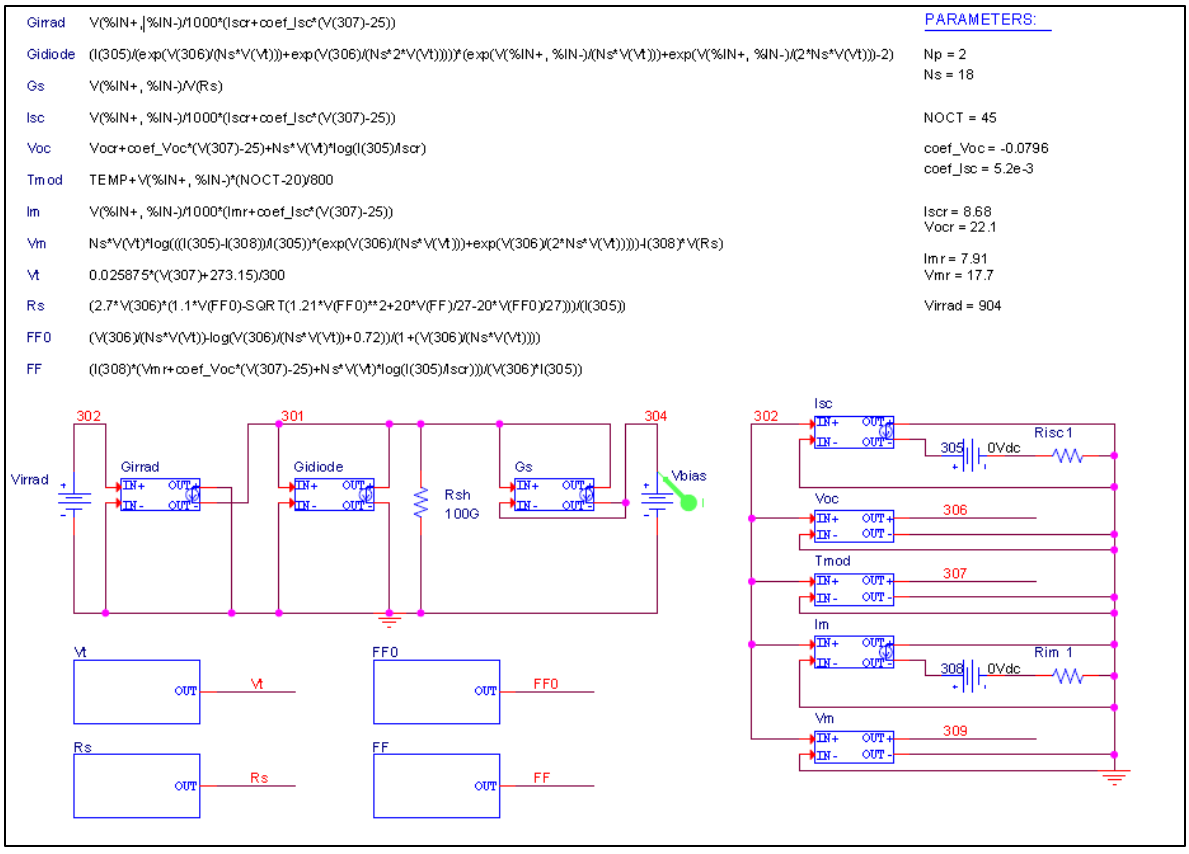

Figure 3-3 Circuit schematic of the proposed model

CHAPTER 4

HYPOTHESIS

Photovoltaic module manufacturers usually give their electrical characteristics, like its maximum power output, under STC. However, when deployed in the field those standard conditions are not found and hence the output from the module varies. When designing a photovoltaic power plant it is important for the operator to know which output can be expected on an average day from the solar modules. Thus, simulations of the solar module output under conditions other than STC are required. The generalized model of a solar cell requires physical data, e.g. diode saturation current or series resistance, as an input, which might not be readily available for newly developed modules. Therefore, it is required to create a model which simulates solar cells based on electrical parameters, e.g. short-circuit current and open-circuit voltage under STC, which are provided by the manufacturer or can easily be determined with the right equipment.

This leads to the research question and its sub-questions, which will be answered in this report:

Can the proposed model accurately simulate the performance of photovoltaic cells/modules using only electrical parameters as inputs?

Can the accuracy, with regards to parasitic temperature effects, of the proposed model be improved, by deploying analog behavioural modelling in addition to the intrinsic diode and resistor models?

How does the proposed model perform compared to the behavioural solar cell model described by Castaner and Silvestre (64) in simulating the temperature effects on the series resistance?

Does the model simulate the influences of parasitic effects on the photovoltaic cell/module output accurately?

Electrical parameters of the photovoltaic module are the short-circuit current, the open-circuit voltage, the voltage and current at the maximum power point, the temperature coefficients for the open-circuit voltage and the short-circuit current and the NOCT. The temperature effects are changes in the module temperature, which is affected by the irradiance and the ambient temperature according to the NOCT model. Parasitic effects are internal resistances present in the photovoltaic module, as well as changing ambient temperature and varying irradiation levels. As for the internal resistances, only the series resistance is considered. The shunt resistance is assumed to be infinite and the contact and wiring resistances are assumed to be practically nil.

Accurately in this case means a maximal deviation of 5% from the experimentally obtained data.

CHAPTER 5

RESEARCH DESIGN

To validate the aforementioned model a research design has been developed. The model verification phase is crucial in showing the model´s functionality. In the validation phase the model is tested for its intended functionalities, i.e. output prediction of unknown or new solar cells, and the accuracy is determined.

5.1 Model verification

In this first phase of the research design the model is verified. It is tested if the model generates outputs as expected, that is if the equations governing this model react to changes in the input as one would expect from the theory. This can be done with any solar cell/module. Tests will be the following:

5.1.1 Comparison of ABM and intrinsic modelling with regard to temperature

To identify if the accuracy of the proposed model can be improved by the use of ABM devices a simple two-diode model is simulated using different intrinsic diode and resistor models and ABM models. The shunt resistance is assumed to be infinite and can thus be ignored. Four different combinations will be compared to each other, however all four use a g-device to compute the photo-generated current and a dc-voltage source to simulate the irradiance:

1. The first model consists of only two diodes in parallel. They simulate the diffusion and recombination diodes. In those models the ideality factors are set to 1 and 2, respectively and the saturation current is calculated according to equation 3-5, where the values of I_{sc} and V_{oc} at STC are used. Furthermore, the series resistance is set within these diode models according to equation 3-6 at STC. The intrinsic model takes the simulation temperature into account and modifies the diodes behaviour accordingly.
2. The second model is similar to the first one, only the series resistance within the diode model is set to 0 and an external resistor is added to simulate it. The value of this resistor is calculated the same way as above, by means of equation 3-6 at STC.
3. In the third model the diodes are simulated using an ABM device, specifically a g-device. Its behaviour is given by equation 3-4. The series resistance is simulated by an external resistor model, just like in the second model. Other e- and g-devices are used to calculate the parameters used in the ABM-device diodes, like I_{sc}, V_{oc} and V_T, at the current simulation temperature.
4. The fourth model makes use of ABM device for the diodes, just as described above. Furthermore does it as well simulate the series resistance with a g-device, where its value is calculated according to equation 3-6. In this model a resistor parallel to the diode model is as well included, similar to a shunt resistance. This resistor is set to be 100GΩ and it is needed for the simulation. Otherwise node 301 would be floating and PSPICE would not be able to start the simulation. However, due to its very large value this resistor will not influence the final results.

The OrCAD circuits and netlists of all four models are shown in Appendix B.

5.1.2 Changes in input irradiance

The proposed model will be evaluated under changing irradiance value. This will show if the model reacts according to the expected changes. It is expected that the short-circuit current will change linearly with the irradiance, whereas the open-circuit voltage will only change logarithmically as seen in chapter 2.3.3. Furthermore, a decrease in R_s is expected with an increase in irradiance. To verify this effect the executed test will be two-fold. First the series resistance is kept at an appropriate constant value, i.e. R_s at STC, to evaluate the expected changes in short-circuit current and open-circuit voltage. In the second part the series resistance will be calculated as proposed. When comparing the two results the effects of a changing irradiance on R_s and in turn the effects of an altered R_s can be observed.

The expectations are that the short-circuit current will decrease greatly, whereas the open-circuit voltage will only decrease slightly with decreasing irradiance. The series resistance will on the other hand increase and hence the fill factor will be decreased.

5.1.3 Changes in ambient temperature

In this test, the ambient temperature, i.e. the simulation temperature, will be altered to analyse the response of the proposed model. Due to the fact, that this will change not only the short-circuit current and the open-circuit voltage, as outlined in chapter 2.3.3, but also the series resistance, the test is split into two parts as described in the chapter above.

It is expected to see a decrease of the open-circuit voltage, a slight increase of the short-circuit current and an increase in R_s, which will result in a higher fill factor, due to a higher maximum power output.

5.2 Model validation

In the model validation process the proposed model will be used to predict the output of a photovoltaic module at various irradiances and ambient temperatures. These predictions are then evaluated against experimental data. Since the expected equipment, i.e. an artificial sun and a semiconductor analyser, was not yet available, measurements were obtained with the Solmetric PVA-600 PV Analyzer. The experiments were conducted outside over one day, to obtain a wide range of irradiance/temperature pairings. The error of the predicted curve towards the experimentally obtained curve was then calculated to determine the overall accuracy of the proposed model. The same was done for the model proposed by Castaner (64), hence a comparison between the two models can be made.

Furthermore, it is necessary to determine the effects that errors of the input parameters have on the output of the proposed model. A good way to determine this error would be by using the Monte Carlo method. In it the simulation will be run several times, with slightly altered inout parameters according to the Monte Carlo variation model. However, this variation model was not available and for the creation of one, the necessary equipment was not available. To assess the effects of erroneous input parameters a much more simplified approach was used. Only the minimum and maximum errors in the input parameters is evaluated which provides an acceptable evaluation base. That is achieved by running the simulation for the same datasets as

above three times. Once with the parameters supplied by the manufacturer and then again at the lower and upper boundary of the parameters. Therefore, the maximum errors in the model output can be evaluated. This method is not the most accurate, however with the available data the error tendencies of the proposed model can be evaluated acceptably.

CHAPTER 6

RESULTS

In this section, the results of the various experiments are presented. The first sub-chapter contains the results and analysis to verify the proposed model. The second sub-chapter is focused on the validation.

6.1 Verification results

6.1.1 Comparison results of intrinsic PSPICE models and ABM devices

The four models described in chapter 5.1.1 are evaluated at three different temperatures, i.e. 25°C, 50°C and 100°C, under an illumination of 1000 W/m^2. The solar cell described in chapter 3.14 of (64) is used for simulation. Its nominal electrical parameters are:

- I_{sc} = 37.5 mA
- V_{oc} = 0.669 V
- I_m = 35.52 mA
- V_m = 0.518 V
- NOCT = 47
- α_I = 12.6 µA/°C
- α_V = -3.1 mV/°C

thus the solar cell has a nominal fill factor of FF = 0.7334. It is obvious that since it is only a single photovoltaic cell both, N_s and N_p, are $N_s = N_p = 1$. From the PSPICE simulation, the key characteristics are extracted and presented in Table 6-1.

	Model 1		Model 2		Model 3		Model 4	
	value	Δ%	value	Δ%	value	Δ%	value	Δ%
				25°C				
I_{sc}	0.0375	0.00	0.0375	0.00	0.0375	0.00	0.0375	0.00
V_{oc}	0.774	15.70	0.694	3.74	0.669	0.00	0.669	0.00
I_m	0.0357	0.51	0.0357	0.51	0.0354	-0.34	0.0354	-0.34
V_m	0.62	19.69	0.54	4.25	0.52	0.39	0.52	0.39
FF	0.7626	3.98	0.7407	1.00	0.7338	0.05	0.7338	0.05

Table 6-1 Comparison of four models using intrinsic diode and resistor models and analog behavioural models, at 25°C, 50°C and 100°C
Showing data extracted from PSPICE and their percentage changes with respect to the nominal values at STC.

	Model 1		Model 2		Model 3		Model 4	
	value	Δ%	value	Δ%	value	Δ%	value	Δ%
				50°C				
I_{sc}	0.0378	0.80	0.0378	0.80	0.0378	0.80	0.0378	0.80
V_{oc}	0.733	9.57	0.652	-2.54	0.592	-11.51	0.592	-11.51
I_m	0.0361	1.63	0.0354	-0.34	0.0354	-0.34	0.035	-1.46
V_m	0.57	10.04	0.5	-3.47	0.44	-15.06	0.45	-13.13
FF	0.7427	1.26	0.7182	-2.08	0.6961	-5.09	0.7038	-4.03
				100°C				
I_{sc}	0.0384	2.40	0.0384	2.40	0.0384	2.40	0.0384	2.40
V_{oc}	0.65	-2.84	0.568	-15.10	0.437	-34.68	0.437	-34.68
I_m	0.0356	0.23	0.0355	-0.06	0.0335	-5.69	0.0336	-5.41
V_m	0.49	-5.41	0.41	-20.85	0.3	-42.08	0.309	-40.35
FF	0.6989	-4.71	0.6673	-9.01	0.5989	-18.34	0.6187	-15.64

Table 6-1 continued

From the table above it can be seen that at 25°C, which represents STC, model 1 and 2 perform poorly. Model 1 exhibits an open-circuit voltage 15.7% higher than the nominal value at STC. And model 2 results in 3.7% higher V_{oc}. On the other hand model 3 and 4 simulate the open-

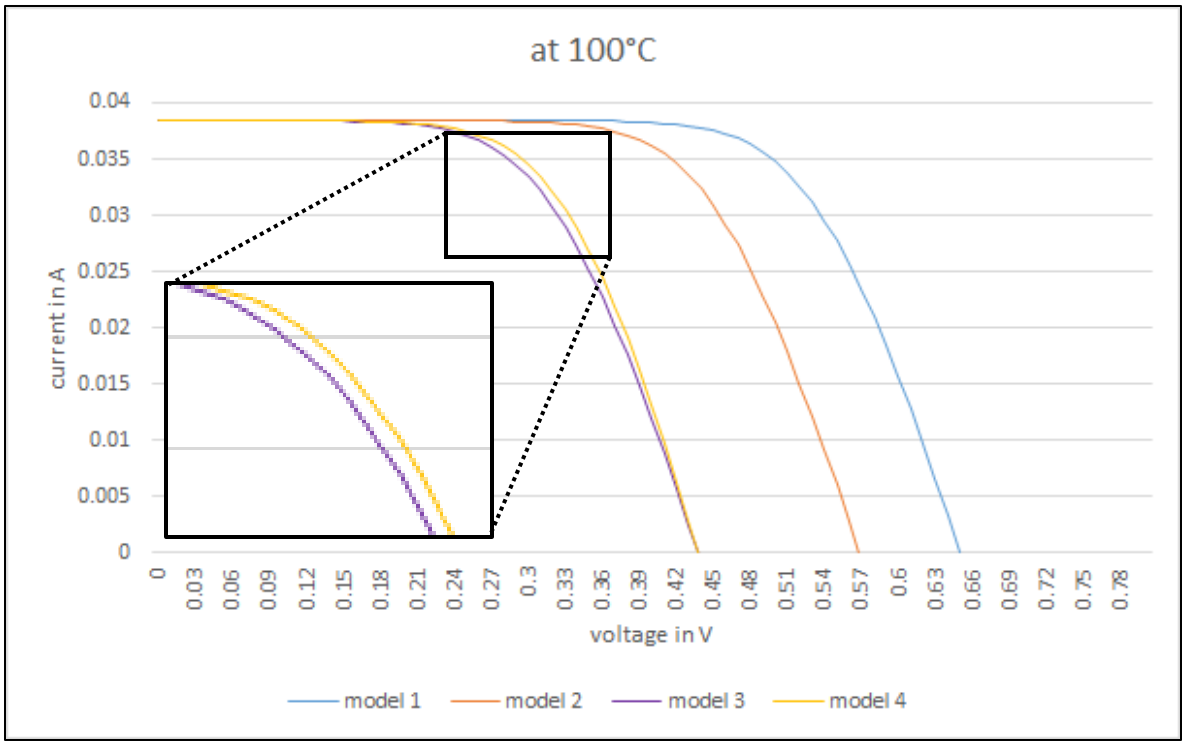

Figure 6-1 Simulation results of the four models at 100°C

circuit voltage perfectly. Furthermore, they reproduce I_m and V_m at STC more accurately, with a deviation of only around 0.4% for each parameter. Model 3 and 4 only differ in the shape of the I-V curve, as seen in Figure 6-1. Model 3 has a slightly flatter I-V curve than model 4. This is due to a difference in the series resistance, which influences this part of the curve greatly. Model 3 uses an intrinsic resistor model to simulate the series resistance, which can only process parameters given in the OrCAD schematic. Thus it calculates the series resistance at STC. Whereas model 4, which uses a g-device to simulate R_s, is able to calculate the resistance at 100°C. At this temperature the series resistance is slightly less than at STC, which results is a more round I-V curve. This leads to a higher fill factor at 50°C and 100°C. Considering these results it was found, that model 4 shows the most promising results. It will therefore be used in the proposed model and the next verification step can be approached.

6.1.2 Results for changes in irradiance

In this test, the proposed model is evaluated under different irradiance conditions where the module temperature is kept constant at 25°C. The module temperature is determined according to the NOCT theorem, i.e. equation 2-3, and is thus dependent on the ambient temperature and the irradiance. Therefore was it necessary to adjust the simulation temperature, which simulates the ambient temperature, with every change in irradiance to achieve the required module temperature. The model was evaluated at four different irradiances, i.e. 1000, 750, 500 and 250 W/m^2. The simulation temperature was set to -6.25, 1.5625, 9.375 and 17.1875°C, respectively, to reach the required module temperature of 25°C. The evaluation is performed with nominal data from Kyocera KD140SX-UFBS solar module. This module is intended to be used for the validation as well. It´s nominal electrical parameters are (70):

- I_{sc} = 8.68A
- V_{oc} = 22.1V
- I_m = 7.91A
- V_m = 17.7V
- NOCT = 45
- α_I = 5.2mA/°C
- α_V = -79.6mV/°C
- N_s = 18
- N_p = 2

	1000 W/m²		750 W/m²		500 W/m²		250 W/m²	
	value	Δ%	value	Δ%	value	Δ%	value	Δ%
I_{sc}	8.68	0.00	6.51	-25.00	4.34	-50.00	2.17	-75.00
V_{oc}	22.10	0.00	21.97	-0.59	21.78	-1.45	21.46	-2.90
I_m	8.36	5.69	6.31	-20.23	4.22	-46.65	2.12	-73.20
V_m	16.80	-5.08	17.50	-1.13	18.20	2.82	18.80	6.21
FF	0.7322	0.31	0.7721	5.78	0.8125	11.32	0.8559	17.26

Table 6-2 Key simulation results for different irradiances with constant R_s
Showing data extracted from PSPICE and their percentage changes with respect to the nominal values at STC.

thus the nominal fill factor is FF = 0.7299. In Table 6-2 the key simulation results, extracted from PSPICE, are listed. In this first step, the series resistance was kept constant at $R_s = 0.452\Omega$. From the table above it is apparent, that the short-circuit current is linearly proportional to the irradiance. For a decrease in irradiance of 25%, I_{sc} decreases by 25% as well. It is further visible, that the open-circuit voltage is logarithmically decreased. The current at the maximum power point decreases as well linearly proportional to the irradiance. However, an increase in V_m visible, due to the series resistance, which is artificially kept low. Hence, the fill factor is increasing for decreasing irradiance.

The same simulations are now executed for a non-constant series resistance. The results are shown in Table 6-3.

	1000 W/m²		750 W/m²		500 W/m²		250 W/m²	
	value	Δ%	value	Δ%	value	Δ%	value	Δ%
I_{sc}	8.68	0.00	6.51	-25.00	4.34	-50.00	2.17	-75.00
V_{oc}	22.10	0.00	21.97	-0.59	21.78	-1.45	21.46	-2.90
I_m	8.36	5.69	6.29	-20.48	4.18	-47.16	2.09	-73.58
V_m	16.80	-5.08	16.60	-6.21	16.50	-6.78	16.20	-8.47
FF	0.7322	0.31	0.7300	0.02	0.7296	-0.03	0.7271	-0.39

Table 6-3 Key simulation results for different irradiances with variable R_s
Showing data extracted from PSPICE and their percentage changes with respect to the nominal values at STC.

The short-circuit current, open-circuit voltage and current at the maximum power point exhibit the same behaviour as in the simulation with fixed series resistance. However, the voltage at the maximum power point shows a decrease with decreasing irradiance at a rate comparable to the decrease of V_{oc}. This results in a relatively stable fill factor. Since all other simulation parameters are the same as in the previous test it can be concluded, that the series resistance is responsible for this behaviour. If the fill factors at the same irradiance levels are compared it is visible that FF is decreasing significantly which is an indication for an increased series resistance. In Figure 6-2 a comparison between the simulation results when the series resistance is kept constant and when it is calculated, as proposed in this report, is shown. It is visible that the curve in the second case is dampened. This is the result of a higher series resistance, which considerably decreases the fill factor, from 0.8559 to 0.7271, as expected from the theory.

The above results show the forecasted behaviour and it was therefore concluded, that this step of the verification process is successfully completed. The results show the expected changes in I_{sc}, V_{oc} and FF. Therefore the next verification step can be approached.

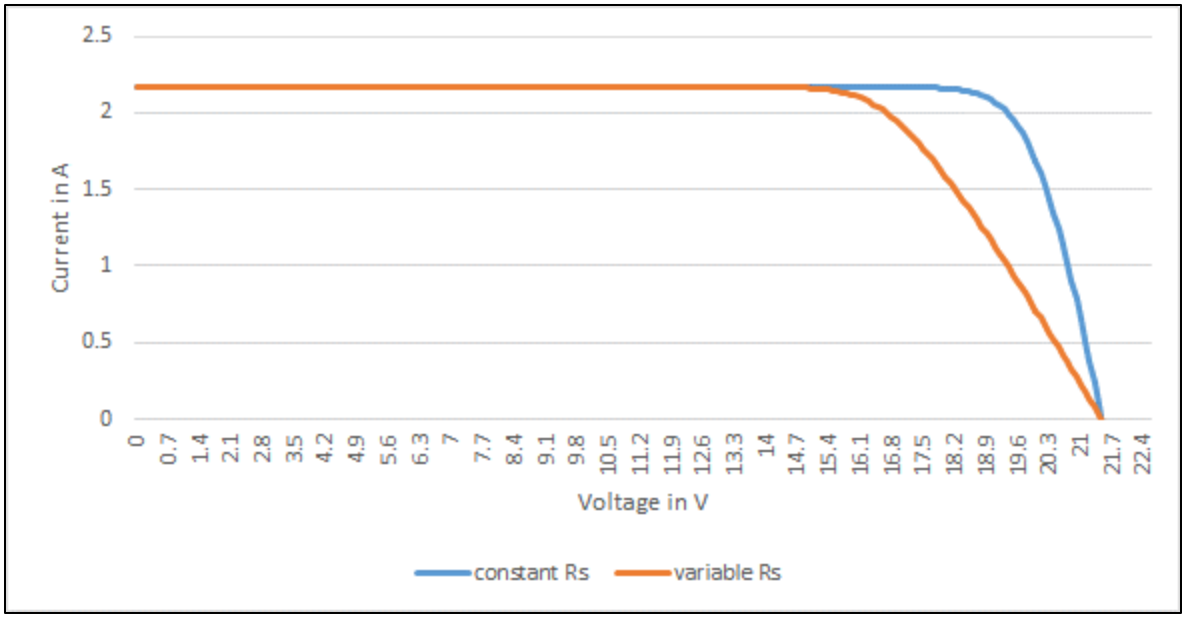

Figure 6-2 Simulation results at 250 W/m^2 and 25°C with variable and constant R_s

6.1.3 Results for changes in ambient temperature

The first phase of this test was executed with an irradiance value of 1000W/m^2 and the series resistance set to a constant value, i.e. $R_s = 0.452\Omega$, the series resistance at STC. Under those conditions the simulation was repeated for ambient temperatures of 0°C, 10°C, 20°C and 30°C. The key simulation results, extracted from PSPICE A/D, are displayed in Table 6-4. From the key simulation results of this test it can be seen that, just as expected, the short-circuit current slightly increases whereas the open-circuit voltage decreases. The voltage and current at the maximum power point do decrease and increase at about the same rate as V_{oc} and I_{sc}, respectively, as well. However, at 30°C a sudden drop in I_m and a less than expected decrease in V_m is observed. Further investigation into this phenomena revealed that the current at the maximum power point periodically decreases instead of the expected increase. At the same time does the voltage at the maximum power point keeps constant when the current drops. This behaviour can be seen in the data in Appendix E.4. Although this observations are unexpected and not aligned with the theory, the behaviour of the maximum power and the fill factor is not affected. In general, the higher decrease in the voltages compared to the increases in the currents results in a decreased fill factor, even though the current and voltage at the maximum

	0°C	10°C	20°C	30°C
I_{sc}	8.71	8.76	8.82	8.87
V_{oc}	21.60	20.81	20.02	19.23
I_m	8.42	8.43	8.45	8.40
V_m	16.20	15.40	14.60	13.90
FF	0.7247	0.7117	0.6990	0.6848

Table 6-4 Key simulation results for different ambient temperatures and constant R_s

power point oscillates. This effect could be the result of the equations governing the model and further investigations are necessary to determine their source. However, considering the above results and keeping in mind that this model is intended to simulate the overall behaviour of a photovoltaic module, rather than acting as a maximum power point tracker, it was concluded that the behaviour can be accepted and that the test can progress to its second phase.

In the second part of this test, the series resistance is not kept constant anymore. It will be calculated for the current module temperature according to equation 3-6. Table 6-5 displays the key simulation results for the second part of the test, together with their percentage change

	0°C		10°C		20°C		30°C	
	value	Δ%	value	Δ%	value	Δ%	value	Δ%
I_{sc}	8.71	0.00	8.76	0.00	8.82	0.00	8.87	0.00
V_{oc}	21.60	0.00	20.81	0.00	20.02	0.00	19.23	0.00
I_m	8.40	-0.24	8.43	0.00	8.44	-0.12	8.46	0.71
V_m	16.30	0.62	15.60	1.30	14.90	2.05	14.20	2.16
FF	0.7274	0.38	0.7210	1.30	0.7125	1.93	0.7046	2.89

Table 6-5 Key simulation results for different ambient temperatures and variable R_s Showing data extracted from PSPICE and their percentage changes with respect to the key simulation results with constant R_s (Table 6-4).

with respect to the first part of this test. From the table above it is clear that the series resistance does not influence the short-circuit current nor the open-circuit voltage. Only the current and voltage at the maximum power point are influenced by R_s. Consequently, the fill factor is influenced as well. Since the fill factor is increasing, it can be concluded that the series resistance decreases with increasing temperature. That is supported by the theory outlined in chapter 2.3.3. The increased percentage change in FF is larger for higher temperatures, which supports the theory that R_s is decreasing with increasing temperature, as well.

Figure 6-3 shows a comparison between the simulation results of the proposed model when the series resistance is constant at $R_s = 0.452\Omega$ and when it is variable, i.e. calculated according to equation 3-6. Both simulations were conducted at an ambient temperature of 30°C and an irradiance of 1000 W/m^2. It is clearly visible that the I-V curve where R_s is constant is flatter, which results in the lower fill factor. The markings on the curve are the maximum power points. In the zoomed section of the figure it is clearly visible that the maximum power point of the blue curve has a larger voltage and a slightly increased current, as a result of the lower series resistance of the photovoltaic module at this ambient temperature.

Considering the results above it was concluded that the proposed model represents changes in the ambient temperature sufficiently. All verification steps were now completed successfully. The model behaves to changes in input parameters as expected and the research can progress to the following step, the model validation.

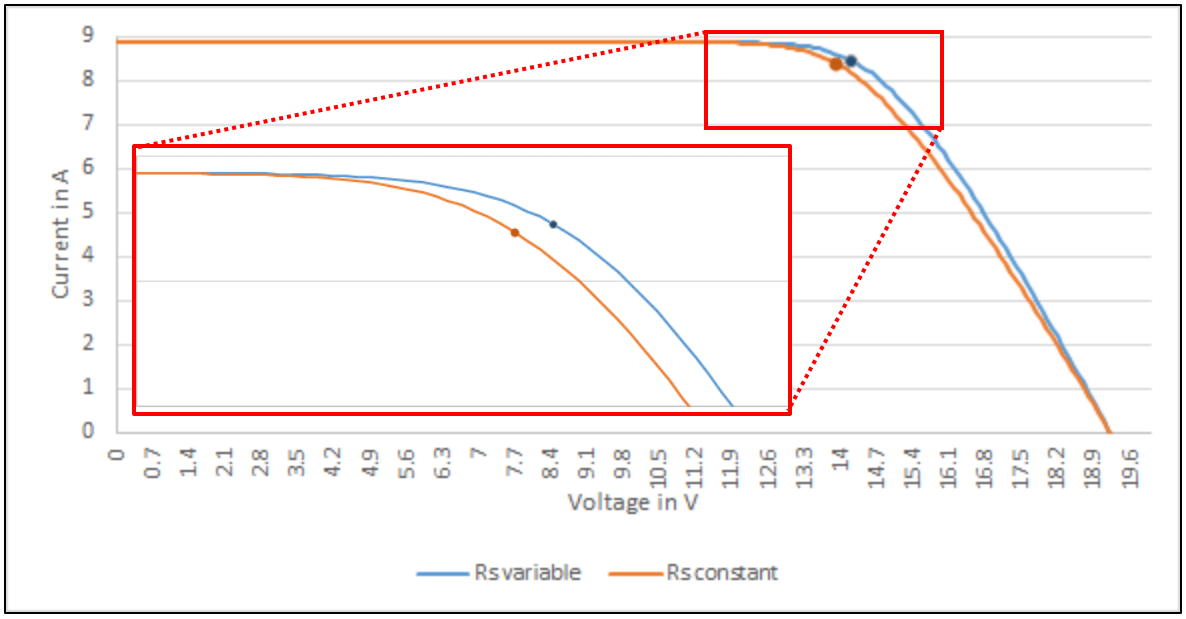

Figure 6-3 Simulation results of the proposed model at 30°C ambient temperature and two different R_s configurations

6.2 Validation results

The validation of the proposed model is performed with the Kyocera KD140SX-UFBS photovoltaic module. Its electrical characteristics are shown in chapter 6.1.2 above. From the obtained data four sets of measurements were chosen to validate the proposed model. These data sets are:

Dataset 1:

- taken at 13:00 on November 4th, 2014
- G = 947 W/m²
- T_{mod} = 57.22 °C
- sunny

Dataset 2:

- taken at 14:00 on November 4th, 2014
- G = 667 W/m²
- T_{mod} = 52.77 °C
- Cirrus clouds were in front of the sun

Dataset 3:

- taken at 14:30 on November 4th, 2014
- G = 423 W/m²
- T_{mod} = 49.44 °C
- Cirrus clouds were in front of the sun

Dataset 4:

- taken at 15:20 on November 4th, 2014
- G = 100 W/m^2
- T_{mod} = 35.00 ºC
- Cirrus clouds were in front of the sun
- The panel was shaded by an adjacent building

All measurements were taken on the grounds of UFMG at latitude -19.8693 and longitude -43.96165. The panel was facing north-east (azimuth of 27 degree) at an angle of 33 degrees.

The datasets, with around 100 measurement points, were imported into MatLab (68) and using its curve fitting tool a double exponential curve was fitted through the points. Due to a large amount of measurement points close to the open-circuit conditions, the double exponential curve exhibited a rather poor fit. Therefore, it was decided to exclude those points from the fitting, to achieve more accuracy at the knee of the curve. The excluded points were then fitted with a linear curve, which can be expected close to the open-circuit conditions. To perform the error analysis both curves were combined. This can be seen in Figure 6-4, where the orange

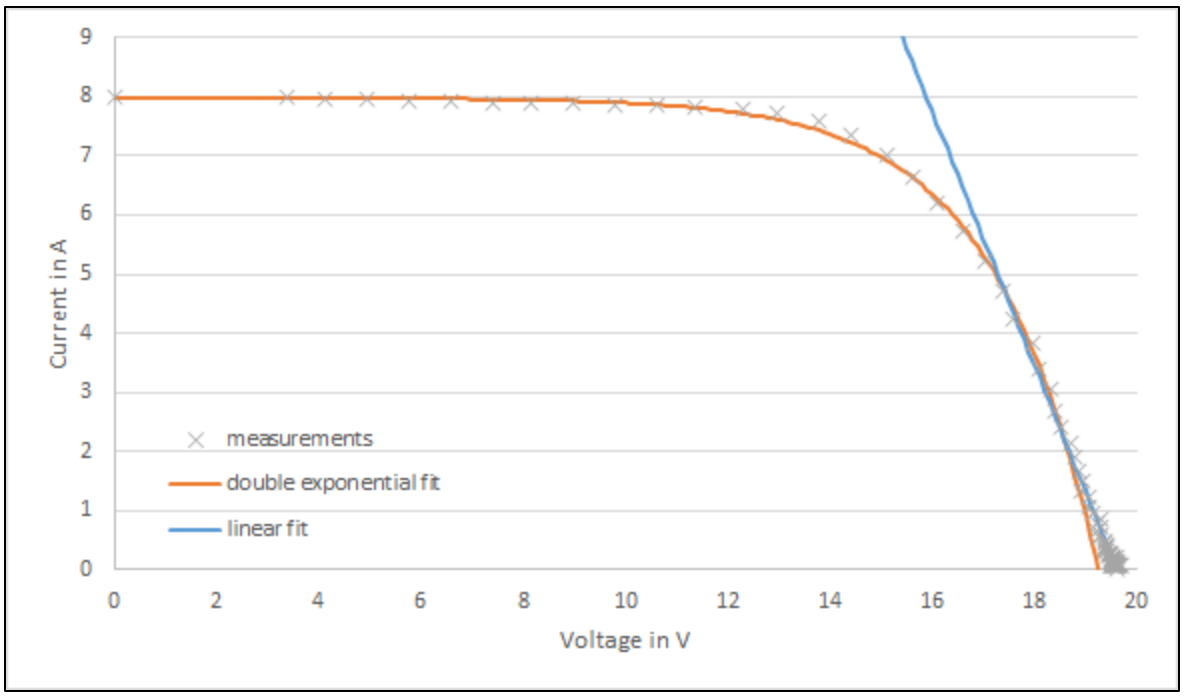

Figure 6-4 Dataset 1 with exponential and linear fit

represents the double exponential fit where all measurement points beyond 18.5 V were excluded. The blue curve is fitted through all points above 18.5 V. It can be seen, that the exponential fit does not represent the measurements close to the open-circuit condition very well, which results in a root mean square of 1.10 A, whereas the linear fit only represents the measurements at those conditions. Therefore a combination of both fitted curves will yield the most accurate approximation, with a root mean square error of only 0.10 A, to the measured

data. This curve together with the simulations results of the proposed model and the model proposed by Castaner (64) is shown in the upper graph of Figure 6-5. Both models yield good simulation results around the short-circuit point, whereas the simulation at the knee of the curve differs greatly from the fitted curve. The proposed model performs well at open-circuit conditions as well, whereas Castaner´s model performs better between the knee of the graph,

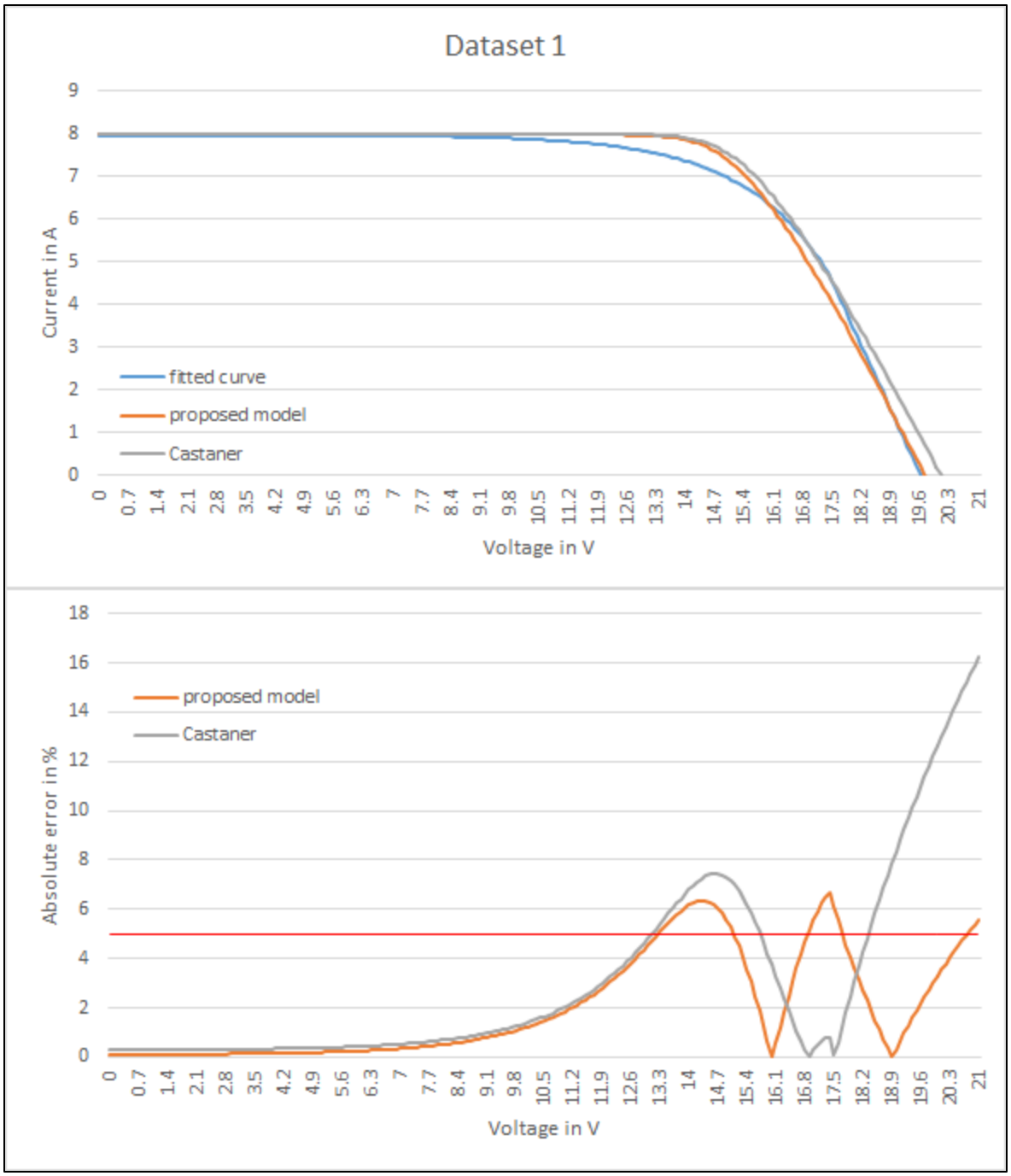

Figure 6-5 Dataset 1 fitted I-V curve and simulation results (up) and absolute error (down)

	Dataset 1	Dataset 2	Dataset 3	Dataset 4
$RSME_{fit}$	0.10	0.07	0.06	0.07
$RSME_c$	0.40	0.60	0.70	0.92
$RSME_p$	0.23	0.30	0.20	0.69
$MADP_c$	3.05	10.06	13.66	46.11
$MADP_p$	2.09	5.34	3.10	15.09
E_c	0.98	0.91	0.75	-0.09
E_p	0.99	0.98	0.98	0.39

Table 6-6 Errors and model efficiency values for the proposed and Castaner´s model

and the open-circuit condition. All of this can be seen in the lower graph in Figure 6-5 as well, where the absolute error of the proposed model (orange) and Castaner´s model (grey) towards the fitted curve is displayed. The red line represents a 5% error. Which is exceeded around the knee of the I-V curve however, the mean absolute deviation percent (MADP) is below that line at 2.09%. It seems that the proposed model mostly exhibits lower errors than Castaner´s model except between 16.5 V and 18.2 V. This is supported by its lower root mean square error (RSME) of $RSME_p$ = 0.23 A, compared to Castaner´s model with an $RSME_c$ = 0.40 A. Additionally, does the proposed model have a lower MADP, i.e. a lower average error, and therefore it approximates the I-V curve more closely. Thus the proposed model performs better on dataset 1 than Castaner´s model. This can as well be seen in the higher Nash-Sutcliffe model efficiency coefficient (E) of E_p = 0.99 compared to E_c = 0.98. A comparison of the root mean square errors and the Nash-Sutcliffe model efficiency coefficients is displayed in Table 6-6. In the table it can be seen, that the fitted curves for each dataset only exhibit marginal root mean square errors. Hence, the validation of the model can be performed with the fitted curve. Further it is visible that the proposed model generally has a lower RSME and a higher Nash-Sutcliffe coefficient than Castaner´s model. Thus, the model proposed in this report is outperforming Castaner´s model, with Nash-Sutcliffe coefficients above 0.95. Only at the fourth dataset was the performance of both models rather poor. That suggests, that either the models are not suited for predicting photovoltaic cell output at low irradiances or that the measurement equipment is not suited to perform low irradiance measurements. In Figure 6-5 is it already visible, that absolute error at the knee of the I-V curve is getting much larger. The same behaviour can be

	Dataset 1				
	measured	proposed model		Castaner	
		value	error (%)	value	error (%)
V_{oc}	19.63	19.72	0.42	20.11	2.36
I_{sc}	7.98	7.98	0.10	8.00	0.29
V_m	14.67	14.60	-0.51	14.80	0.85
I_m	7.25	7.65	5.27	7.67	5.44
P_m	106.40	111.75	4.79	113.49	6.25

Table 6-7 Measurements and simulation results of key parameters together with their respective errors

	measured	proposed model		Castaner	
		value	error (%)	value	error (%)
Dataset 2					
V_{oc}	19.57	19.69	0.61	20.23	3.24
I_{sc}	5.65	5.89	4.01	5.93	4.79
V_m	15.40	14.60	-5.46	15.80	2.55
I_m	5.16	5.63	8.37	5.72	9.72
P_m	79.48	82.24	3.36	90.33	12.02
Dataset 3					
V_{oc}	19.26	19.73	2.37	20.48	5.93
I_{sc}	3.71	3.73	0.54	3.80	2.46
V_m	15.10	14.60	-3.46	17.00	11.15
I_m	3.42	3.57	4.29	3.67	6.88
P_m	51.66	52.18	0.99	62.44	17.26
Dataset 4					
V_{oc}	18.76	20.20	7.13	21.58	13.02
I_{sc}	0.83	0.87	4.39	0.92	9.26
V_m	15.37	15.00	-2.46	19.40	20.78
I_m	0.77	0.84	8.29	0.90	13.98
P_m	11.84	12.60	6.04	17.38	31.85

Table 6-7 continued

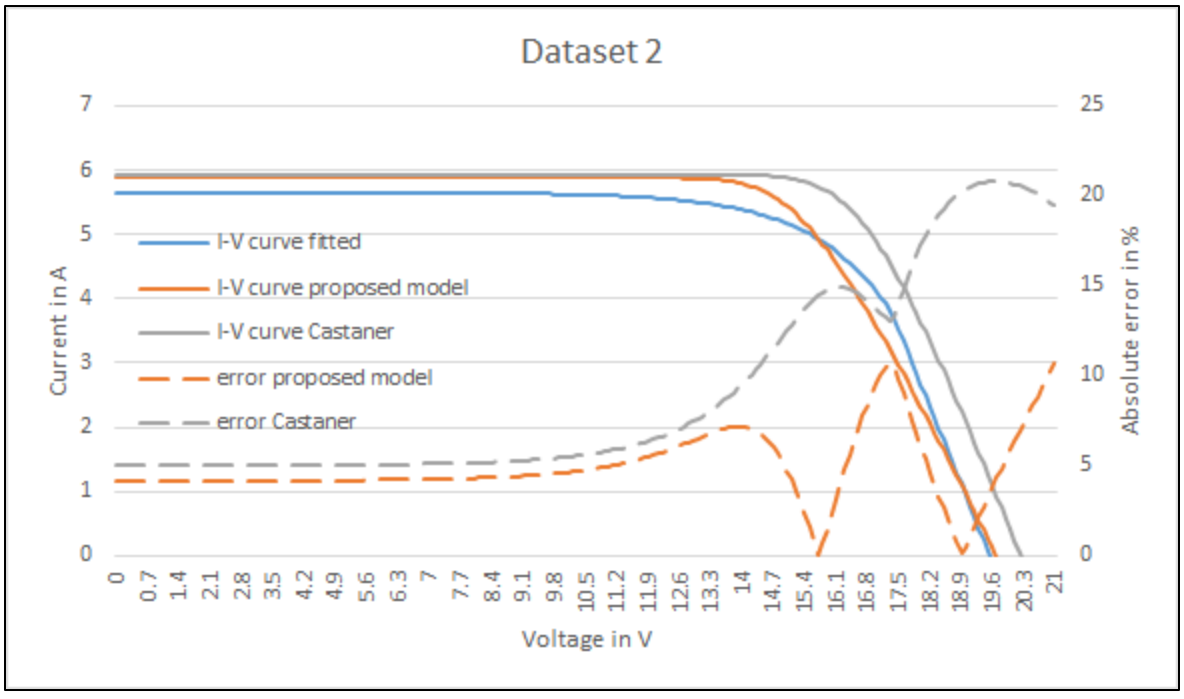

Figure 6-6 I-V curves and error plots of the fitted curve and the simulations for Dataset 2

seen in Figure 6-6 as well, where the error around the knee of the I-V curve is generally large. However, even though the error around the maximum power point seems to be large, the maximum power output of the panel is predicted with less than 5% error. Table 6-7 displays the measured and simulated key parameters, together with their simulation errors. The voltage at the maximum power point is generally lower in the simulations, whereas the current at the maximum power point is higher than the measured value. This leads to an overall acceptable prediction of the maximum power output. Only the last dataset shows errors larger than 5% for the open-circuit voltage, the maximum power and the MADP. This behaviour is largely attributed to the low Nash-Sutcliffe efficiency coefficient. This means that the model does not perform well in the simulation of dataset 4. In Table 6-7 it is as well visible, that Castaner´s model performs even worse than the proposed model.

As a last step the effects of errors in the input parameters have to be analysed. The Kyocera KD140SX-UFBS photovoltaic module has a tolerance for the module power output of +7% / -0%. Due to lack of tolerance ratings for the voltages and currents it is assumed that the power tolerance is equally shared between the voltage and current at the maximum power point. It is further assumed that the open-circuit voltage and the short-circuit current exhibit the same tolerances. Therefore, the tolerances for V_{oc}, I_{sc}, I_m and V_m are +3.5% / -0%. Since the negative error in the input parameters is 0% the simulation only has to be performed at the positive maximum error. The errors, given in percent, in the output compared to simulation run at nominal input parameters are shown in Table 6-8. It is apparent, that the errors are constant

	Dataset 1	Dataset 2	Dataset 3	Dataset 4
V_{oc}	+3.92	+3.94	+3.92	+3.83
I_{sc}	+3.44	+3.44	+3.45	+3.48
V_m	+4.11	+4.11	+4.11	+4.00
I_m	+3.40	+3.40	+3.41	+3.43

Table 6-8 Output errors (in %) of the model for maximum error of the input parameters

over all datasets, hence they are independent of the irradiance and ambient temperature. Furthermore, it is visible that the output errors for the short-circuit current and the current at the maximum power point are slightly lower than the 3.5% in the input parameters. On the other hand, the errors for the open-circuit voltage and the voltage at the maximum power point are higher, ranging around 3.9% and 4.1%, respectively. Only for the fourth dataset are the errors dissimilar to the other values, however only by a small margin. Overall it can be concluded, that the proposed model will transmit errors in the input parameter through the model, which results in errors of approximate the same magnitude in the model output. The slightly higher errors magnitude in the output voltages can be attributed to the behaviour of the model. It is however acceptable, since the proposed model only yields an approximation.

Considering all the results above it is concluded that the proposed model is validated. It performs within appropriate error margins of less than 5% and efficiently simulates the I-V

curve of the photovoltaic panel at different irradiance and temperature levels. The model only performs weak at low irradiance levels, with errors between 5 and 10%. Overall, the proposed model outperforms Castaner´s model, for all four datasets.

CHAPTER 7

CONCLUSION

This section will summarize the findings of Chapter 6 and answer the research questions, as presented in Chapter 4.

Can the proposed model accurately simulate the performance of photovoltaic cells/modules using only electrical parameters as inputs?

From the results in the previous chapter, we find that the proposed model can precisely simulate the I-V curve of a solar panel, for high and medium irradiance values, with a Nash-Sutcliffe coefficients of more than 0.95. It as well accurately predicts the open-circuit voltage, short-circuit current and maximum power output of the panel, with errors between 0.10% and 4.80%. This is within the acceptance criteria of no more than 5% deviation.

The MADP is within the acceptance criteria for dataset 1 and 3. For dataset 2 it is slightly above the 5% boundary. This is believed to be due to significantly lower short-circuit current in the measured data than it would be expected for this irradiance. For datasets 1 and 3 the proposed model was within 1% of the measured V_{oc} and the subsequent linear part of the I-V curve until it´s knee. Therefore it is concluded, that the measurements for dataset 2 are faulty. However, if the more accurate Monte Carlo Analysis was to be used, the MADP for dataset 2 might very well be below 5%. Another explanation for the large error in dataset 2 is that the irradiation sensor was shielded by a cloud or light smoke, which was not detected when the measurements were performed. Which is as well supported by the large offset in the short-circuit current as seen in figure Figure 6-6.

For the fourth dataset the performance of the model was well below the expectations. The simulated results varied from the measurements by up to 7.15%. However, the maximum power for this dataset was only 11.86 W, due to the low irradiance of 100 W/m^2. This explains the high error of 6.04%, whereas the absolute error is only 0.76 W and therefore less than the absolute errors in simulating dataset 1 and 2. Hence, the proposed model still performed very well on dataset 4.

The current and voltage values at the maximum power point would usually be significantly lower and higher, respectively, than the measured values. Those deviations in the current and voltage are not ideal, but the most important parameter, namely the maximum output power, is only slightly affected by that. After all, the model was conceived and developed to predict the output of a photovoltaic cell or module. It is not intended as a maximum power point tracker and hence the inaccuracies at the maximum power point are acceptable. It is further possible that rather poor performance around the knee of the I-V curve, thus around the maximum power point, is attributed to the shunt resistance. R_{sh} degrades the fill factor, by "flattening" the knee of the I-V curve (71). In the proposed model, this effect is assumed marginal and was therefore neglected.

In summary we can conclude, that the proposed model can accurately simulate the performance of a photovoltaic module using only electrical input parameters, as long as the irradiance is sufficiently high. Unfortunately were we not able to evaluate the performance for other solar panels, due to bureaucratic hurdles and delivery delays. However, for other multi-crystal photovoltaic modules similar results are expected.

Can the accuracy, with regards to parasitic temperature effects, of the proposed model be improved, by deploying analog behavioural modelling in addition to the intrinsic diode and resistor models?

The results in chapter 6.1.1 show that analog behavioural modelling greatly improves the expected accuracy of the proposed model. When using only intrinsic diode and resistor models it was not even possible to reproduce the I-V curve correctly at STC. Analog behavioural model (ABM) improved the accuracy to an error of less than 0.4% at STC. Therefore we can assume that ABM is performing much better at higher temperatures as well. Furthermore, the intrinsic resistor model was not able to simulate the changes in the series resistance as described in chapter 2.3.3.3, however an ABM device was able to simulate those effects.

Therefore, we can conclude, that by deploying analog behavioural models the accuracy of the proposed model can be improved with respect to parasitic temperature effects.

How does the proposed model perform compared to the behavioural solar cell model described by Castaner and Silvestre (64) in simulating the temperature effects on the series resistance?

This research question was answered when performing research, to answer the previous question. Since Castaner and Silvestre are using an intrinsic resistor model to simulate the series resistance, they cannot model the temperature effects on the series resistance. The intrinsic resistor model does only accept constants as inputs, and therefore only the electrical characteristics at STC can be used to calculate the resistance. The proposed model on the other hand uses a g-device to simulate the series resistance. In it, electrical characteristics calculated by other ABM devices can be used to determine the resistance. Since those characteristics are dependent on the module temperature and the irradiance, the resistance is calculated, while taking temperature effects into account.

During the validation of the proposed model, its performance was compared to Castaner´s model. During those comparisons we found, that the proposed model generally outperforms Castaner´s model. It exhibits lower errors in the key parameter simulations and it represents the I-V curve more efficiently and accurately, as the Nash-Sutcliffe coefficients show.

Does the model simulate the influences of parasitic effects on the photovoltaic cell/module output accurately?

From the results in chapters 6.1.2 and 6.1.3 we find that the model simulates the influences well. The model behaves as expected from the theory presented in chapter 2.3.3. For a decrease in irradiance the short-circuit current is decreased linearly and the open-circuit voltage logarithmically. Furthermore, the series resistance is increased for lower irradiance values. The effects of parasitic temperature are as well simulated correctly. With an increase in module temperature, the open-circuit voltage decreased, whereas the short-circuit current increases. The series resistance decreases at the same time, which improves the fill factor of the solar module.

These results suggest that the proposed model simulated the influences of parasitic effects accurately. However, exact measurements with photovoltaic cells or modules could not be conducted under laboratory conditions, due to bureaucratic hurdles and delivery delays for the necessary equipment. Therefore, this sub-question cannot be answered fully at this point in time, although the results collected until now look very promising.

CHAPTER 8

RECOMMENDATIONS

This chapter discusses possibilities to enhance the research results and potential improvements for the proposed model.

In Chapter 6.1.3 an oscillating behaviour of the current at the maximum power point was observed. It was determined, that this oscillation is acceptable, although not accurate, due to the fact, that the behaviour of the maximum power and the fill factor was not influenced by this anomaly. However, to improve the accuracy of the model an analysis of this effect is recommended. This analysis should be designed to determine the origin of the oscillation of the current at the maximum power point and subsequently it can be eliminated.

To enhance the research results it is desirable to perform measurements on multiple photovoltaic cells and modules under monitored laboratory conditions. That way all parasitic effects can be controlled and interferences can be ruled out. Laboratory experiments are also necessary to answer the last research sub-question with certainty. The attempt to answer that question, presented in this report, is only based on theoretical analysis and no measured data was available to support the assumptions.

Furthermore, it can be of great value to validate the proposed model on other multi-crystalline photovoltaic modules as well. Unfortunately, at the time of the test only one photovoltaic module was available. The results from other modules might give more insight into the possible shortcomings of the model and could be used to improve it. It would be interesting as well to evaluate the prediction performance for the proposed model for other types of photovoltaic cells or modules, e.g. organic or multi-junction.

As discussed in Chapter 7, the shunt resistance might have more influence on the simulation results than expected. An adaption of the model to accurately simulate the effects of the shunt resistance on the photovoltaic module could improve the overall accuracy of the model greatly. However, it would be important to still maintain the condition of using only electrical parameters as inputs. After all, that is the main advantage of the proposed model over other models.

Additionally could it be of great value to investigate the theory for the series resistance as indicated in Chapter 2.3.3.3 further. The photovoltaic and semiconductor community interpret series resistance differently, while calling it both the same. Further research into this anomalies could improve the understanding of it and it will clarify its possible connection. A proper understanding of the various theories could as well enhance already existing photovoltaic models and therefore increase the accuracy of photovoltaic modelling.

REFERENCES

1. Skarbek A, Jotzo F, Jones A, Denis A, Kelly R, Ferraro S, et al. pathways to deep decarbonization. 2014.
2. United Nations Framework Convention on Climate Change, Conference of the Parties. Report of the Conference of the Parties on its fifteenth session, held in Copenhagen from 7 to 19 December 2009. Addendum. Part Two: Action taken by the Conference of the Parties at its fifteenth session. Geneva (Switzerland): 2010 Contract No.: FCCC/CP/2009/11/Add.1.
3. Barrucho L. Brazil drought stokes worries over energy shortages. BBC Brasil. 2013.
4. Rother L. Energy Crisis in Brazil is Bringing Dimmer Lights and Altered Lives. The New York Times. 2001 June 6.
5. Skoplaki E, Palyvos J. On the temperature dependence of photovoltaic module electrical performance: A review of efficiency/power correlations. Solar energy. 2009;83(5):614-24.
6. Fan JCC. Theoretical temperature dependence of solar cell parameters. Solar Cells. 1986;17(2–3):309-15.
7. Singh P, Singh SN, Lal M, Husain M. Temperature dependence of I–V characteristics and performance parameters of silicon solar cell. Solar Energy Materials and Solar Cells. 2008;92(12):1611-6.
8. Green MA. General temperature dependence of solar cell performance and implications for device modelling. Progress in Photovoltaics: Research and Applications. 2003;11(5):333-40.
9. United Nations - Departement of Economy and Social Affairs - Population Division. World Population Prospects: The 2012 Revision online1980 - 2010 [23/09/2014]. Available from: http://esa.un.org/wpp/Excel-Data/population.htm.
10. Frei C, Whitney R, Schiffer H-W, Rose K, Rieser DA, Al-Qahtani A, et al. World Energy Scenarios: Composing energy futures to 2050. London, UK: World Energy Council, 2013.
11. Øvergaard S. Issue paper: definition of primary and secondary energy. Oslo: 2008.
12. United States Energy Information Administration. International Energy Statistics - Total Primary Energy Production online1980 - 2010 [23/09/2014]. Available from: http://www.eia.gov/cfapps/ipdbproject/iedindex3.cfm?tid=44&pid=44&aid=1&cid=ww,&syid=1980&eyid=2010&unit=QBTU.
13. United Nations Framework Convention on Climate Change. Kyoto Protocol to the United Nations Framework COnvention on CLimate Change. 1998.
14. United Nations Framework Convention on Climate Change. Doha Amendment to the Kyoto Protocol. New York, NY, United States of America: 2012 Contract No.: C.N.718.2012.TREATIES-XXVII.7.c.
15. Lima Call for Climate Action Puts World on Track to Paris 2015 [press release]. [online]: UNFCCC Press Office2014.
16. Green Climate Fund. GCF - Background [online]2014 [19/12/2014]. Available from: http://www.gcfund.org/about/the-fund.html.
17. United States Environmental Protection Agency. Global Greenhouse Gas Emissions Data 2004 [24/09/2014]. Available from: http://www.epa.gov/climatechange/ghgemissions/global.html.
18. Miller O. Geothermal Energy: Modern Uses and Environmental Issues. Indiana University, 2010.

19. Salmon JP, Meurice J, Wobus N, Stern F, Duaime M. Guidebook to Geothermal Power Finance. In: Laboratory NRE, editor. Cole Boulevard - CO, USA2011.
20. Organisation for Economic Co-operation and Development, International Energy Agency. World Energy Outlook 2013. 2013.
21. United States Energy Information Administration. International Energy Statistics - Per Capita Carbon Dioxide Emissions from the Consumption of Energy online2011 [25/09/2014]. Available from: http://www.eia.gov/cfapps/ipdbproject/iedindex3.cfm?tid=90&pid=45&aid=8&cid=regions&syid=2007&eyid=2011&unit=MMTCD.
22. Empresta de Pesquisa Energética. Balanço Energético Nacional 2014: Ano base 2013 - Brazilian Energy Balance 2014 Year 2013. Rio de Janeiro: 2014. Table 1.2.b, Primary Energy Production, p. 21.
23. Empresta de Pesquisa Energética. Balanço Energético Nacional 2014: Ano base 2013 - Brazilian Energy Balance 2014 Year 2013. Rio de Janeiro: 2014. Chart 1.1, Domestic Electricity Supply by source, p. 16.
24. Rosenzweig C, Iglesias A, Yang X, Epstein PR, Chivian E. Climate change and extreme weather events; implications for food production, plant diseases, and pests. Global change & human health. 2001;2(2):90-104.
25. Pereira EB, Martins FR, de Abreu SL, Rüther R. Atlas brasileiro de energia solar. São Jose de Campos: INPE; 2006. Figure, Radiação Solar no Plano Inclinado Média anual, p. 38.
26. Empresta de Pesquisa Energética. Análise da Inserção da Geração Solar na Matriz Elétrica Brasileira. Rio de Janeiro: Ministerio de Minas e Energia,, 2012.
27. Wenham SR, Green MA, Watt ME, Corkish R. Applied Photovoltaics: Earthscan; 2007.
28. Spanggaard H, Krebs FC. A brief history of the development of organic and polymeric photovoltaics. Solar Energy Materials and Solar Cells. 2004;83(2–3):125-46.
29. Chapin D, Fuller C, Pearson G. A new silicon p-n junction photocell for converting solar radiation into electrical power. Journal of Applied Physics. 1954;25(5):676-7.
30. Morales-Acevedo A, Casados-Cruz G. Forecasting the Development of Different Solar Cell Technologies. International Journal of Photoenergy. 2013;2013(Article ID 202747):5.
31. Robson G. Electron shell 014 Silicon - no label [Figure]. wikipedia.org; 2012. Available from: http://nn.wikipedia.org/wiki/Halvleiar#mediaviewer/File:Electron_shell_014_Silicon_-_no_label.svg.
32. Kininger F. Photovoltaic Systems Technology. Kassel: Universität Kassel, Institut für Rationelle Energiewandlung; 2003. Figure 3-1, Schematic drawing of a silicon solar cell, p. 32.
33. Kininger F. Photovoltaic Systems Technology. Kassel: Universität Kassel, Institut für Rationelle Energiewandlung; 2003.
34. Kininger F. Photovoltaic Systems Technology. Kassel: Universität Kassel, Institut für Rationelle Energiewandlung; 2003. Figure 3-4, Operating principle of a solar cell (schematic), p. 36.
35. Hersch P, Zweibel K. Basic photovoltaic principles and methods. Solar Energy Research Institute (SERI), 1982 SERI/SP-290-1448 Contract No.: SERI/SP-290-1448.
36. Fraunhofer-Institut für Solare Energiesysteme ISE. STC Measurements [Internet]. Fraunhofer-Institut für Solare Energiesysteme ISE; 2014 [cited 02/10/2014]. Available from: http://www.ise.fraunhofer.de/en/service-units/callab-pv-cells-callab-pv-modules/callab-pv-modules/stc-measurements.

37. Alonso García MC, Balenzategui JL. Estimation of photovoltaic module yearly temperature and performance based on Nominal Operation Cell Temperature calculations. Renewable Energy. 2004;29(12):1997-2010.
38. Castaner L, Silvestre S. Modelling photovoltaic systems using PSpice: John Wiley and Sons; 2002. Figure 3.4, I(V) plots of a solar cell under several irradiance values, p. 46.
39. Castaner L, Silvestre S. Modelling photovoltaic systems using PSpice: John Wiley and Sons; 2002. Figure 3.11, Effects of temperature, p. 61.
40. Castaner L, Silvestre S. Modelling photovoltaic systems using PSpice: John Wiley and Sons; 2002. Figure 3.7, Series resistance effects, p. 54.
41. Pierret RF. Semiconductor device fundamentals: Addison Wesley; 1996.
42. Nagel LW, Pederson DO. SPICE: Simulation program with integrated circuit emphasis. Berkeley, CA, United States of America: Electronics Research Laboratory, College of Engineering, University of California; 1973.
43. Nagel L, Rohrer R. Computer analysis of nonlinear circuits, excluding radiation (CANCER). Solid-State Circuits, IEEE Journal of. 1971;6(4):166-82.
44. Division CPS. OrCAD Capture - Fast, intuitive PCB schematic design solution. 2014.
45. Cadence PCB Systems Division. PSpice Reference Guide: Cadence PCB Systems Division,; 2000. Available from: http://www.seas.upenn.edu/~jan/spice/PSpice_ReferenceguideOrCAD.pdf.
46. Cadence Design Systems. OrCAD Capture CIS Lite (Version 16.6) [Computer Software]. Cadence Design Systems; 2014 [cited 18/09/2014]. Available from: http://www.orcad.com/resources/orcad-downloads.
47. Cadence PCB Systems Division. PSpice User Guide. Portland, OR, United States of America: Cadence Design Systems; 2000.
48. Weidong X, Dunford WG, Capel A, editors. A novel modeling method for photovoltaic cells. Power Electronics Specialists Conference, 2004 PESC 04 2004 IEEE 35th Annual; 2004 20-25 June 2004.
49. De Soto W, Klein SA, Beckman WA. Improvement and validation of a model for photovoltaic array performance. Solar Energy. 2006;80(1):78-88.
50. Merten J, Asensi JM, Voz C, Shah AV, Platz R, Andreu J. Improved equivalent circuit and analytical model for amorphous silicon solar cells and modules. Electron Devices, IEEE Transactions on. 1998;45(2):423-9.
51. Villalva MG, Gazoli JR, Filho ER. Comprehensive Approach to Modeling and Simulation of Photovoltaic Arrays. Power Electronics, IEEE Transactions on. 2009;24(5):1198-208.
52. Sera D, Teodorescu R, Rodriguez P, editors. PV panel model based on datasheet values. Industrial Electronics, 2007 ISIE 2007 IEEE International Symposium on; 2007 4-7 June 2007.
53. Koutroulis E, Kalaitzakis K, Tzitzilonis V, editors. Development of an FPGA-based System for Real-Time Simulation of Photovoltaic Modules. Rapid System Prototyping, 2006 Seventeenth IEEE International Workshop on; 2006 14-16 June 2006.
54. Ahmad GE, Hussein HMS, El-Ghetany HH. Theoretical analysis and experimental verification of PV modules. Renewable Energy. 2003;28(8):1159-68.
55. Yeong-Chan K, Tsorng-Juu L, Jiann-Fuh C. Novel maximum-power-point-tracking controller for photovoltaic energy conversion system. Industrial Electronics, IEEE Transactions on. 2001;48(3):594-601.
56. van Dyk EE, Meyer EL. Analysis of the effect of parasitic resistances on the performance of photovoltaic modules. Renewable Energy. 2004;29(3):333-44.
57. Ishaque K, Salam Z, Taheri H. Simple, fast and accurate two-diode model for photovoltaic modules. Solar Energy Materials and Solar Cells. 2011;95(2):586-94.

58. Gow JA, Manning CD. Development of a photovoltaic array model for use in power-electronics simulation studies. Electric Power Applications, IEE Proceedings -. 1999;146(2):193-200.
59. Chowdhury S, Taylor GA, Chowdhury SP, Saha AK, Song YH, editors. Modelling, simulation and performance analysis of a PV array in an embedded environment. Universities Power Engineering Conference, 2007 UPEC 2007 42nd International; 2007 4-6 Sept. 2007.
60. Hyvarinen J, Karila J, editors. New analysis method for crystalline silicon cells. Photovoltaic Energy Conversion, 2003 Proceedings of 3rd World Conference on; 2003 18-18 May 2003.
61. Silvestre S, Boronat A, Chouder A. Study of bypass diodes configuration on PV modules. Applied Energy. 2009;86(9):1632-40.
62. Nishioka K, Sakitani N, Uraoka Y, Fuyuki T. Analysis of multicrystalline silicon solar cells by modified 3-diode equivalent circuit model taking leakage current through periphery into consideration. Solar Energy Materials and Solar Cells. 2007;91(13):1222-7.
63. Dhass AD, Natarajan E, Ponnusamy L, editors. Influence of shunt resistance on the performance of solar photovoltaic cell. Emerging Trends in Electrical Engineering and Energy Management (ICETEEEM), 2012 International Conference on; 2012 13-15 Dec. 2012; Chennai.
64. Castaner L, Silvestre S. Modelling photovoltaic systems using PSpice: John Wiley and Sons; 2002.
65. Nordcad Systems A/S. Analog Behavioural Moddeling Applications: Nordcad Systems A/S; n.d. Available from: http://www.nordcad.dk/download/Forum/PSpice/abm.pdf.
66. Sah C-T. Fundamentals of solid-state electronics. Singapore: World Scientific; 1991.
67. Green MA. Accuracy of analytical expressions for solar cell fill factors. Solar Cells. 1982;7(3):337-40.
68. MathWorks. MATLAB R2009a. version 7.8.0 ed2009.
69. Green MA. Solar cell fill factors: General graph and empirical expressions. Solid-State Electronics. 1981;24(8):788-9.
70. Kyocera Solar. High efficiency Multicrystal module KD140F, SX Series. [Datasheet]n.d. Available from: http://www.kyocerasolar.com/assets/001/5340.pdf.
71. Markvart T, Castañer L. Practical handbook of photovoltaics fundamentals and applications. New York: Elsevier Advanced Technology; 2003. Available from: http://www.sciencedirect.com/science/book/9781856173902.

APPENDICES

APPENDIX A

EQUATION DERIVATION

Appendix A.1 Module conversion

From equation 2-8, with the assumption that R_{shC} is infinite, we get:

$$I_C = I_{phC} - I_{01}\left(e^{\frac{V_C + I_C R_{sC}}{n_1 V_T}} - 1\right) - I_{02}\left(e^{\frac{V_C + I_C R_{sC}}{n_2 V_T}} - 1\right)$$

To convert this for usage with a solar module simple scaling rules are applied. Those rules are:

$$I = N_p I_C$$

$$I_{ph} = N_p I_{phC}$$

$$V = N_s V_C$$

$$R_s = \frac{N_s}{N_p} R_{sC}$$

Applying the rules on the above equation yields:

$$\frac{I}{N_p} = \frac{I_{ph}}{N_p} - I_{01}\left(e^{\frac{\frac{V}{N_s} + \frac{I}{N_p}\frac{N_p}{N_s} R_s}{n_1 V_T}} - 1\right) - I_{02}\left(e^{\frac{\frac{V}{N_s} + \frac{I}{N_p}\frac{N_p}{N_s} R_s}{n_1 V_T}} - 1\right)$$

The N_p in the exponentials reduce each other, thus only leaving N_s. We now multiply both sides by N_p to reach:

$$I = I_{ph} - N_p I_{01}\left(e^{\frac{V + I R_S}{N_s n_1 V_T}} - 1\right) - N_p I_{02}\left(e^{\frac{V + I R_S}{N_s n_2 V_T}} - 1\right)$$

which is the basis for many equations derived in Chapter 3 and this Appendix.

Appendix A.2 Open-circuit voltage - V_{oc}

Equation 3-1 at open-circuit conditions, i.e. I=0 and V=V_{oc}, yields:

$$0 = I_{ph} - N_p I_0\left(e^{\left[\frac{V_{oc}}{N_s V_T}\right]} + e^{\left[\frac{V_{oc}}{2N_s V_T}\right]} - 2\right)$$

Since the terms $e^{\left[\frac{V_{oc}}{N_s V_T}\right]}$ and $e^{\left[\frac{V_{oc}}{2N_s V_T}\right]}$ are very large we can neglect the '-2'. Rearranging we get:

$$\frac{I_{ph}}{N_p I_0} = e^{\left[\frac{V_{oc}}{N_s V_T}\right]} + e^{\left[\frac{V_{oc}}{2N_s V_T}\right]}$$

If we now use the binomial theorem

$$e^x + e^{\frac{x}{2}} = \left(e^{\frac{x}{2}} + \frac{1}{2}\right)^2 - \frac{1}{4}$$

where

$$x = \frac{V_{oc}}{N_s V_T}$$

we get

$$\frac{I_{ph}}{N_p I_0} = \left(e^{\left[\frac{V_{oc}}{2N_s V_T}\right]} + \frac{1}{2}\right)^2 - \frac{1}{4}$$

Here again we can neglect some terms, i.e. $\frac{1}{2}$ and $\frac{1}{4}$, due to the size of $e^{\frac{V_{oc}}{2N_s V_T}}$

$$\frac{I_{ph}}{N_p I_0} = \left(e^{\left[\frac{V_{oc}}{2N_s V_T}\right]}\right)^2$$

Which is the same as:

$$\frac{I_{ph}}{N_p I_0} = e^{\left[\frac{V_{oc}}{N_s V_T}\right]}$$

Rearranging this and assuming that $I_{ph} = I_{sc}$ results in

$$V_{oc} = N_S V_T \, ln\left[\frac{I_{sc}}{N_p I_0}\right]$$

Castaner et al. (64) has determined that the temperature coefficient of the open-circuit voltage is calculated by:

$$\alpha_V(T_{cell} - 25°C) = V_T \, ln\left[\frac{I_{scr}}{I_0}\right] - V_{ocr}$$

We have to adjust this equation to our intended use with photovoltaic modules, hence

$$\alpha_V(T_{cell} - 25°C) = N_S V_T \, ln\left[\frac{I_{scr}}{N_p I_0}\right] - V_{ocr}$$

From here on we follow their derivation with our adjusted equation. They added and subtracted V_{oc} at the RHS

$$\alpha_V(T_{cell} - 25°C) = N_S V_T \, ln\left[\frac{I_{scr}}{N_p I_0}\right] - V_{ocr} + V_{oc} - V_{oc}$$

Now they substituted one V_{oc} with the earlier from equation 3-1 derived equation and rearranged the above equation to get:

$$V_{ocr} + \alpha_V(T_{cell} - 25°C) + N_S V_T \, ln\left[\frac{I_{sc}}{N_p I_0}\right] - N_S V_T \, ln\left[\frac{I_{scr}}{N_p I_0}\right] = V_{oc}$$

Which they then combined to

$$V_{oc} = V_{ocr} + \alpha_V(T_{cell} - 25°C) + N_S V_T \, ln\left[\frac{\frac{I_{sc}}{N_p I_0}}{\frac{I_{scr}}{N_p I_0}}\right]$$

The $N_p I_0$ in the numerator and denominator of the natural logarithm reduce each other, thus leaving us with

$$V_{oc} = V_{ocr} + \alpha_V(T_{cell} - 25°C) + N_S V_T \, ln\left[\frac{I_{sc}}{I_{scr}}\right]$$

Appendix A.3 Series resistance - R_s

Green (69) proposed a method to determine the ideal fill factor, FF_0, while only using the open-circuit and thermal voltage.

$$FF_0 = \frac{\frac{V_{oc}}{V_T} - ln\left[\frac{V_{oc}}{V_T} + 0.72\right]}{1 + \frac{V_{oc}}{V_T}}$$

We have to adjust this equation for our use with solar modules. The V_{oc} used by Green will be equal to $\frac{V_{oc}}{N_s}$. The equation we will thus use is:

$$FF_0 = \frac{\frac{V_{oc}}{N_s V_T} - ln\left[\frac{V_{oc}}{N_s V_T} + 0.72\right]}{1 + \frac{V_{oc}}{N_s V_T}}$$

In another work Green (67) proposed a relationship between the fill factor and the ideal fill factor

$$FF = FF_0(1 - 1.1 r_s) + \frac{{r_s}^2}{5.4}$$

where $r_s = \frac{I_{sc} R_s}{V_{oc}}$. This has to be converted for use with solar modules as well, however, when applying the rules shown in Appendix A.1 the N_s and N_p brought into the equation by V_{oc} and

I_{sc} reduce each other with $\frac{N_p}{N_s}$, which was used to convert R_s. Thus the equation does not change. We can then rearrange the above quadratic equation to the form $0 = ax^2+bx+c$ where $R_s = x$:

$$0 = \frac{{I_{sc}}^2}{5.4{V_{oc}}^2}{R_s}^2 - \frac{1.1FF_0 I_{sc}}{V_{oc}}R_s + FF_0 - FF$$

We can solve this equation in MATLAB (68) to get the following two solutions:

$$R_{s_1} = \frac{2.7V_{oc}\left\{1.1FF_0 + \sqrt{\left[1.21{FF_0}^2 + \frac{20}{27}(FF - FF_0)\right]}\right\}}{I_{sc}}$$

$$R_{s_2} = \frac{2.7V_{oc}\left\{1.1FF_0 - \sqrt{\left[1.21{FF_0}^2 + \frac{20}{27}(FF - FF_0)\right]}\right\}}{I_{sc}}$$

The first solution would result in large resistance values (around 100Ω), which is highly unlikely for solar cells and modules. However, the second solutions returns results around 1Ω which is to be expected. The FF can further more be substituted by equation 2-2, which gives us the equation for the approximation of the series resistance:

$$R_s = \frac{2.7V_{oc}\left\{1.1FF_0 - \sqrt{\left[1.21{FF_0}^2 + \frac{20}{27}\left(\frac{I_m V_m}{I_{sc}V_{oc}} - FF_0\right)\right]}\right\}}{I_{sc}}$$

In this equation the I_m, V_{oc}, I_{sc} and FF_0 can be easily determined using the appropriate equations. Only V_m cannot be determined, since it is dependent on R_s as can be seen in equation 3-9. However, to calculate the series resistance it is assumed that V_m is scale proportional to V_{oc}, hence it can be approximated by:

$$V_m = V_{mr} + \alpha_V(T_{cell} - 25°C) + N_S V_T \, ln\frac{I_{sc}}{I_{scr}}$$

Appendix A.4 Diode saturation current - I_o

If we evaluate equation 3-1 at open-circuit conditions, i.e. I=0 and V=V_{oc}:

$$0 = I_{ph} - N_p I_0\left(e^{\left[\frac{V_{oc}}{N_s V_T}\right]} + e^{\left[\frac{V_{oc}}{2N_s V_T}\right]} - 2\right)$$

We can rearrange the equation to:

$$I_{ph} = N_p I_0\left(e^{\left[\frac{V_{oc}}{N_s V_T}\right]} + e^{\left[\frac{V_{oc}}{2N_s V_T}\right]} - 2\right)$$

If we now evaluate equation 3-1 at the short-circuit conditions, i.e. I=I_{sc} and V=0:

$$I_{sc} = I_{ph} - N_p I_0 \left(e^{\left[\frac{I_{sc} R_s}{N_s V_T}\right]} + e^{\left[\frac{I_{sc} R_s}{2 N_s V_T}\right]} - 2 \right)$$

We can substitute I_{ph} to get:

$$I_{sc} = N_P I_0 \left(e^{\left[\frac{V_{oc}}{N_S V_t}\right]} - e^{\left[\frac{I_{sc} R_s}{N_S V_t}\right]} + e^{\left[\frac{V_{oc}}{2 N_S V_t}\right]} - e^{\left[\frac{I_{sc} R_s}{2 N_S V_t}\right]} - 2 + 2 \right)$$

Here we can neglect the terms $e^{\left[\frac{I_{sc} R_s}{N_S V_t}\right]}$ and $e^{\left[\frac{I_{sc} R_s}{2 N_S V_t}\right]}$, because compared to $e^{\left[\frac{V_{oc}}{N_S V_t}\right]}$ and $e^{\left[\frac{V_{oc}}{2 N_S V_t}\right]}$ they are very small. Doing so and rearranging the equation leads us to:

$$I_0 = \frac{I_{sc}}{N_P \left(e^{\left[\frac{V_{oc}}{N_S V_t}\right]} + e^{\left[\frac{V_{oc}}{2 N_S V_t}\right]} \right)}$$

Appendix A.5 Voltage at the maximum power point - V_m

Equation 3-1 at maximum power point conditions, i.e. $I=I_m$ and $V=V_m$, yields:

$$I_m = I_{ph} - N_p I_0 \left(e^{\left[\frac{V_m + I_m R_s}{N_s V_T}\right]} + e^{\left[\frac{V_m + I_m R_s}{2 N_s V_T}\right]} - 2 \right)$$

Since the terms $e^{\left[\frac{V_m + I_m R_s}{N_s V_T}\right]}$ and $e^{\left[\frac{V_m + I_m R_s}{2 N_s V_T}\right]}$ are very large we can neglect the '-2'. Rearranging we get:

$$\frac{I_{ph} - I_m}{N_p I_0} = e^{\left[\frac{V_m + I_m R_s}{N_s V_T}\right]} + e^{\left[\frac{V_m + I_m R_s}{2 N_s V_T}\right]}$$

If we now use the binomial theorem

$$e^x + e^{\frac{x}{2}} = \left(e^{\frac{x}{2}} + \frac{1}{2} \right)^2 - \frac{1}{4}$$

where

$$x = \frac{V_m + I_m R_s}{N_s V_T}$$

we get

$$\frac{I_{ph} - I_m}{N_p I_0} = \left(e^{\left[\frac{V_m + I_m R_s}{2 N_s V_T}\right]} + \frac{1}{2} \right)^2 - \frac{1}{4}$$

Here again we can neglect some terms, i.e. $\frac{1}{2}$ and $\frac{1}{4}$, due to the size of $e^{\left[\frac{V_m + I_m R_s}{2 N_s V_T}\right]}$

$$\frac{I_{ph} - I_m}{N_p I_0} = \left(e^{\left[\frac{V_m + I_m R_s}{2 N_s V_T}\right]} \right)^2$$

Which is the same as:

$$\frac{I_{ph} - I_m}{N_p I_0} = e^{\left[\frac{V_m + I_m R_s}{N_s V_T}\right]}$$

Rearranging this and assuming that $I_{ph} = I_{sc}$ results in

$$V_m = N_S V_T \, ln \left[\frac{I_{sc} - I_m}{N_p I_0} \right] - I_m R_s$$

Now can substitute the equation for I_0, which we derived in Appendix A.4 into the above equation, to arrive at:

$$V_m = N_S V_T \, ln \left[\frac{I_{sc} - I_m}{I_{sc}} \left(e^{\left[\frac{V_{oc}}{N_S V_t}\right]} + e^{\left[\frac{V_{oc}}{2 N_S V_t}\right]} \right) \right] - I_m R_s$$

APPENDIX B

ORCAD CIRCUITS

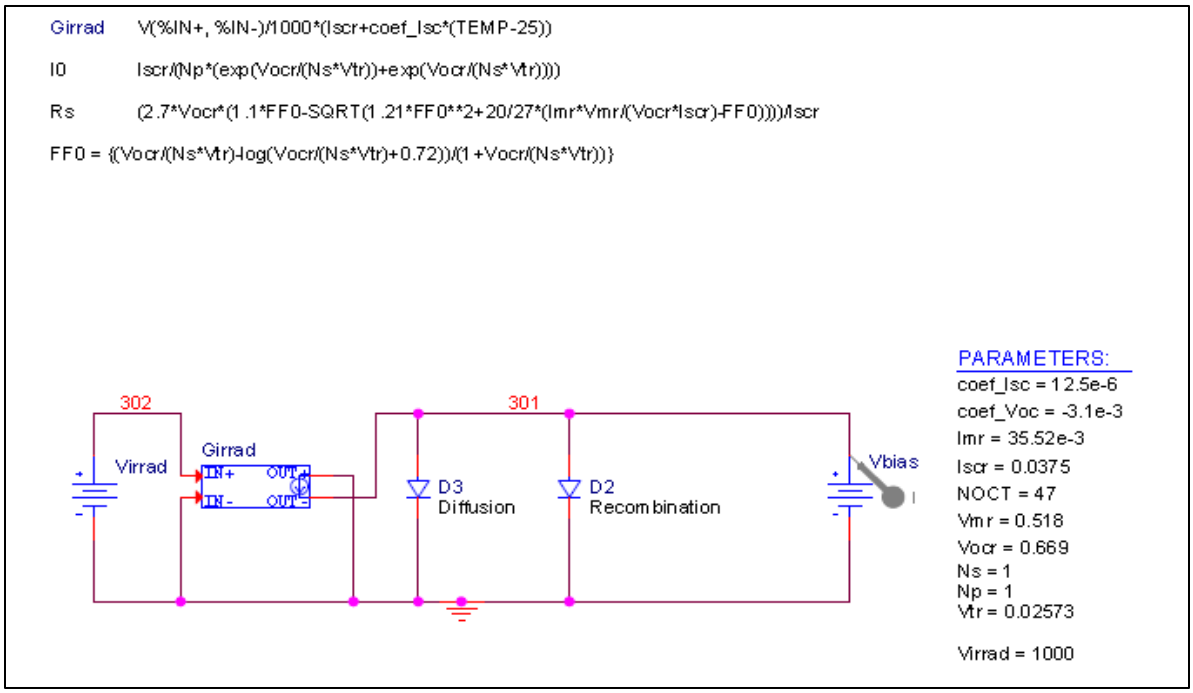

Figure B-1 OrCAD circuit of the first model used in chapter 5.1.1
Consisting of two intrinsic diode models, where the series resistance is set within the PSPICE diode model

The net list of the first model used in chapter 5.1.1 is:

```
V_Virrad 302 0 {Virrad}
G_Girrad 0 301 VALUE {V(302,0)/1000*(Iscr+coef_Isc*(TEMP
+ -25))}
D_D2 301 0 Recombination
.model Recombination D Is={I0} n=2 rs={Rs}
V_Vbias 301 0 0
D_D3 301 0 Diffusion
.model Diffusion D Is={I0} n=1 rs={Rs}
.PARAM rs={(2.7*vocr*(1.1*ff0-sqrt(1.21*ff0**2+20/27*(imr*
+ vmr/(vocr*iscr)-ff0))))/iscr} noct=47 np=1 vmr=0.518 ns=1
+ virrad=1000 vocr=0.669 iscr=0.0375 imr=35.52e-3
+ coef_voc=-3.1e-3 coef_isc=12.5e-6 i0={iscr/(np*(exp(vocr/
+ (ns*vtr))+exp(vocr/(ns*vtr))))} ff0={(vocr/(ns*vtr)-log
+ (vocr/(ns*vtr)+0.72))/(1+vocr/(ns*vtr))} vtr=0.02573
```

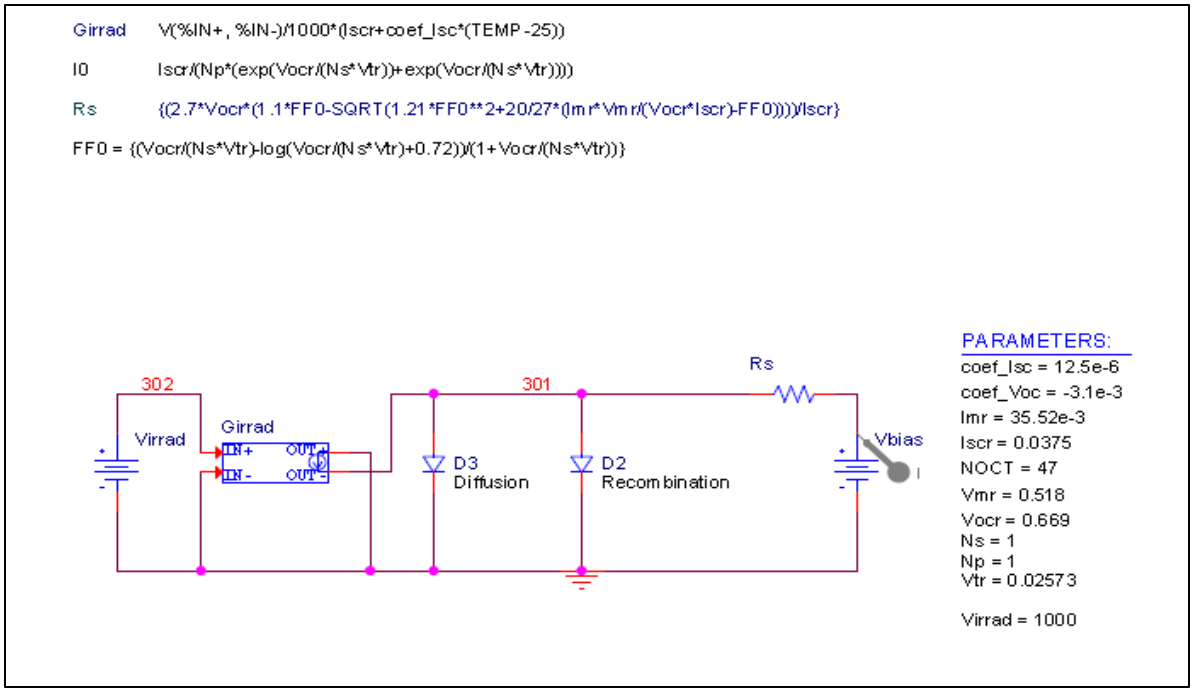

Figure B-2 OrCAD circuit of the second model used in chapter 5.1.1 Consisting of two intrinsic diode models and an intrinsic resistor model

The net list of the second model used in chapter 5.1.1 is:

```
V_Virrad 302 0 {Virrad}
G_Girrad 0 301 VALUE {V(302,0)/1000*(Iscr+coef_Isc*(TEMP
+ -25)) }
D_D2 301 0 Recombination
.model Recombination D Is={I0} n=2
R_Rs 301 N02729 {(2.7*Vocr*(1.1*FF0-SQRT(1.21*FF0**2+20/27
+ *(Imr*Vmr/(Vocr*Iscr)-FF0))))/Iscr} TC=0,0
V_Vbias N02729 0 0
D_D3 301 0 Diffusion
.model Diffusion D Is={I0} n=1
.PARAM noct=47 np=1 vmr=0.518 ns=1 virrad=1000 vocr=0.669
+ iscr=0.0375 imr=35.52e-3 coef_voc=-3.1e-3 coef_isc=
+ 12.5e-6 i0={iscr/(np*(exp(vocr/(ns*vtr))+exp(vocr/(ns*
+ vtr))))} ff0={(vocr/(ns*vtr)-log(vocr/(ns*vtr)+0.72))
+ /(1+vocr/(ns*vtr))} vtr=0.02573
```

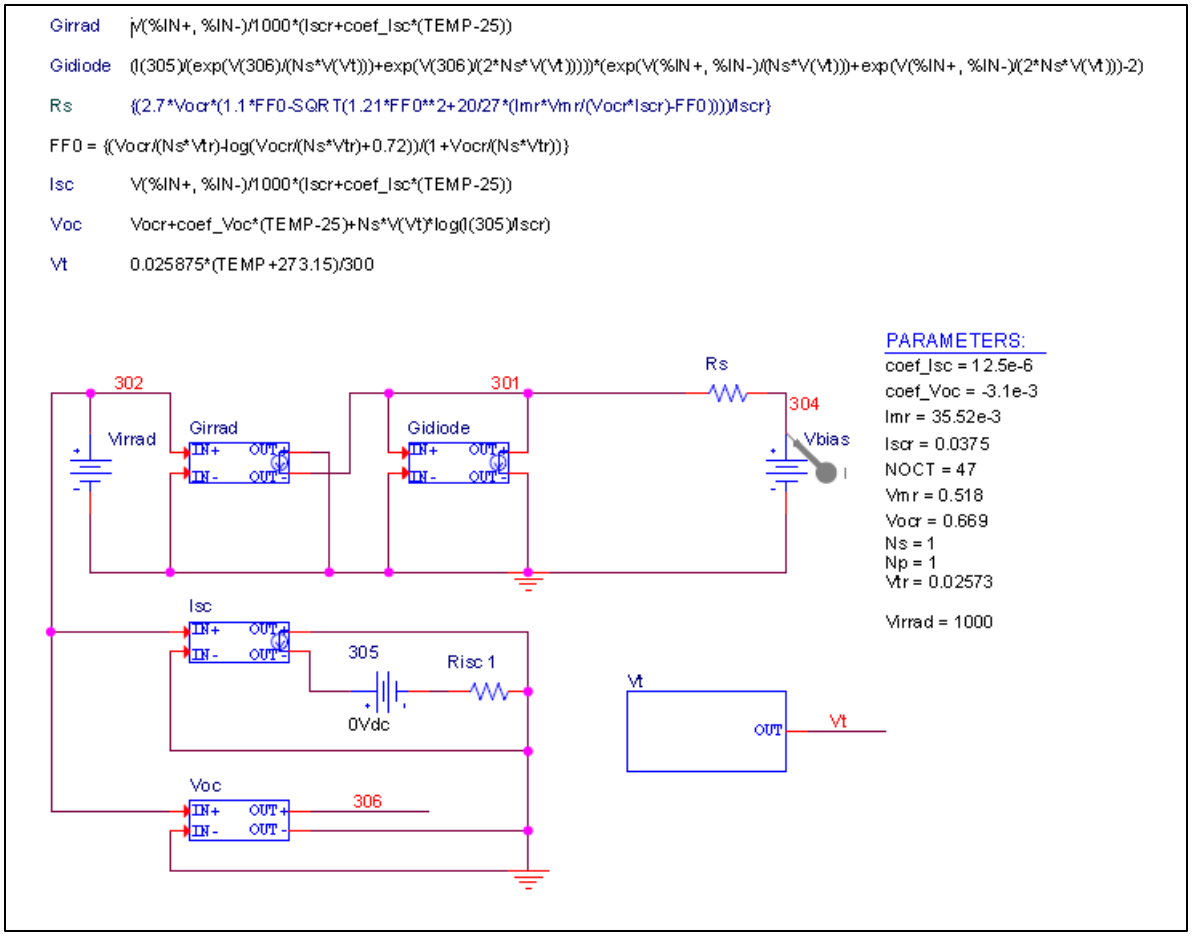

Figure B-3 OrCAD circuit of the third model used in chapter 5.1.1
Consisting of a g-device (Gidiode) to model the diodes and an intrinsic resistor model. Other g- and e-devices calculate the parameters used in Gidiode, i.e. Isc, Voc and VT

The net list of the third model used in chapter 5.1.1 is:

```
G_Girrad 0 301 VALUE{V(302,0)/1000*(Iscr+coef_Isc*(TEMP
+ -25))}
V_Virrad 302 0 {Virrad}
V_Vbias 304 0 0
R_Rs 301 304 {(2.7*Vocr*(1.1*FF0-SQRT(1.21*FF0**2+20/27*
+ (Imr*Vmr/(Vocr*Iscr)-FF0))))/Iscr} TC=0,0
G_Gidiode 301 0 VALUE{(I(V_305)/(exp(V(306)/(Ns*V(Vt)))
+ +exp(V(306)/(2*Ns*V(Vt)))))*(exp(V(301,0)/(Ns*V(Vt)))
+ +exp(V(301, 0)/(2*Ns*V(Vt)))-2)}
G_Isc 0 N02837 VALUE{V(302,0)/1000*(Iscr+coef_Isc*(TEMP
+ -25))}
E_Voc 306 0 VALUE { Vocr+coef_Voc*(TEMP-25)+Ns*V(Vt)*log
+ (I(V_305)/Iscr)}
V_305 N02837 N02874 0Vdc
R_Risc N02874 0  1 TC=0,0
E_Vt VT 0 VALUE{0.025875*(TEMP+273.15)/300}
.PARAM noct=47 np=1 vmr=0.518 ns=1 virrad=1000 imr=35.52e-3
+ iscr=0.0375 vocr=0.669 coef_isc=12.5e-6 coef_voc=-3.1e-3
+ vtr=0.02573 ff0={(vocr/(ns*vtr)-log(vocr/(ns*vtr)+0.72))
+ /(1+vocr/(ns*vtr))}
```

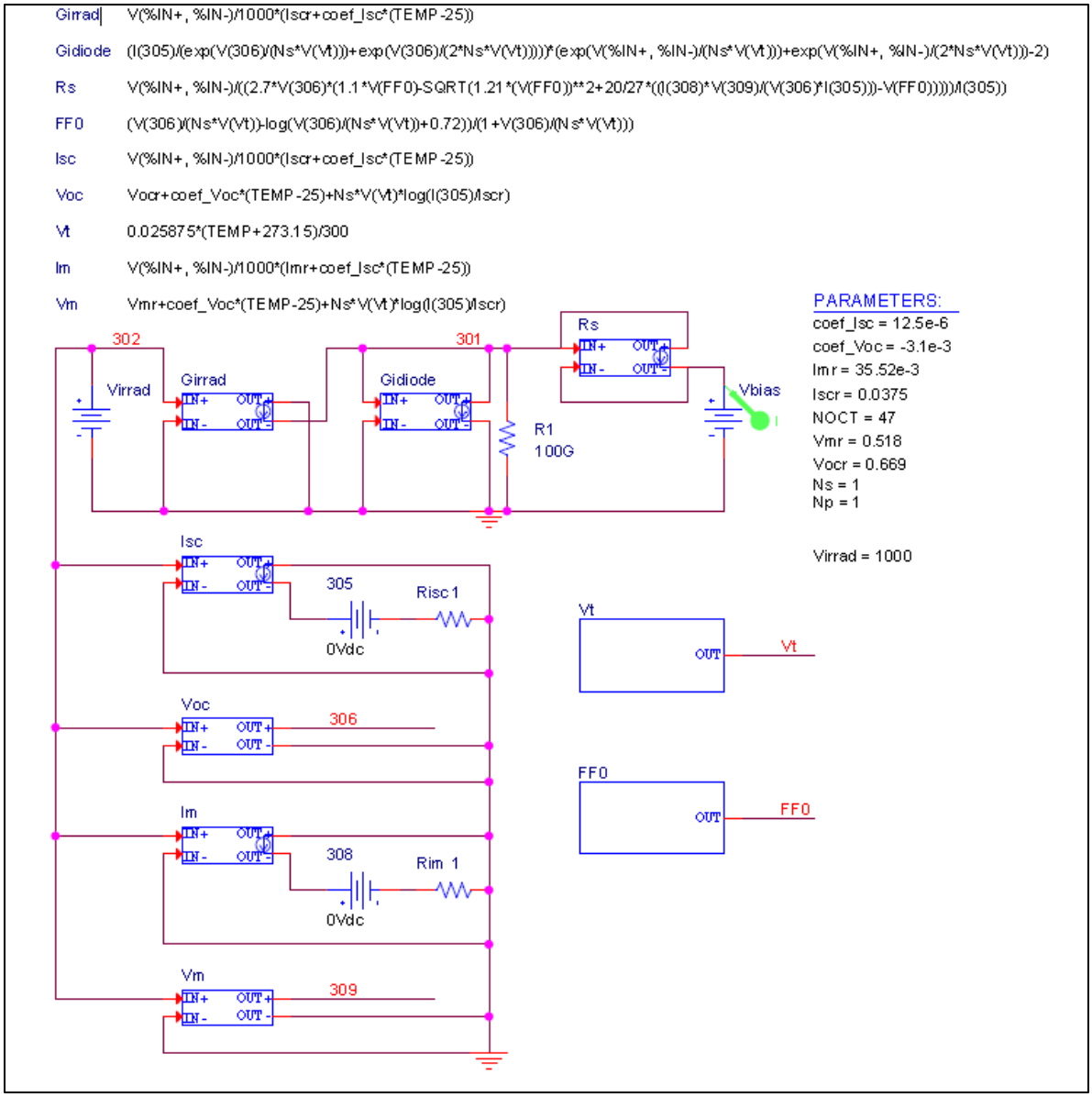

Figure B-4 OrCAD circuit of the fourth model used in chapter 5.1.1
Consisting of a g-device (Gidiode) to model the diodes and a g-device (Rs) to model the series resistance. Other g- and e- devices calculate the parameters used in Gidiode and Rs, i.e. I_{sc}, V_{oc}, V_T, I_m, V_m and FF_o

The net list of the fourth model used in chapter 5.1.1 is:

```
G_Girrad 0 301 VALUE{V(302,0)/1000*(Iscr+coef_Isc*(TEMP
+ -25))}
V_Virrad 302 0 {Virrad}
V_Vbias N03965 0 0
G_Gidiode 301 0 VALUE{(I(V_305)/(exp(V(306)/(Ns*V(Vt)))
+ +exp(V(306)/(2*Ns*V(Vt)))))*(exp(V(301,0)/(Ns*V(Vt)))
+ +exp(V(301, 0)/(2*Ns*V(Vt)))-2)}
G_Isc 0 N02837 VALUE{V(302,0)/1000*(Iscr+coef_Isc*(TEMP
+ -25))}
E_Voc 306 0 VALUE { Vocr+coef_Voc*(TEMP-25)+Ns*V(Vt)*log
+ (I(V_305)/Iscr)}
V_305 N02837 N02874 0Vdc
R_Risc N02874 0  1 TC=0,0
E_Vt VT 0 VALUE{0.025875*(TEMP+273.15)/300}
G_Rs 301 N03965 VALUE { V(301,N03965)/((2.7*V(306)*(1.1*
+ V(FF0)-SQRT(1.21*(V(FF0))**2+20/27*((I(V_308)*V(309)/(V
+ (306)*I(V_305)))-V(FF0)))))/I(V_305))}
G_Im 0 N04156 VALUE{V(302,0)/1000*(Imr+coef_Isc*(TEMP-25))}
R_Rim N04170 0  1 TC=0,0
V_308 N04156 N04170 0Vdc
R_R1 0 301  100G TC=0,0
E_FF0 FF0 0 VALUE{(V(306)/(Ns*V(Vt))-log(V(306)/(Ns*V(Vt)
+ )+0.72))/(1+V(306)/(Ns*V(Vt)))}
E_Vm 309 0 VALUE{Vmr+coef_Voc*(TEMP-25)+Ns*V(Vt)*log(
+ I(V_305)/Iscr)}
E_ABM1 RS1 0 VALUE {((2.7*V(306)*(1.1*V(FF0)-SQRT(1.21*(V
+ (FF0))**2+20/27*((I(V_308)*V(309)/(V(306)*I(V_305)))-V(
+ FF0)))))/I(V_305))}
.PARAM noct=47 np=1 vmr=0.518 ns=1 virrad=1000 vocr=0.669
+ iscr=0.0375 imr=35.52e-3 coef_voc=-3.1e-3 coef_isc=
+ 12.5e-6 vtr=0.02573
```

APPENDIX C

MATLAB

Appendix C.1 MatLab Fitting Options

To fit a double exponential curve through the measurements a costume equation was created in MatLab´s curve fitting tool. The equation is as follows:

$$f(x) = I_{sc} - a * (e^{bx} - 1) - c * (e^{dx} - 1)$$

where a, b, c and d are parameters which will be determined by MatLab, to find the best fit through the data. The fit options for this costume equation are:

Method	**NonLinearLeastSquare**		
Robust			Off
Algorithm			Trust-Region
DiffMinChange			1.0E-15
DiffMaxChange			0.1
MaxFunEvals			10000
MaxIter			1000
TolFun			1.0E-12
TolX			1.0E-12
Unknowns	StartPoint	Lower	Upper
a	0.218	0	1.000
b	0.896	0	40.000
c	0.448	0	1.000
d	0.729	0	20.000

For the linear fit around the open-circuit conditions a linear polynomial fit was chosen. It exhibits the following form:

$$f(x) = p_1 x + p_2$$

where p_1 and p_2 are again parameters, which will be determined by MatLab to achieve the best fit through the data points. The fit options for it were left at the default settings, namely:

Method	**LinearLeastSquare**	
Robust		Off
Unknowns	Lower	Upper
p1	-Inf	Inf
p2	-Inf	Inf

Appendix C.2 MatLab code

At first the data to be analysed was imported into MatLab. The voltage values into the vector '`Vdata`' and the current values into vector '`Idata`'. Furthermore were the current values of the simulation with the proposed model imported into vector '`Iprop`' and the current values of Castaner´s model were imported into '`Icast`'. Then the curve fitting tools was used to fit the exponential and linear curve through the data. Both fitted curves were visually inspected in the curve fitting tool, to determine the best transition point (Ptrans), at which the smoothest transition from the exponential curve to the linear curve can be achieved. For dataset 1 this point was at 17.4V, for dataset 2 at 17.3V and for dataset 3 at 18.8V. For dataset 4 only the exponentially fitted curve was used, since it showed a very good fit. The two fitted curves were then exported to the MatLab workspace as '`fitExp`' and '`fitLin`' for the exponential and linear fit, respectively. After that the following code was executed, to achieve the results shown in chapter 6.2:

```
Vcomp=[0:0.1:21].'
vecExp=fitExp(Vcomp)
vecLin=fitLin(Vcomp)
IrealFit=[vecExp(1:Ptrans);vecLin(Ptrans:length(Vcomp))]
diffProp=abs(IrealFit - Iprop)
diffCast=abs(IrealFit – Icast)
RSMEprop=sqrt(mean((IrealFit – Iprop).^2))
RSMEcast=sqrt(mean((IrealFit – Icast).^2))
Eprop=1 – (sum((IrealFit – Iprop).^2)) / (sum((IrealFit –
     (mean(IrealFit))).^2))
Ecast=1 – (sum((IrealFit – Icast).^2)) / (sum((IrealFit –
     (mean(IrealFit))).^2))
MADPprop=mean(diffProp) / mean(abs(IrealFit))
MADPcast=mean(diffCast) / mean(abs(IrealFit))
vecExp=fitExp(Vdata)
vecLin=fitLin(Vdata)
IfitValid=[vecExp(1:Ptrans);vecLin(Ptrans:length(Vdata))]
RSMEfit=sqrt(mean((Idata – IfitValid).^2))
```

Now the needed data can be extracted from MatLab, e.g. root mean square error, mean absolute deviation percent, Nash-Sutcliffe coefficient, I-V curves.

APPENDIX D

ERROR CALCULATIONS

In the formulas in the section the following parameters are used:

- t index
- a_t actual value at index t
- $\bar{a}$ mean of the actual values
- f_t forecasted value at index t
- n number of elements

To calculate the root mean square error, the mean absolute derivation percent and the Nash-Sutcliffe model efficiency coefficient the following formulas were used:

$$RSME = \sqrt{\frac{\sum_{t=1}^{n}(a_t - f_t)^2}{n}}$$

$$MADP = \frac{\sum_{t=1}^{n}|f_t - a_t|}{\sum_{t=1}^{n}|a_t|}$$

$$E = 1 - \frac{\sum_{t=1}^{n}(a_t - f_t)^2}{\sum_{t=1}^{n}(a_t - \bar{a})^2}$$

APPENDIX E

VERIFICATION RAW DATA

Appendix E.1 Comparison between ABM and intrinsic modelling

In this section the simulation raw data of the first verification step, the comparison between ABM and intrinsic modelling, are shown, as extracted from PSPICE.

	25°C				50°C			
V	I(model 1)	I(model 2)	I(model 3)	I(model 4)	I(model 1)	I(model 2)	I(model 3)	I(model 4)
0.00	0.03750	0.03750	0.03750	0.03750	0.03781	0.03781	0.03781	0.03781
0.01	0.03750	0.03750	0.03750	0.03750	0.03781	0.03781	0.03781	0.03781
0.02	0.03750	0.03750	0.03750	0.03750	0.03781	0.03781	0.03781	0.03781
0.03	0.03750	0.03750	0.03750	0.03750	0.03781	0.03781	0.03781	0.03781
0.04	0.03750	0.03750	0.03750	0.03750	0.03781	0.03781	0.03781	0.03781
0.05	0.03750	0.03750	0.03750	0.03750	0.03781	0.03781	0.03781	0.03781
0.06	0.03750	0.03750	0.03750	0.03750	0.03781	0.03781	0.03781	0.03781
0.07	0.03750	0.03750	0.03750	0.03750	0.03781	0.03781	0.03781	0.03781
0.08	0.03750	0.03750	0.03750	0.03750	0.03781	0.03781	0.03781	0.03781
0.09	0.03750	0.03750	0.03750	0.03750	0.03781	0.03781	0.03781	0.03781
0.10	0.03750	0.03750	0.03750	0.03750	0.03781	0.03781	0.03781	0.03781
0.11	0.03750	0.03750	0.03750	0.03750	0.03781	0.03781	0.03781	0.03781
0.12	0.03750	0.03750	0.03750	0.03750	0.03781	0.03781	0.03781	0.03781
0.13	0.03750	0.03750	0.03750	0.03750	0.03781	0.03781	0.03781	0.03781
0.14	0.03750	0.03750	0.03750	0.03750	0.03781	0.03781	0.03781	0.03781
0.15	0.03750	0.03750	0.03750	0.03750	0.03781	0.03781	0.03781	0.03781
0.16	0.03750	0.03750	0.03750	0.03750	0.03781	0.03781	0.03781	0.03781
0.17	0.03750	0.03750	0.03750	0.03750	0.03781	0.03781	0.03781	0.03781
0.18	0.03750	0.03750	0.03750	0.03750	0.03781	0.03781	0.03781	0.03781
0.19	0.03750	0.03750	0.03750	0.03750	0.03781	0.03781	0.03781	0.03781
0.20	0.03750	0.03750	0.03750	0.03750	0.03781	0.03781	0.03781	0.03781
0.21	0.03750	0.03750	0.03750	0.03750	0.03781	0.03781	0.03781	0.03781
0.22	0.03750	0.03750	0.03750	0.03750	0.03781	0.03781	0.03781	0.03781
0.23	0.03750	0.03750	0.03750	0.03750	0.03781	0.03781	0.03781	0.03781
0.24	0.03750	0.03750	0.03750	0.03750	0.03781	0.03781	0.03781	0.03781
0.25	0.03750	0.03750	0.03750	0.03750	0.03781	0.03781	0.03781	0.03781
0.26	0.03750	0.03750	0.03750	0.03750	0.03781	0.03781	0.03781	0.03781
0.27	0.03750	0.03750	0.03750	0.03750	0.03781	0.03781	0.03781	0.03781
0.28	0.03750	0.03750	0.03750	0.03750	0.03781	0.03781	0.03781	0.03781
0.29	0.03750	0.03750	0.03750	0.03750	0.03781	0.03781	0.03781	0.03781
0.30	0.03750	0.03750	0.03750	0.03750	0.03781	0.03781	0.03781	0.03781
0.31	0.03750	0.03750	0.03750	0.03750	0.03781	0.03781	0.03778	0.03779
0.32	0.03750	0.03750	0.03750	0.03750	0.03781	0.03781	0.03777	0.03778
0.33	0.03750	0.03750	0.03750	0.03750	0.03781	0.03781	0.03776	0.03777
0.34	0.03750	0.03750	0.03750	0.03750	0.03781	0.03780	0.03773	0.03775
0.35	0.03750	0.03750	0.03750	0.03750	0.03781	0.03780	0.03770	0.03772
0.36	0.03750	0.03750	0.03749	0.03749	0.03781	0.03779	0.03765	0.03768
0.37	0.03750	0.03750	0.03749	0.03749	0.03781	0.03779	0.03758	0.03762
0.38	0.03750	0.03750	0.03749	0.03749	0.03781	0.03777	0.03748	0.03754
0.39	0.03750	0.03749	0.03748	0.03748	0.03781	0.03776	0.03734	0.03743
0.40	0.03750	0.03749	0.03748	0.03748	0.03781	0.03773	0.03715	0.03727
0.41	0.03750	0.03749	0.03746	0.03746	0.03781	0.03770	0.03688	0.03704
0.42	0.03750	0.03748	0.03745	0.03745	0.03780	0.03765	0.03651	0.03674
0.43	0.03750	0.03747	0.03742	0.03742	0.03780	0.03758	0.03602	0.03632

Table E-1 Raw data of the comparison between ABM and intrinsic modelling at 25°C and 50°C

	25°C				50°C			
V	I(model 1)	I(model 2)	I(model 3)	I(model 4)	I(model 1)	I(model 2)	I(model 3)	I(model 4)
0.44	0.03750	0.03746	0.03739	0.03739	0.03779	0.03749	0.03537	0.03576
0.45	0.03750	0.03744	0.03733	0.03733	0.03779	0.03735	0.03453	0.03502
0.46	0.03750	0.03741	0.03726	0.03726	0.03777	0.03716	0.03348	0.03407
0.47	0.03749	0.03736	0.03715	0.03714	0.03776	0.03690	0.03219	0.03289
0.48	0.03749	0.03730	0.03698	0.03698	0.03774	0.03654	0.03066	0.03145
0.49	0.03749	0.03720	0.03675	0.03675	0.03770	0.03606	0.02888	0.02974
0.50	0.03748	0.03707	0.03643	0.03643	0.03766	0.03542	0.02685	0.02776
0.51	0.03747	0.03687	0.03598	0.03597	0.03759	0.03460	0.02460	0.02553
0.52	0.03746	0.03660	0.03536	0.03536	0.03749	0.03356	0.02214	0.02306
0.53	0.03744	0.03621	0.03455	0.03455	0.03736	0.03228	0.01949	0.02036
0.54	0.03741	0.03568	0.03351	0.03350	0.03717	0.03077	0.01667	0.01746
0.55	0.03736	0.03497	0.03221	0.03221	0.03692	0.02900	0.01370	0.01439
0.56	0.03730	0.03404	0.03065	0.03064	0.03656	0.02699	0.01059	0.01115
0.57	0.03720	0.03286	0.02881	0.02881	0.03609	0.02475	0.00737	0.00777
0.58	0.03707	0.03143	0.02672	0.02672	0.03546	0.02230	0.00403	0.00426
0.59	0.03687	0.02972	0.02439	0.02439	0.03465	0.01966	0.00060	0.00064
0.60	0.03659	0.02775	0.02184	0.02184	0.03362	0.01685	-0.00291	-0.00308
0.61	0.03621	0.02553	0.01910	0.01909	0.03236	0.01389	-0.00650	-0.00689
0.62	0.03567	0.02308	0.01618	0.01618	0.03086	0.01078	-0.01016	-0.01078
0.63	0.03496	0.02042	0.01311	0.01311	0.02910	0.00756	-0.01387	-0.01474
0.64	0.03403	0.01759	0.00991	0.00990	0.02711	0.00423	-0.01765	-0.01877
0.65	0.03285	0.01458	0.00659	0.00658	0.02488	0.00081	-0.02147	-0.02285
0.66	0.03141	0.01144	0.00316	0.00316	0.02244	-0.00270	-0.02533	-0.02699
0.67	0.02970	0.00817	-0.00036	-0.00036	0.01981	-0.00629	-0.02924	-0.03117
0.68	0.02773	0.00479	-0.00395	-0.00395	0.01701	-0.00994	-0.03319	-0.03540
0.69	0.02550	0.00132	-0.00762	-0.00762	0.01406	-0.01365	-0.03717	-0.03966
0.70	0.02305	-0.00224	-0.01136	-0.01135	0.01096	-0.01742	-0.04118	-0.04397
0.71	0.02040	-0.00588	-0.01515	-0.01514	0.00775	-0.02124	-0.04522	-0.04831
0.72	0.01756	-0.00959	-0.01899	-0.01898	0.00442	-0.02511	-0.04929	-0.05267
0.73	0.01455	-0.01335	-0.02288	-0.02287	0.00100	-0.02901	-0.05338	-0.05707
0.74	0.01141	-0.01717	-0.02681	-0.02680	-0.00250	-0.03296	-0.05750	-0.06149
0.75	0.00814	-0.02104	-0.03078	-0.03077	-0.00608	-0.03694	-0.06163	-0.06594
0.76	0.00476	-0.02495	-0.03479	-0.03477	-0.00973	-0.04095	-0.06579	-0.07041
0.77	0.00128	-0.02891	-0.03883	-0.03881	-0.01344	-0.04499	-0.06997	-0.07491
0.78	-0.00228	-0.03290	-0.04289	-0.04287	-0.01721	-0.04905	-0.07416	-0.07942
0.79	-0.00592	-0.03692	-0.04699	-0.04697	-0.02103	-0.05315	-0.07837	-0.08395
0.80	-0.00963	-0.04098	-0.05111	-0.05108	-0.02489	-0.05726	-0.08260	-0.08850

Table E-1 continued

	100°C			
V	I(model 1)	I(model 2)	I(model 3)	I(model 4)
0.00	0.03844	0.03844	0.03844	0.03844
0.01	0.03844	0.03844	0.03844	0.03844
0.02	0.03844	0.03844	0.03844	0.03844
0.03	0.03844	0.03844	0.03844	0.03844
0.04	0.03844	0.03844	0.03844	0.03844
0.05	0.03844	0.03844	0.03843	0.03844
0.06	0.03844	0.03844	0.03843	0.03843
0.07	0.03844	0.03844	0.03843	0.03843
0.08	0.03844	0.03844	0.03843	0.03843
0.09	0.03844	0.03844	0.03843	0.03843
0.10	0.03844	0.03844	0.03842	0.03843
0.11	0.03844	0.03844	0.03842	0.03842
0.12	0.03844	0.03844	0.03841	0.03842
0.13	0.03844	0.03844	0.03840	0.03841

Table E-2 Raw data of the comparison between ABM and intrinsic modelling at 100°C

	100°C			
V	I(model 1)	I(model 2)	I(model 3)	I(model 4)
0.14	0.03844	0.03844	0.03839	0.03840
0.15	0.03844	0.03844	0.03837	0.03839
0.16	0.03844	0.03844	0.03835	0.03837
0.17	0.03844	0.03844	0.03832	0.03835
0.18	0.03844	0.03843	0.03827	0.03832
0.19	0.03844	0.03843	0.03821	0.03828
0.20	0.03844	0.03843	0.03813	0.03822
0.21	0.03844	0.03843	0.03803	0.03814
0.22	0.03844	0.03843	0.03788	0.03804
0.23	0.03844	0.03842	0.03769	0.03790
0.24	0.03844	0.03842	0.03743	0.03771
0.25	0.03844	0.03841	0.03710	0.03747
0.26	0.03843	0.03840	0.03667	0.03714
0.27	0.03843	0.03839	0.03611	0.03671
0.28	0.03843	0.03837	0.03541	0.03615
0.29	0.03843	0.03835	0.03454	0.03545
0.30	0.03843	0.03832	0.03348	0.03456
0.31	0.03842	0.03828	0.03222	0.03347
0.32	0.03842	0.03822	0.03074	0.03215
0.33	0.03841	0.03815	0.02905	0.03059
0.34	0.03841	0.03804	0.02715	0.02878
0.35	0.03839	0.03790	0.02504	0.02672
0.36	0.03838	0.03772	0.02274	0.02442
0.37	0.03836	0.03747	0.02026	0.02189
0.38	0.03833	0.03714	0.01762	0.01914
0.39	0.03829	0.03672	0.01483	0.01618
0.40	0.03823	0.03618	0.01190	0.01305
0.41	0.03816	0.03549	0.00885	0.00974
0.42	0.03806	0.03463	0.00569	0.00629
0.43	0.03793	0.03359	0.00243	0.00270
0.44	0.03776	0.03235	-0.00091	-0.00102
0.45	0.03752	0.03089	-0.00434	-0.00484
0.46	0.03721	0.02922	-0.00785	-0.00877
0.47	0.03681	0.02733	-0.01142	-0.01278
0.48	0.03629	0.02524	-0.01505	-0.01688
0.49	0.03563	0.02296	-0.01874	-0.02106
0.50	0.03481	0.02049	-0.02247	-0.02530
0.51	0.03380	0.01787	-0.02626	-0.02960
0.52	0.03260	0.01508	-0.03008	-0.03396
0.53	0.03118	0.01217	-0.03395	-0.03837
0.54	0.02955	0.00913	-0.03785	-0.04283
0.55	0.02771	0.00598	-0.04178	-0.04734
0.56	0.02565	0.00272	-0.04575	-0.05188
0.57	0.02341	-0.00062	-0.04974	-0.05646
0.58	0.02097	-0.00405	-0.05376	-0.06108
0.59	0.01838	-0.00754	-0.05780	-0.06573
0.60	0.01562	-0.01111	-0.06187	-0.07041
0.61	0.01273	-0.01474	-0.06596	-0.07511
0.62	0.00971	-0.01842	-0.07007	-0.07985
0.63	0.00658	-0.02215	-0.07420	-0.08461
0.64	0.00335	-0.02594	-0.07835	-0.08939
0.65	0.00002	-0.02976	-0.08251	-0.09419
0.66	-0.00339	-0.03362	-0.08669	-0.09901
0.67	-0.00688	-0.03752	-0.09089	-0.10385
0.68	-0.01043	-0.04145	-0.09510	-0.10872
0.69	-0.01405	-0.04541	-0.09932	-0.11359

Table E-2 continued

	100°C			
V	I(model 1)	I(model 2)	I(model 3)	I(model 4)
0.70	-0.01772	-0.04941	-0.10356	-0.11849
0.71	-0.02144	-0.05342	-0.10780	-0.12340
0.72	-0.02522	-0.05747	-0.11206	-0.12832
0.73	-0.02903	-0.06153	-0.11633	-0.13326
0.74	-0.03289	-0.06562	-0.12062	-0.13821
0.75	-0.03678	-0.06973	-0.12491	-0.14317
0.76	-0.04070	-0.07386	-0.12921	-0.14815
0.77	-0.04466	-0.07801	-0.13352	-0.15314
0.78	-0.04865	-0.08217	-0.13784	-0.15813
0.79	-0.05266	-0.08635	-0.14216	-0.16314
0.80	-0.05670	-0.09054	-0.14650	-0.16816

Table E-2 continued

Appendix E.2 Changes in input irradiance

In this section the simulation raw data of the second verification step, the changes in irradiance, are shown, as extracted from PSPICE.

	R_s constant				R_s variable			
V	I(1000W/m²)	I(750W/m²)	I(500W/m²)	I(250W/m²)	I(1000W/m²)	I(750W/m²)	I(500W/m²)	I(250W/m²)
0.0	8.68000	6.51000	4.34000	2.17000	8.68000	6.51000	4.34000	2.17000
0.1	8.68000	6.51000	4.34000	2.17000	8.68000	6.51000	4.34000	2.17000
0.2	8.68000	6.51000	4.34000	2.17000	8.68000	6.51000	4.34000	2.17000
0.3	8.68000	6.51000	4.34000	2.17000	8.68000	6.51000	4.34000	2.17000
0.4	8.68000	6.51000	4.34000	2.17000	8.68000	6.51000	4.34000	2.17000
0.5	8.68000	6.51000	4.34000	2.17000	8.68000	6.51000	4.34000	2.17000
0.6	8.68000	6.51000	4.34000	2.17000	8.68000	6.51000	4.34000	2.17000
0.7	8.68000	6.51000	4.34000	2.17000	8.68000	6.51000	4.34000	2.17000
0.8	8.68000	6.51000	4.34000	2.17000	8.68000	6.51000	4.34000	2.17000
0.9	8.68000	6.51000	4.34000	2.17000	8.68000	6.51000	4.34000	2.17000
1.0	8.68000	6.51000	4.34000	2.17000	8.68000	6.51000	4.34000	2.17000
1.1	8.68000	6.51000	4.34000	2.17000	8.68000	6.51000	4.34000	2.17000
1.2	8.68000	6.51000	4.34000	2.17000	8.68000	6.51000	4.34000	2.17000
1.3	8.68000	6.51000	4.34000	2.17000	8.68000	6.51000	4.34000	2.17000
1.4	8.68000	6.51000	4.34000	2.17000	8.68000	6.51000	4.34000	2.17000
1.5	8.68000	6.51000	4.34000	2.17000	8.68000	6.51000	4.34000	2.17000
1.6	8.68000	6.51000	4.34000	2.17000	8.68000	6.51000	4.34000	2.17000
1.7	8.68000	6.51000	4.34000	2.17000	8.68000	6.51000	4.34000	2.17000
1.8	8.68000	6.51000	4.34000	2.17000	8.68000	6.51000	4.34000	2.17000
1.9	8.68000	6.51000	4.34000	2.17000	8.68000	6.51000	4.34000	2.17000
2.0	8.68000	6.51000	4.34000	2.17000	8.68000	6.51000	4.34000	2.17000
2.1	8.68000	6.51000	4.34000	2.17000	8.68000	6.51000	4.34000	2.17000
2.2	8.68000	6.51000	4.34000	2.17000	8.68000	6.51000	4.34000	2.17000
2.3	8.68000	6.51000	4.34000	2.17000	8.68000	6.51000	4.34000	2.17000
2.4	8.68000	6.51000	4.34000	2.17000	8.68000	6.51000	4.34000	2.17000
2.5	8.68000	6.51000	4.34000	2.17000	8.68000	6.51000	4.34000	2.17000
2.6	8.68000	6.51000	4.34000	2.17000	8.68000	6.51000	4.34000	2.17000
2.7	8.68000	6.51000	4.34000	2.17000	8.68000	6.51000	4.34000	2.17000
2.8	8.68000	6.51000	4.34000	2.17000	8.68000	6.51000	4.34000	2.17000
2.9	8.68000	6.51000	4.34000	2.17000	8.68000	6.51000	4.34000	2.17000
3.0	8.68000	6.51000	4.34000	2.17000	8.68000	6.51000	4.34000	2.17000
3.1	8.68000	6.51000	4.34000	2.17000	8.68000	6.51000	4.34000	2.17000
3.2	8.68000	6.51000	4.34000	2.17000	8.68000	6.51000	4.34000	2.17000
3.3	8.68000	6.51000	4.34000	2.17000	8.68000	6.51000	4.34000	2.17000

Table E-3 Raw data of simulation with changes in irradiance, where R_s in constant and variable

	R_s constant				R_s variable			
V	I(1000W/m²)	I(750W/m²)	I(500W/m²)	I(250W/m²)	I(1000W/m²)	I(750W/m²)	I(500W/m²)	I(250W/m²)
3.4	8.68000	6.51000	4.34000	2.17000	8.68000	6.51000	4.34000	2.17000
3.5	8.68000	6.51000	4.34000	2.17000	8.68000	6.51000	4.34000	2.17000
3.6	8.68000	6.51000	4.34000	2.17000	8.68000	6.51000	4.34000	2.17000
3.7	8.68000	6.51000	4.34000	2.17000	8.68000	6.51000	4.34000	2.17000
3.8	8.68000	6.51000	4.34000	2.17000	8.68000	6.51000	4.34000	2.17000
3.9	8.68000	6.51000	4.34000	2.17000	8.68000	6.51000	4.34000	2.17000
4.0	8.68000	6.51000	4.34000	2.17000	8.68000	6.51000	4.34000	2.17000
4.1	8.68000	6.51000	4.34000	2.17000	8.68000	6.51000	4.34000	2.17000
4.2	8.68000	6.51000	4.34000	2.17000	8.68000	6.51000	4.34000	2.17000
4.3	8.68000	6.51000	4.34000	2.17000	8.68000	6.51000	4.34000	2.17000
4.4	8.68000	6.51000	4.34000	2.17000	8.68000	6.51000	4.34000	2.17000
4.5	8.68000	6.51000	4.34000	2.17000	8.68000	6.51000	4.34000	2.17000
4.6	8.68000	6.51000	4.34000	2.17000	8.68000	6.51000	4.34000	2.17000
4.7	8.68000	6.51000	4.34000	2.17000	8.68000	6.51000	4.34000	2.17000
4.8	8.68000	6.51000	4.34000	2.17000	8.68000	6.51000	4.34000	2.17000
4.9	8.68000	6.51000	4.34000	2.17000	8.68000	6.51000	4.34000	2.17000
5.0	8.68000	6.51000	4.34000	2.17000	8.68000	6.51000	4.34000	2.17000
5.1	8.68000	6.51000	4.34000	2.17000	8.68000	6.51000	4.34000	2.17000
5.2	8.68000	6.51000	4.34000	2.17000	8.68000	6.51000	4.34000	2.17000
5.3	8.68000	6.51000	4.34000	2.17000	8.68000	6.51000	4.34000	2.17000
5.4	8.68000	6.51000	4.34000	2.17000	8.68000	6.51000	4.34000	2.17000
5.5	8.68000	6.51000	4.34000	2.17000	8.68000	6.51000	4.34000	2.17000
5.6	8.68000	6.51000	4.34000	2.17000	8.68000	6.51000	4.34000	2.17000
5.7	8.68000	6.51000	4.34000	2.17000	8.68000	6.51000	4.34000	2.17000
5.8	8.68000	6.51000	4.34000	2.17000	8.68000	6.51000	4.34000	2.17000
5.9	8.68000	6.51000	4.34000	2.17000	8.68000	6.51000	4.34000	2.17000
6.0	8.68000	6.51000	4.34000	2.17000	8.68000	6.51000	4.34000	2.17000
6.1	8.68000	6.51000	4.34000	2.17000	8.68000	6.51000	4.34000	2.17000
6.2	8.68000	6.51000	4.34000	2.17000	8.68000	6.51000	4.34000	2.17000
6.3	8.68000	6.51000	4.34000	2.17000	8.68000	6.51000	4.34000	2.17000
6.4	8.68000	6.51000	4.34000	2.17000	8.68000	6.51000	4.34000	2.17000
6.5	8.68000	6.51000	4.34000	2.17000	8.68000	6.51000	4.34000	2.17000
6.6	8.68000	6.51000	4.34000	2.17000	8.68000	6.51000	4.34000	2.17000
6.7	8.68000	6.51000	4.34000	2.17000	8.68000	6.51000	4.34000	2.17000
6.8	8.68000	6.51000	4.34000	2.17000	8.68000	6.51000	4.34000	2.17000
6.9	8.68000	6.51000	4.34000	2.17000	8.68000	6.51000	4.34000	2.17000
7.0	8.68000	6.51000	4.34000	2.17000	8.68000	6.51000	4.34000	2.17000
7.1	8.68000	6.51000	4.34000	2.17000	8.68000	6.51000	4.34000	2.17000
7.2	8.68000	6.51000	4.34000	2.17000	8.68000	6.51000	4.34000	2.17000
7.3	8.68000	6.51000	4.34000	2.17000	8.68000	6.51000	4.34000	2.17000
7.4	8.68000	6.51000	4.34000	2.17000	8.68000	6.51000	4.34000	2.17000
7.5	8.68000	6.51000	4.34000	2.17000	8.68000	6.51000	4.34000	2.17000
7.6	8.68000	6.51000	4.34000	2.17000	8.68000	6.51000	4.34000	2.17000
7.7	8.68000	6.51000	4.34000	2.17000	8.68000	6.51000	4.34000	2.17000
7.8	8.68000	6.51000	4.34000	2.17000	8.68000	6.51000	4.34000	2.17000
7.9	8.68000	6.51000	4.34000	2.17000	8.68000	6.51000	4.34000	2.17000
8.0	8.68000	6.51000	4.34000	2.17000	8.68000	6.51000	4.34000	2.17000
8.1	8.68000	6.51000	4.34000	2.17000	8.68000	6.51000	4.34000	2.17000
8.2	8.68000	6.51000	4.34000	2.17000	8.68000	6.51000	4.34000	2.17000
8.3	8.68000	6.51000	4.34000	2.17000	8.68000	6.51000	4.34000	2.17000
8.4	8.68000	6.51000	4.34000	2.17000	8.68000	6.51000	4.34000	2.17000
8.5	8.68000	6.51000	4.34000	2.17000	8.68000	6.51000	4.34000	2.17000
8.6	8.68000	6.51000	4.34000	2.17000	8.68000	6.51000	4.34000	2.17000
8.7	8.68000	6.51000	4.34000	2.17000	8.68000	6.51000	4.34000	2.17000
8.8	8.68000	6.51000	4.34000	2.17000	8.68000	6.51000	4.34000	2.17000
8.9	8.68000	6.51000	4.34000	2.17000	8.68000	6.51000	4.34000	2.17000
9.0	8.68000	6.51000	4.34000	2.17000	8.68000	6.51000	4.34000	2.17000

Table E-3 continued

	R_s constant				R_s variable			
V	I(1000W/m²)	I(750W/m²)	I(500W/m²)	I(250W/m²)	I(1000W/m²)	I(750W/m²)	I(500W/m²)	I(250W/m²)
9.1	8.68000	6.51000	4.34000	2.17000	8.68000	6.51000	4.34000	2.17000
9.2	8.68000	6.51000	4.34000	2.17000	8.68000	6.51000	4.34000	2.17000
9.3	8.68000	6.51000	4.34000	2.17000	8.68000	6.51000	4.34000	2.17000
9.4	8.68000	6.51000	4.34000	2.17000	8.68000	6.51000	4.34000	2.17000
9.5	8.68000	6.51000	4.34000	2.17000	8.68000	6.51000	4.34000	2.17000
9.6	8.68000	6.51000	4.34000	2.17000	8.68000	6.51000	4.34000	2.17000
9.7	8.68000	6.51000	4.34000	2.17000	8.68000	6.51000	4.34000	2.17000
9.8	8.68000	6.51000	4.34000	2.17000	8.68000	6.51000	4.34000	2.17000
9.9	8.68000	6.51000	4.34000	2.17000	8.68000	6.51000	4.34000	2.17000
10.0	8.68000	6.51000	4.34000	2.17000	8.68000	6.51000	4.34000	2.17000
10.1	8.68000	6.51000	4.34000	2.17000	8.68000	6.51000	4.34000	2.17000
10.2	8.68000	6.51000	4.34000	2.17000	8.68000	6.51000	4.34000	2.17000
10.3	8.68000	6.51000	4.34000	2.17000	8.68000	6.51000	4.34000	2.17000
10.4	8.68000	6.51000	4.34000	2.17000	8.68000	6.51000	4.34000	2.17000
10.5	8.68000	6.51000	4.34000	2.17000	8.68000	6.51000	4.34000	2.17000
10.6	8.68000	6.51000	4.34000	2.17000	8.68000	6.51000	4.34000	2.17000
10.7	8.68000	6.51000	4.34000	2.17000	8.68000	6.51000	4.34000	2.17000
10.8	8.68000	6.51000	4.34000	2.17000	8.68000	6.51000	4.34000	2.17000
10.9	8.68000	6.51000	4.34000	2.17000	8.68000	6.51000	4.34000	2.17000
11.0	8.68000	6.51000	4.34000	2.17000	8.68000	6.51000	4.34000	2.17000
11.1	8.68000	6.51000	4.34000	2.17000	8.68000	6.51000	4.34000	2.17000
11.2	8.68000	6.51000	4.34000	2.17000	8.68000	6.51000	4.34000	2.17000
11.3	8.68000	6.51000	4.34000	2.17000	8.68000	6.51000	4.34000	2.17000
11.4	8.68000	6.51000	4.34000	2.17000	8.68000	6.51000	4.34000	2.17000
11.5	8.68000	6.51000	4.34000	2.17000	8.68000	6.51000	4.34000	2.17000
11.6	8.67999	6.51000	4.34000	2.17000	8.67999	6.50999	4.33999	2.16999
11.7	8.67999	6.51000	4.34000	2.17000	8.67999	6.50999	4.33999	2.16999
11.8	8.67999	6.51000	4.34000	2.17000	8.67999	6.50999	4.33999	2.16999
11.9	8.67999	6.51000	4.34000	2.17000	8.67999	6.50999	4.33999	2.16999
12.0	8.67999	6.51000	4.34000	2.17000	8.67999	6.50999	4.33999	2.16999
12.1	8.67998	6.51000	4.34000	2.17000	8.67998	6.50998	4.33998	2.16998
12.2	8.67998	6.51000	4.34000	2.17000	8.67998	6.50998	4.33998	2.16998
12.3	8.67997	6.51000	4.34000	2.17000	8.67997	6.50997	4.33997	2.16997
12.4	8.67997	6.51000	4.34000	2.17000	8.67997	6.50997	4.33997	2.16997
12.5	8.67996	6.51000	4.34000	2.17000	8.67996	6.50996	4.33996	2.16996
12.6	8.67995	6.50999	4.34000	2.17000	8.67995	6.50995	4.33995	2.16995
12.7	8.67994	6.50999	4.34000	2.17000	8.67994	6.50994	4.33994	2.16994
12.8	8.67992	6.50999	4.34000	2.17000	8.67992	6.50992	4.33992	2.16993
12.9	8.67990	6.50999	4.34000	2.17000	8.67990	6.50990	4.33991	2.16991
13.0	8.67988	6.50999	4.34000	2.17000	8.67988	6.50988	4.33988	2.16989
13.1	8.67985	6.50998	4.34000	2.17000	8.67985	6.50985	4.33985	2.16986
13.2	8.67981	6.50998	4.34000	2.17000	8.67981	6.50982	4.33982	2.16983
13.3	8.67977	6.50997	4.34000	2.17000	8.67977	6.50977	4.33978	2.16978
13.4	8.67971	6.50997	4.34000	2.17000	8.67971	6.50972	4.33972	2.16973
13.5	8.67964	6.50996	4.33999	2.17000	8.67964	6.50965	4.33965	2.16967
13.6	8.67956	6.50995	4.33999	2.17000	8.67956	6.50956	4.33957	2.16959
13.7	8.67945	6.50993	4.33999	2.17000	8.67945	6.50946	4.33947	2.16949
13.8	8.67932	6.50992	4.33999	2.17000	8.67932	6.50933	4.33934	2.16936
13.9	8.67915	6.50990	4.33999	2.17000	8.67915	6.50916	4.33918	2.16921
14.0	8.67895	6.50987	4.33998	2.17000	8.67895	6.50896	4.33898	2.16902
14.1	8.67869	6.50984	4.33998	2.17000	8.67869	6.50871	4.33874	2.16878
14.2	8.67838	6.50981	4.33998	2.17000	8.67838	6.50840	4.33844	2.16849
14.3	8.67799	6.50976	4.33997	2.17000	8.67799	6.50802	4.33806	2.16813
14.4	8.67751	6.50970	4.33996	2.17000	8.67751	6.50754	4.33759	2.16768
14.5	8.67691	6.50963	4.33996	2.16999	8.67691	6.50695	4.33702	2.16713
14.6	8.67616	6.50954	4.33994	2.16999	8.67616	6.50622	4.33630	2.16645
14.7	8.67524	6.50943	4.33993	2.16999	8.67524	6.50532	4.33542	2.16561

Table E-3 continued

	R_s constant				R_s variable			
V	I(1000W/m²)	I(750W/m²)	I(500W/m²)	I(250W/m²)	I(1000W/m²)	I(750W/m²)	I(500W/m²)	I(250W/m²)
14.8	8.67410	6.50929	4.33991	2.16999	8.67410	6.50420	4.33433	2.16457
14.9	8.67269	6.50912	4.33989	2.16999	8.67269	6.50281	4.33298	2.16329
15.0	8.67094	6.50891	4.33987	2.16998	8.67094	6.50110	4.33132	2.16173
15.1	8.66878	6.50865	4.33984	2.16998	8.66878	6.49898	4.32926	2.15981
15.2	8.66612	6.50832	4.33980	2.16998	8.66612	6.49637	4.32674	2.15746
15.3	8.66282	6.50792	4.33975	2.16997	8.66282	6.49315	4.32364	2.15461
15.4	8.65876	6.50742	4.33969	2.16996	8.65876	6.48919	4.31985	2.15115
15.5	8.65377	6.50680	4.33961	2.16995	8.65377	6.48434	4.31521	2.14698
15.6	8.64764	6.50603	4.33952	2.16994	8.64764	6.47839	4.30957	2.14198
15.7	8.64013	6.50507	4.33941	2.16993	8.64013	6.47114	4.30273	2.13602
15.8	8.63096	6.50389	4.33926	2.16991	8.63096	6.46232	4.29448	2.12897
15.9	8.61979	6.50243	4.33908	2.16989	8.61979	6.45164	4.28458	2.12068
16.0	8.60626	6.50062	4.33886	2.16986	8.60626	6.43877	4.27278	2.11103
16.1	8.58992	6.49839	4.33859	2.16983	8.58992	6.42335	4.25880	2.09991
16.2	8.57032	6.49563	4.33825	2.16979	8.57032	6.40499	4.24239	2.08719
16.3	8.54694	6.49222	4.33783	2.16974	8.54694	6.38329	4.22328	2.07280
16.4	8.51926	6.48802	4.33731	2.16968	8.51926	6.35785	4.20122	2.05667
16.5	8.48674	6.48286	4.33666	2.16960	8.48674	6.32829	4.17601	2.03877
16.6	8.44886	6.47652	4.33586	2.16950	8.44886	6.29424	4.14746	2.01909
16.7	8.40512	6.46876	4.33487	2.16938	8.40512	6.25540	4.11546	1.99765
16.8	8.35511	6.45929	4.33364	2.16923	8.35511	6.21153	4.07993	1.97447
16.9	8.29847	6.44776	4.33211	2.16905	8.29847	6.16247	4.04086	1.94962
17.0	8.23496	6.43380	4.33023	2.16882	8.23496	6.10810	3.99826	1.92315
17.1	8.16443	6.41697	4.32790	2.16853	8.16443	6.04844	3.95222	1.89515
17.2	8.08683	6.39679	4.32503	2.16818	8.08683	5.98352	3.90283	1.86570
17.3	8.00222	6.37274	4.32148	2.16774	8.00222	5.91347	3.85022	1.83487
17.4	7.91071	6.34431	4.31711	2.16720	7.91071	5.83845	3.79454	1.80276
17.5	7.81254	6.31094	4.31174	2.16652	7.81254	5.75867	3.73597	1.76944
17.6	7.70795	6.27213	4.30515	2.16569	7.70795	5.67435	3.67465	1.73500
17.7	7.59726	6.22739	4.29709	2.16465	7.59726	5.58575	3.61077	1.69952
17.8	7.48075	6.17630	4.28725	2.16337	7.48075	5.49310	3.54448	1.66305
17.9	7.35879	6.11855	4.27529	2.16178	7.35879	5.39667	3.47595	1.62568
18.0	7.23170	6.05388	4.26081	2.15982	7.23170	5.29669	3.40533	1.58747
18.1	7.09981	5.98217	4.24337	2.15740	7.09981	5.19341	3.33276	1.54847
18.2	6.96344	5.90339	4.22249	2.15440	6.96344	5.08705	3.25838	1.50874
18.3	6.82289	5.81761	4.19765	2.15071	6.82289	4.97782	3.18232	1.46833
18.4	6.67846	5.72496	4.16831	2.14617	6.67846	4.86593	3.10468	1.42728
18.5	6.53041	5.62568	4.13395	2.14058	6.53041	4.75155	3.02558	1.38564
18.6	6.37899	5.52002	4.09403	2.13373	6.37899	4.63486	2.94512	1.34344
18.7	6.22444	5.40829	4.04810	2.12535	6.22444	4.51602	2.86339	1.30073
18.8	6.06697	5.29081	3.99576	2.11513	6.06697	4.39517	2.78048	1.25752
18.9	5.90678	5.16792	3.93670	2.10272	5.90678	4.27246	2.69646	1.21387
19.0	5.74405	5.03995	3.87069	2.08771	5.74405	4.14799	2.61140	1.16978
19.1	5.57896	4.90723	3.79762	2.06966	5.57896	4.02189	2.52537	1.12529
19.2	5.41166	4.77007	3.71749	2.04806	5.41166	3.89426	2.43843	1.08043
19.3	5.24229	4.62879	3.63038	2.02240	5.24229	3.76521	2.35064	1.03521
19.4	5.07098	4.48365	3.53645	1.99214	5.07098	3.63481	2.26204	0.98965
19.5	4.89785	4.33494	3.43592	1.95674	4.89785	3.50314	2.17269	0.94377
19.6	4.72302	4.18290	3.32907	1.91571	4.72302	3.37030	2.08262	0.89759
19.7	4.54658	4.02775	3.21622	1.86858	4.54658	3.23634	1.99189	0.85113
19.8	4.36864	3.86972	3.09767	1.81498	4.36864	3.10132	1.90052	0.80440
19.9	4.18927	3.70899	2.97378	1.75459	4.18927	2.96532	1.80855	0.75742
20.0	4.00857	3.54576	2.84488	1.68724	4.00857	2.82838	1.71601	0.71019
20.1	3.82660	3.38018	2.71128	1.61282	3.82660	2.69055	1.62294	0.66273
20.2	3.64343	3.21242	2.57331	1.53134	3.64343	2.55188	1.52936	0.61505
20.3	3.45914	3.04260	2.43127	1.44290	3.45914	2.41242	1.43529	0.56716
20.4	3.27376	2.87087	2.28543	1.34769	3.27376	2.27221	1.34076	0.51908

Table E-3 continued

	R_s constant				R_s variable			
V	I(1000W/m²)	I(750W/m²)	I(500W/m²)	I(250W/m²)	I(1000W/m²)	I(750W/m²)	I(500W/m²)	I(250W/m²)
20.5	3.08738	2.69733	2.13606	1.24593	3.08738	2.13128	1.24579	0.47080
20.6	2.90002	2.52211	1.98340	1.13791	2.90002	1.98966	1.15041	0.42234
20.7	2.71175	2.34530	1.82769	1.02393	2.71175	1.84740	1.05463	0.37371
20.8	2.52260	2.16699	1.66913	0.90434	2.52260	1.70452	0.95847	0.32491
20.9	2.33262	1.98727	1.50791	0.77946	2.33262	1.56106	0.86195	0.27596
21.0	2.14185	1.80623	1.34421	0.64963	2.14185	1.41703	0.76508	0.22685
21.1	1.95032	1.62393	1.17820	0.51518	1.95032	1.27246	0.66788	0.17760
21.2	1.75807	1.44044	1.01003	0.37640	1.75807	1.12739	0.57037	0.12820
21.3	1.56513	1.25583	0.83984	0.23361	1.56513	0.98182	0.47255	0.07867
21.4	1.37153	1.07016	0.66775	0.08708	1.37153	0.83578	0.37444	0.02902
21.5	1.17729	0.88347	0.49389	-0.06294	1.17729	0.68930	0.27605	-0.02077
21.6	0.98245	0.69583	0.31835	-0.21620	0.98245	0.54238	0.17739	-0.07067
21.7	0.78703	0.50727	0.14124	-0.37248	0.78703	0.39504	0.07847	-0.12068
21.8	0.59106	0.31785	-0.03734	-0.53156	0.59106	0.24731	-0.02069	-0.17081
21.9	0.39454	0.12760	-0.21732	-0.69327	0.39454	0.09920	-0.12009	-0.22104
22.0	0.19752	-0.06344	-0.39861	-0.85742	0.19752	-0.04928	-0.21972	-0.27138
22.1	0.00000	-0.25522	-0.58114	-1.02385	0.00000	-0.19811	-0.31957	-0.32182
22.2	-0.19799	-0.44773	-0.76485	-1.19242	-0.19799	-0.34728	-0.41964	-0.37235
22.3	-0.39645	-0.64092	-0.94966	-1.36299	-0.39645	-0.49679	-0.51991	-0.42297
22.4	-0.59534	-0.83477	-1.13554	-1.53543	-0.59534	-0.64660	-0.62037	-0.47369
22.5	-0.79466	-1.02925	-1.32241	-1.70962	-0.79466	-0.79673	-0.72103	-0.52449

Table E-3 continued

Appendix E.3 Changes in ambient temperature

In this section the simulation raw data of the third verification step, changes in ambient temperature, are shown, as extracted from PSPICE.

	R_s constant				R_s variable			
V	I(0°C)	I(10°C)	I(20°C)	I(30°C)	I(0°C)	I(10°C)	I(20°C)	I(30°C)
0.0	8.71250	8.76450	8.81650	8.86850	8.71250	8.76450	8.81650	8.86850
0.1	8.71250	8.76450	8.81650	8.86850	8.71250	8.76450	8.81650	8.86850
0.2	8.71250	8.76450	8.81650	8.86850	8.71250	8.76450	8.81650	8.86850
0.3	8.71250	8.76450	8.81650	8.86850	8.71250	8.76450	8.81650	8.86850
0.4	8.71250	8.76450	8.81650	8.86850	8.71250	8.76450	8.81650	8.86850
0.5	8.71250	8.76450	8.81650	8.86850	8.71250	8.76450	8.81650	8.86850
0.6	8.71250	8.76450	8.81650	8.86850	8.71250	8.76450	8.81650	8.86850
0.7	8.71250	8.76450	8.81650	8.86850	8.71250	8.76450	8.81650	8.86850
0.8	8.71250	8.76450	8.81650	8.86850	8.71250	8.76450	8.81650	8.86850
0.9	8.71250	8.76450	8.81650	8.86850	8.71250	8.76450	8.81650	8.86850
1.0	8.71250	8.76450	8.81650	8.86850	8.71250	8.76450	8.81650	8.86850
1.1	8.71250	8.76450	8.81650	8.86850	8.71250	8.76450	8.81650	8.86850
1.2	8.71250	8.76450	8.81650	8.86850	8.71250	8.76450	8.81650	8.86850
1.3	8.71250	8.76450	8.81650	8.86850	8.71250	8.76450	8.81650	8.86850
1.4	8.71250	8.76450	8.81650	8.86850	8.71250	8.76450	8.81650	8.86850
1.5	8.71250	8.76450	8.81650	8.86850	8.71250	8.76450	8.81650	8.86850
1.6	8.71250	8.76450	8.81650	8.86850	8.71250	8.76450	8.81650	8.86850
1.7	8.71250	8.76450	8.81650	8.86850	8.71250	8.76450	8.81650	8.86850
1.8	8.71250	8.76450	8.81650	8.86850	8.71250	8.76450	8.81650	8.86850
1.9	8.71250	8.76450	8.81650	8.86850	8.71250	8.76450	8.81650	8.86850
2.0	8.71250	8.76450	8.81650	8.86850	8.71250	8.76450	8.81650	8.86850
2.1	8.71250	8.76450	8.81650	8.86850	8.71250	8.76450	8.81650	8.86850
2.2	8.71250	8.76450	8.81650	8.86850	8.71250	8.76450	8.81650	8.86850
2.3	8.71250	8.76450	8.81650	8.86850	8.71250	8.76450	8.81650	8.86850
2.4	8.71250	8.76450	8.81650	8.86850	8.71250	8.76450	8.81650	8.86850
2.5	8.71250	8.76450	8.81650	8.86850	8.71250	8.76450	8.81650	8.86850

Table E-4 Raw data of simulation with changes in ambient temperature, where R_s is constant and variable

	R_s constant				R_s variable			
V	I(0°C)	I(10°C)	I(20°C)	I(30°C)	I(0°C)	I(10°C)	I(20°C)	I(30°C)
2.6	8.71250	8.76450	8.81650	8.86850	8.71250	8.76450	8.81650	8.86850
2.7	8.71250	8.76450	8.81650	8.86850	8.71250	8.76450	8.81650	8.86850
2.8	8.71250	8.76450	8.81650	8.86850	8.71250	8.76450	8.81650	8.86850
2.9	8.71250	8.76450	8.81650	8.86850	8.71250	8.76450	8.81650	8.86850
3.0	8.71250	8.76450	8.81650	8.86850	8.71250	8.76450	8.81650	8.86850
3.1	8.71250	8.76450	8.81650	8.86850	8.71250	8.76450	8.81650	8.86850
3.2	8.71250	8.76450	8.81650	8.86850	8.71250	8.76450	8.81650	8.86850
3.3	8.71250	8.76450	8.81650	8.86850	8.71250	8.76450	8.81650	8.86850
3.4	8.71250	8.76450	8.81650	8.86850	8.71250	8.76450	8.81650	8.86850
3.5	8.71250	8.76450	8.81650	8.86850	8.71250	8.76450	8.81650	8.86850
3.6	8.71250	8.76450	8.81650	8.86850	8.71250	8.76450	8.81650	8.86850
3.7	8.71250	8.76450	8.81650	8.86850	8.71250	8.76450	8.81650	8.86850
3.8	8.71250	8.76450	8.81650	8.86850	8.71250	8.76450	8.81650	8.86850
3.9	8.71250	8.76450	8.81650	8.86850	8.71250	8.76450	8.81650	8.86850
4.0	8.71250	8.76450	8.81650	8.86850	8.71250	8.76450	8.81650	8.86850
4.1	8.71250	8.76450	8.81650	8.86850	8.71250	8.76450	8.81650	8.86850
4.2	8.71250	8.76450	8.81650	8.86850	8.71250	8.76450	8.81650	8.86850
4.3	8.71250	8.76450	8.81650	8.86850	8.71250	8.76450	8.81650	8.86850
4.4	8.71250	8.76450	8.81650	8.86850	8.71250	8.76450	8.81650	8.86850
4.5	8.71250	8.76450	8.81650	8.86850	8.71250	8.76450	8.81650	8.86850
4.6	8.71250	8.76450	8.81650	8.86850	8.71250	8.76450	8.81650	8.86850
4.7	8.71250	8.76450	8.81650	8.86850	8.71250	8.76450	8.81650	8.86850
4.8	8.71250	8.76450	8.81650	8.86850	8.71250	8.76450	8.81650	8.86850
4.9	8.71250	8.76450	8.81650	8.86850	8.71250	8.76450	8.81650	8.86850
5.0	8.71250	8.76450	8.81650	8.86850	8.71250	8.76450	8.81650	8.86850
5.1	8.71250	8.76450	8.81650	8.86850	8.71250	8.76450	8.81650	8.86850
5.2	8.71250	8.76450	8.81650	8.86850	8.71250	8.76450	8.81650	8.86850
5.3	8.71250	8.76450	8.81650	8.86850	8.71250	8.76450	8.81650	8.86850
5.4	8.71250	8.76450	8.81650	8.86850	8.71250	8.76450	8.81650	8.86850
5.5	8.71250	8.76450	8.81650	8.86850	8.71250	8.76450	8.81650	8.86850
5.6	8.71250	8.76450	8.81650	8.86850	8.71250	8.76450	8.81650	8.86850
5.7	8.71250	8.76450	8.81650	8.86850	8.71250	8.76450	8.81650	8.86850
5.8	8.71250	8.76450	8.81650	8.86850	8.71250	8.76450	8.81650	8.86850
5.9	8.71250	8.76450	8.81650	8.86850	8.71250	8.76450	8.81650	8.86850
6.0	8.71250	8.76450	8.81650	8.86850	8.71250	8.76450	8.81650	8.86850
6.1	8.71250	8.76450	8.81650	8.86850	8.71250	8.76450	8.81650	8.86850
6.2	8.71250	8.76450	8.81650	8.86850	8.71250	8.76450	8.81650	8.86850
6.3	8.71250	8.76450	8.81650	8.86850	8.71250	8.76450	8.81650	8.86850
6.4	8.71250	8.76450	8.81650	8.86850	8.71250	8.76450	8.81650	8.86850
6.5	8.71250	8.76450	8.81650	8.86850	8.71250	8.76450	8.81650	8.86850
6.6	8.71250	8.76450	8.81650	8.86850	8.71250	8.76450	8.81650	8.86850
6.7	8.71250	8.76450	8.81650	8.86850	8.71250	8.76450	8.81650	8.86850
6.8	8.71250	8.76450	8.81650	8.86850	8.71250	8.76450	8.81650	8.86850
6.9	8.71250	8.76450	8.81650	8.86850	8.71250	8.76450	8.81650	8.86850
7.0	8.71250	8.76450	8.81650	8.86850	8.71250	8.76450	8.81650	8.86850
7.1	8.71250	8.76450	8.81650	8.86850	8.71250	8.76450	8.81650	8.86850
7.2	8.71250	8.76450	8.81650	8.86850	8.71250	8.76450	8.81650	8.86850
7.3	8.71250	8.76450	8.81650	8.86850	8.71250	8.76450	8.81650	8.86850
7.4	8.71250	8.76450	8.81650	8.86850	8.71250	8.76450	8.81650	8.86850
7.5	8.71250	8.76450	8.81650	8.86850	8.71250	8.76450	8.81650	8.86850
7.6	8.71250	8.76450	8.81650	8.86850	8.71250	8.76450	8.81650	8.86850
7.7	8.71250	8.76450	8.81650	8.86850	8.71250	8.76450	8.81650	8.86850
7.8	8.71250	8.76450	8.81650	8.86849	8.71250	8.76450	8.81650	8.86850
7.9	8.71250	8.76450	8.81650	8.86849	8.71250	8.76450	8.81650	8.86850
8.0	8.71250	8.76450	8.81650	8.86849	8.71250	8.76450	8.81650	8.86850
8.1	8.71250	8.76450	8.81650	8.86849	8.71250	8.76450	8.81650	8.86850
8.2	8.71250	8.76450	8.81650	8.86849	8.71250	8.76450	8.81650	8.86849

Table E-4 continued

	R_s constant				R_s variable			
V	I(0°C)	I(10°C)	I(20°C)	I(30°C)	I(0°C)	I(10°C)	I(20°C)	I(30°C)
8.3	8.71250	8.76450	8.81650	8.86849	8.71250	8.76450	8.81650	8.86849
8.4	8.71250	8.76450	8.81650	8.86848	8.71250	8.76450	8.81650	8.86849
8.5	8.71250	8.76450	8.81650	8.86848	8.71250	8.76450	8.81650	8.86849
8.6	8.71250	8.76450	8.81650	8.86847	8.71250	8.76450	8.81650	8.86849
8.7	8.71250	8.76450	8.81650	8.86847	8.71250	8.76450	8.81650	8.86849
8.8	8.71250	8.76450	8.81649	8.86846	8.71250	8.76450	8.81650	8.86848
8.9	8.71250	8.76450	8.81649	8.86845	8.71250	8.76450	8.81650	8.86848
9.0	8.71250	8.76450	8.81649	8.86844	8.71250	8.76450	8.81650	8.86847
9.1	8.71250	8.76450	8.81649	8.86843	8.71250	8.76450	8.81649	8.86847
9.2	8.71250	8.76450	8.81649	8.86842	8.71250	8.76450	8.81649	8.86846
9.3	8.71250	8.76450	8.81649	8.86840	8.71250	8.76450	8.81649	8.86846
9.4	8.71250	8.76450	8.81648	8.86838	8.71250	8.76450	8.81649	8.86845
9.5	8.71250	8.76450	8.81648	8.86835	8.71250	8.76450	8.81649	8.86843
9.6	8.71250	8.76450	8.81648	8.86832	8.71250	8.76450	8.81649	8.86842
9.7	8.71250	8.76450	8.81647	8.86828	8.71250	8.76450	8.81648	8.86840
9.8	8.71250	8.76450	8.81646	8.86824	8.71250	8.76450	8.81648	8.86838
9.9	8.71250	8.76449	8.81645	8.86818	8.71250	8.76450	8.81648	8.86836
10.0	8.71250	8.76449	8.81644	8.86812	8.71250	8.76450	8.81647	8.86833
10.1	8.71250	8.76449	8.81643	8.86804	8.71250	8.76449	8.81646	8.86829
10.2	8.71250	8.76449	8.81642	8.86794	8.71250	8.76449	8.81646	8.86825
10.3	8.71250	8.76449	8.81640	8.86782	8.71250	8.76449	8.81645	8.86819
10.4	8.71250	8.76448	8.81638	8.86767	8.71250	8.76449	8.81643	8.86813
10.5	8.71250	8.76448	8.81635	8.86750	8.71250	8.76449	8.81642	8.86805
10.6	8.71250	8.76448	8.81632	8.86728	8.71250	8.76448	8.81640	8.86795
10.7	8.71250	8.76447	8.81628	8.86703	8.71250	8.76448	8.81638	8.86784
10.8	8.71250	8.76446	8.81623	8.86671	8.71250	8.76448	8.81635	8.86770
10.9	8.71249	8.76446	8.81617	8.86633	8.71250	8.76447	8.81632	8.86753
11.0	8.71249	8.76445	8.81610	8.86588	8.71249	8.76446	8.81628	8.86732
11.1	8.71249	8.76443	8.81601	8.86532	8.71249	8.76445	8.81623	8.86707
11.2	8.71249	8.76442	8.81590	8.86465	8.71249	8.76444	8.81617	8.86677
11.3	8.71249	8.76440	8.81577	8.86383	8.71249	8.76443	8.81610	8.86640
11.4	8.71248	8.76438	8.81561	8.86284	8.71249	8.76442	8.81601	8.86595
11.5	8.71248	8.76435	8.81541	8.86165	8.71248	8.76440	8.81591	8.86542
11.6	8.71248	8.76431	8.81518	8.86020	8.71248	8.76437	8.81578	8.86476
11.7	8.71247	8.76427	8.81489	8.85846	8.71248	8.76435	8.81562	8.86397
11.8	8.71246	8.76422	8.81453	8.85635	8.71247	8.76431	8.81543	8.86301
11.9	8.71246	8.76415	8.81410	8.85380	8.71246	8.76427	8.81519	8.86185
12.0	8.71245	8.76408	8.81357	8.85072	8.71245	8.76421	8.81491	8.86045
12.1	8.71243	8.76398	8.81293	8.84701	8.71244	8.76415	8.81456	8.85875
12.2	8.71242	8.76386	8.81215	8.84255	8.71243	8.76407	8.81413	8.85670
12.3	8.71240	8.76372	8.81120	8.83719	8.71241	8.76397	8.81361	8.85422
12.4	8.71237	8.76354	8.81005	8.83075	8.71239	8.76385	8.81298	8.85123
12.5	8.71234	8.76332	8.80864	8.82303	8.71237	8.76370	8.81221	8.84762
12.6	8.71231	8.76305	8.80693	8.81381	8.71234	8.76352	8.81127	8.84327
12.7	8.71226	8.76272	8.80485	8.80283	8.71230	8.76330	8.81012	8.83804
12.8	8.71221	8.76232	8.80232	8.78978	8.71225	8.76303	8.80873	8.83175
12.9	8.71214	8.76182	8.79926	8.77433	8.71219	8.76269	8.80704	8.82420
13.0	8.71205	8.76122	8.79554	8.75612	8.71212	8.76228	8.80498	8.81517
13.1	8.71195	8.76047	8.79104	8.73476	8.71203	8.76178	8.80248	8.80438
13.2	8.71182	8.75956	8.78560	8.70984	8.71191	8.76116	8.79944	8.79153
13.3	8.71165	8.75845	8.77903	8.68092	8.71178	8.76040	8.79576	8.77629
13.4	8.71145	8.75708	8.77112	8.64757	8.71160	8.75948	8.79129	8.75826
13.5	8.71121	8.75541	8.76162	8.60940	8.71139	8.75834	8.78589	8.73704
13.6	8.71091	8.75336	8.75025	8.56601	8.71113	8.75695	8.77937	8.71218
13.7	8.71053	8.75086	8.73668	8.51706	8.71081	8.75525	8.77151	8.68321
13.8	8.71007	8.74781	8.72055	8.46225	8.71042	8.75317	8.76206	8.64965
13.9	8.70950	8.74408	8.70146	8.40138	8.70993	8.75062	8.75072	8.61104

Table E-4 continued

	R_s constant				R_s variable			
V	I(0°C)	I(10°C)	I(20°C)	I(30°C)	I(0°C)	I(10°C)	I(20°C)	I(30°C)
14.0	8.70879	8.73954	8.67899	8.33429	8.70932	8.74751	8.73717	8.56691
14.1	8.70792	8.73403	8.65270	8.26090	8.70857	8.74372	8.72103	8.51686
14.2	8.70685	8.72733	8.62213	8.18121	8.70765	8.73910	8.70190	8.46050
14.3	8.70552	8.71922	8.58683	8.09528	8.70652	8.73347	8.67932	8.39754
14.4	8.70389	8.70942	8.54637	8.00323	8.70512	8.72665	8.65282	8.32776
14.5	8.70188	8.69763	8.50037	7.90523	8.70339	8.71838	8.62191	8.25101
14.6	8.69941	8.68350	8.44848	7.80148	8.70127	8.70839	8.58611	8.16722
14.7	8.69637	8.66662	8.39043	7.69222	8.69865	8.69636	8.54493	8.07641
14.8	8.69264	8.64658	8.32603	7.57769	8.69544	8.68192	8.49793	7.97867
14.9	8.68807	8.62290	8.25516	7.45817	8.69150	8.66468	8.44472	7.87415
15.0	8.68248	8.59512	8.17779	7.33391	8.68667	8.64417	8.38497	7.76304
15.1	8.67564	8.56275	8.09396	7.20519	8.68076	8.61993	8.31842	7.64558
15.2	8.66732	8.52532	8.00378	7.07226	8.67354	8.59146	8.24491	7.52205
15.3	8.65721	8.48238	7.90741	6.93538	8.66475	8.55824	8.16437	7.39273
15.4	8.64497	8.43354	7.80504	6.79477	8.65409	8.51978	8.07680	7.25790
15.5	8.63023	8.37848	7.69694	6.65069	8.64119	8.47561	7.98228	7.11788
15.6	8.61255	8.31696	7.58337	6.50333	8.62566	8.42530	7.88097	6.97295
15.7	8.59146	8.24880	7.46460	6.35292	8.60706	8.36850	7.77307	6.82341
15.8	8.56646	8.17394	7.34090	6.19962	8.58489	8.30494	7.65882	6.66952
15.9	8.53705	8.09238	7.21258	6.04362	8.55866	8.23443	7.53851	6.51156
16.0	8.50271	8.00423	7.07990	5.88510	8.52783	8.15688	7.41242	6.34978
16.1	8.46295	7.90964	6.94313	5.72419	8.49188	8.07230	7.28087	6.18441
16.2	8.41731	7.80880	6.80252	5.56105	8.45032	7.98075	7.14416	6.01568
16.3	8.36541	7.70198	6.65833	5.39581	8.40269	7.88241	7.00259	5.84380
16.4	8.30694	7.58945	6.51078	5.22859	8.34863	7.77747	6.85646	5.66895
16.5	8.24170	7.47150	6.36008	5.05950	8.28783	7.66620	6.70605	5.49133
16.6	8.16954	7.34844	6.20644	4.88866	8.22008	7.54888	6.55163	5.31110
16.7	8.09046	7.22056	6.05005	4.71615	8.14529	7.42582	6.39346	5.12842
16.8	8.00452	7.08817	5.89107	4.54208	8.06344	7.29734	6.23177	4.94342
16.9	7.91187	6.95154	5.72967	4.36653	7.97464	7.16374	6.06680	4.75626
17.0	7.81271	6.81095	5.56599	4.18957	7.87902	7.02535	5.89875	4.56705
17.1	7.70729	6.66667	5.40019	4.01128	7.77682	6.88246	5.72782	4.37590
17.2	7.59592	6.51892	5.23238	3.83174	7.66829	6.73537	5.55418	4.18294
17.3	7.47889	6.36795	5.06268	3.65099	7.55375	6.58435	5.37801	3.98825
17.4	7.35653	6.21396	4.89121	3.46911	7.43351	6.42965	5.19946	3.79193
17.5	7.22916	6.05715	4.71807	3.28615	7.30789	6.27152	5.01868	3.59407
17.6	7.09709	5.89771	4.54335	3.10215	7.17722	6.11019	4.83580	3.39474
17.7	6.96064	5.73580	4.36713	2.91718	7.04183	5.94587	4.65094	3.19403
17.8	6.82009	5.57158	4.18951	2.73127	6.90202	5.77874	4.46422	2.99200
17.9	6.67572	5.40519	4.01055	2.54447	6.75809	5.60900	4.27574	2.78872
18.0	6.52778	5.23678	3.83033	2.35682	6.61031	5.43681	4.08560	2.58425
18.1	6.37653	5.06646	3.64891	2.16835	6.45895	5.26232	3.89390	2.37864
18.2	6.22219	4.89434	3.46636	1.97910	6.30426	5.08567	3.70071	2.17196
18.3	6.06496	4.72054	3.28272	1.78911	6.14645	4.90700	3.50612	1.96424
18.4	5.90504	4.54515	3.09806	1.59840	5.98573	4.72643	3.31020	1.75554
18.5	5.74261	4.36826	2.91242	1.40701	5.82232	4.54406	3.11302	1.54590
18.6	5.57783	4.18996	2.72584	1.21496	5.65637	4.36001	2.91464	1.33537
18.7	5.41085	4.01031	2.53838	1.02228	5.48805	4.17437	2.71512	1.12397
18.8	5.24181	3.82941	2.35007	0.82899	5.31753	3.98723	2.51451	0.91175
18.9	5.07085	3.64730	2.16095	0.63512	5.14493	3.79867	2.31288	0.69875
19.0	4.89807	3.46405	1.97106	0.44069	4.97039	3.60877	2.11026	0.48498
19.1	4.72360	3.27973	1.78042	0.24572	4.79402	3.41760	1.90670	0.27050
19.2	4.54752	3.09438	1.58908	0.05023	4.61594	3.22522	1.70225	0.05531
19.3	4.36994	2.90805	1.39706	-0.14576	4.43625	3.03170	1.49694	-0.16054
19.4	4.19093	2.72080	1.20439	-0.34223	4.25504	2.83710	1.29081	-0.37704
19.5	4.01058	2.53267	1.01109	-0.53917	4.07239	2.64146	1.08390	-0.59416
19.6	3.82897	2.34369	0.81719	-0.73656	3.88840	2.44484	0.87624	-0.81187

Table E-4 continued

	R_s constant				R_s variable			
V	I(0°C)	I(10°C)	I(20°C)	I(30°C)	I(0°C)	I(10°C)	I(20°C)	I(30°C)
19.7	3.64615	2.15391	0.62272	-0.93438	3.70312	2.24728	0.66786	-1.03016
19.8	3.46220	1.96335	0.42769	-1.13263	3.51663	2.04883	0.45879	-1.24899
19.9	3.27718	1.77207	0.23213	-1.33128	3.32900	1.84953	0.24906	-1.46837
20.0	3.09113	1.58008	0.03605	-1.53032	3.14028	1.64942	0.03869	-1.68826
20.1	2.90411	1.38742	-0.16052	-1.72974	2.95052	1.44852	-0.17229	-1.90864
20.2	2.71616	1.19411	-0.35757	-1.92953	2.75979	1.24689	-0.38386	-2.12951
20.3	2.52734	1.00019	-0.55507	-2.12967	2.56813	1.04454	-0.59600	-2.35084
20.4	2.33768	0.80567	-0.75302	-2.33016	2.37557	0.84151	-0.80867	-2.57261
20.5	2.14722	0.61058	-0.95140	-2.53099	2.18217	0.63783	-1.02188	-2.79483
20.6	1.95600	0.41494	-1.15019	-2.73213	1.98797	0.43352	-1.23559	-3.01746
20.7	1.76405	0.21878	-1.34938	-2.93360	1.79299	0.22860	-1.44979	-3.24050
20.8	1.57140	0.02211	-1.54895	-3.13537	1.59728	0.02311	-1.66446	-3.46393
20.9	1.37809	-0.17504	-1.74890	-3.33743	1.40086	-0.18294	-1.87958	-3.68774
21.0	1.18414	-0.37267	-1.94922	-3.53979	1.20377	-0.38953	-2.09515	-3.91193
21.1	0.98958	-0.57075	-2.14988	-3.74242	1.00603	-0.59663	-2.31113	-4.13647
21.2	0.79443	-0.76926	-2.35088	-3.94533	0.80768	-0.80422	-2.52754	-4.36136
21.3	0.59872	-0.96820	-2.55221	-4.14850	0.60873	-1.01230	-2.74433	-4.58659
21.4	0.40247	-1.16754	-2.75386	-4.35192	0.40922	-1.22084	-2.96152	-4.81215
21.5	0.20570	-1.36728	-2.95582	-4.55560	0.20916	-1.42982	-3.17907	-5.03803
21.6	0.00843	-1.56740	-3.15807	-4.75952	0.00857	-1.63923	-3.39699	-5.26422
21.7	-0.18932	-1.76789	-3.36062	-4.96368	-0.19252	-1.84906	-3.61526	-5.49071
21.8	-0.38754	-1.96873	-3.56346	-5.16808	-0.39410	-2.05929	-3.83387	-5.71749
21.9	-0.58620	-2.16991	-3.76656	-5.37269	-0.59615	-2.26991	-4.05280	-5.94456
22.0	-0.78529	-2.37143	-3.96994	-5.57753	-0.79865	-2.48091	-4.27206	-6.17190

Table E-4 continued

Appendix E.4 Oscillating behaviour of I_m and V_m

In this section the analysis of the oscillating behavior of I_m for changing ambient temperature is shown. Key simulation results are extracted from PSPICE and visualized in graphs.

T_a	V_{oc}	I_{sc}	P_m	V_m	I_m	FF
15	20.4148	8.7905	126.6174	15.0000	8.4412	0.7056
16	20.3355	8.7957	125.9649	14.9999	8.3977	0.7042
17	20.2562	8.8009	125.3177	14.9000	8.4106	0.7030
18	20.1769	8.8061	124.6656	14.8000	8.4234	0.7016
19	20.0976	8.8113	124.0090	14.7000	8.4360	0.7003
20	20.0183	8.8165	123.3477	14.6000	8.4485	0.6989
21	19.9391	8.8217	122.6945	14.5999	8.4037	0.6975
22	19.8598	8.8269	122.0450	14.5000	8.4169	0.6962
23	19.7805	8.8321	121.3907	14.4000	8.4299	0.6948
24	19.7013	8.8373	120.7317	14.3000	8.4428	0.6934
25	19.6220	8.8425	120.0681	14.2000	8.4555	0.6920
26	19.5427	8.8477	119.4158	14.1999	8.4096	0.6906
27	19.4634	8.8529	118.7637	14.1000	8.4230	0.6893
28	19.3842	8.8581	118.1068	14.0000	8.4362	0.6878
29	19.3049	8.8633	117.4452	13.9000	8.4493	0.6864
30	19.2256	8.8685	116.7792	13.8883	8.4075	0.6848
31	19.1464	8.8737	116.1291	13.8000	8.4152	0.6835
32	19.0671	8.8789	115.4742	13.7000	8.4288	0.6821
33	18.9879	8.8841	114.8145	13.6000	8.4422	0.6806
34	18.9086	8.8893	114.1502	13.5000	8.4556	0.6791
35	18.8293	8.8945	113.4882	13.4999	8.4065	0.6776

Table E-5 Key simulation results different ambient temperatures and constant Rs
An oscillating behaviour in I_m can be seen and when I_m decreases, V_m stays constant.

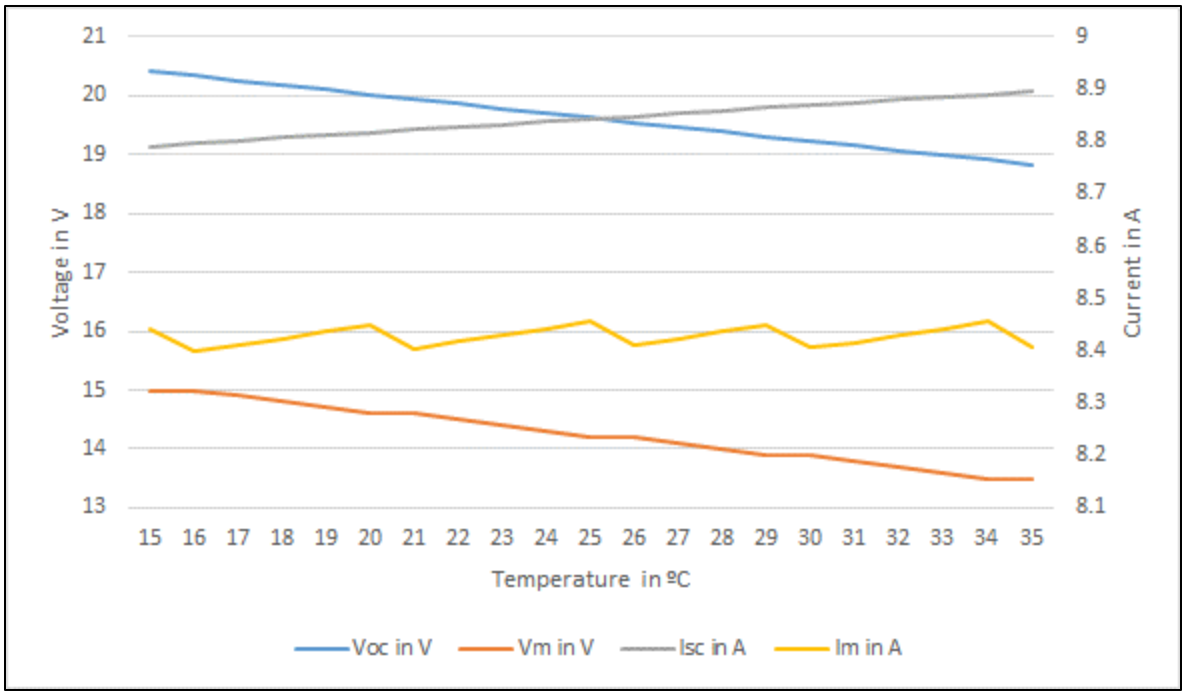

Figure E-1 V_{oc}, I_{sc}, V_m and I_m for different ambient temperatures
I_m decreases periodically. When I_m drops, V_m stays constant.

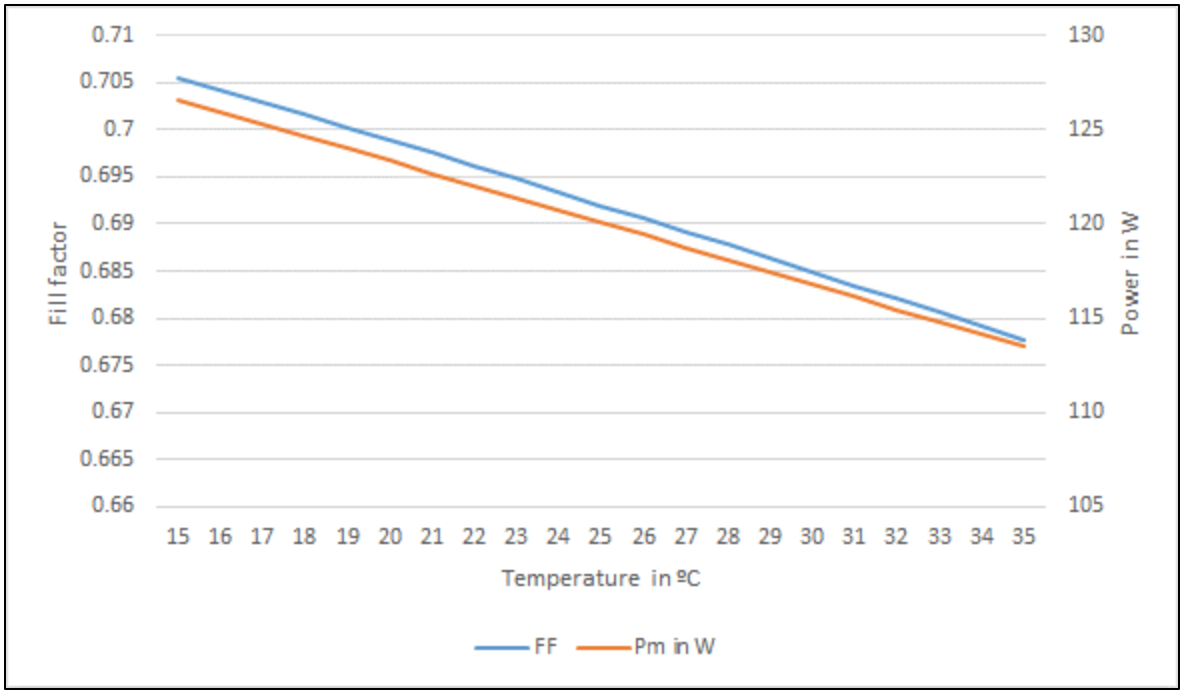

Figure E-2 FF and P_m for different ambient temperatures
Both parameters seem to be not affected by the oscillating behaviour of I_m and decrease as the theory suggests.

APPENDIX F

VALIDATION RAW DATA

In this section the simulation raw data of the validation step is shown.

Dataset 1		Dataset 2		Dataset 3		Dataset 4	
V	I	V	I	V	I	V	I
0.00000	7.97672	0.00000	5.65004	0.00000	3.70520	0.00000	0.83487
3.38897	7.97672	3.97534	5.65004	3.32825	3.70520	2.45696	0.83163
4.11259	7.94760	5.60301	5.64356	5.05969	3.69873	3.04695	0.83487
4.94333	7.94112	7.26437	5.63062	6.47226	3.65342	3.28951	0.83487
5.77316	7.92818	8.75295	5.62091	7.99462	3.64048	3.77373	0.83163
6.60300	7.91524	10.45041	5.61768	9.41302	3.62754	4.25977	0.83487
7.39773	7.89906	12.00684	5.59826	10.96829	3.60488	4.84885	0.83487
8.15962	7.89582	13.59403	5.55296	12.49006	3.58870	5.12425	0.82840
8.98855	7.87640	15.04136	5.26819	13.83625	3.55958	5.64403	0.82840
9.81929	7.86993	16.40985	4.68894	15.22669	3.39131	6.09632	0.83487
10.61493	7.86022	17.15295	3.88965	16.36961	3.00299	6.54589	0.83163
11.37365	7.83434	17.80374	3.07742	17.26003	2.43022	7.03011	0.82840
12.30518	7.80521	18.24875	2.34932	17.89856	1.82832	7.54989	0.82840
12.98870	7.73726	18.57949	1.77331	18.27263	1.32350	8.17272	0.82516
13.79861	7.58193	18.79668	1.34292	18.57173	0.96107	8.41348	0.81869
14.42483	7.35217	19.00199	1.01608	18.77464	0.69572	8.82930	0.81869
15.10586	7.01886	19.11188	0.78633	18.82514	0.50480	9.28249	0.82840
15.63215	6.62407	19.23803	0.61806	18.95405	0.39154	9.80137	0.82516
16.11617	6.18398	19.23639	0.49185	19.02080	0.29769	10.32205	0.82840
16.59935	5.72123	19.23512	0.40124	18.99770	0.23944	10.70141	0.82192
17.04341	5.21641	19.31213	0.33329	19.05418	0.20708	11.18745	0.82516
17.38593	4.72778	19.32625	0.28151	19.07728	0.17796	11.60146	0.81869
17.59228	4.25532	19.34679	0.24592	19.06317	0.14236	12.05103	0.81545
17.97178	3.81846	19.33781	0.22326	19.12862	0.13266	12.53435	0.80898
18.10630	3.41072	19.46102	0.18443	19.12349	0.11971	13.05413	0.80898
18.31711	3.04182	19.45460	0.16825	19.12349	0.11971	13.43530	0.80898
18.42326	2.70204	19.41353	0.15207	19.10799	0.09382	13.95417	0.80574
18.53762	2.40756	19.47771	0.13913	19.19827	0.08412	14.37000	0.80574
18.72452	2.12927	19.43536	0.11971	19.19372	0.08088	14.81685	0.79280
18.81517	1.89951	19.43407	0.11648	19.22837	0.08088	15.22905	0.77986
18.87143	1.68270	19.49953	0.10677	19.32321	0.07441	15.60297	0.75397
18.97017	1.50148	19.49824	0.10353	19.21925	0.07441	16.04620	0.72808
18.93315	1.33321	19.51925	0.09059	19.24935	0.07117	16.41921	0.69896
19.08149	1.21995	19.51470	0.08735	19.23568	0.06146	16.75577	0.66336
19.08411	1.07433	19.50103	0.07764	19.23568	0.06146	17.08507	0.60188
19.16353	0.97078	19.50103	0.07764	19.22201	0.05176	17.38154	0.54686
19.30779	0.86723	19.52656	0.07117	19.22201	0.05176	17.60390	0.48214
19.25230	0.79280	19.49647	0.07441	19.29131	0.05176	17.75150	0.41742
19.29896	0.71190	19.50103	0.07764	19.18736	0.05176	17.97610	0.37212
19.24799	0.65365	19.48736	0.06794	19.29131	0.05176	18.09674	0.32682
19.30280	0.60188	19.55666	0.06794	19.22656	0.05499	18.24562	0.26533
19.28830	0.55010	19.47369	0.05823	19.26598	0.04205	18.33803	0.23621
19.37757	0.49832	19.47369	0.05823	19.25667	0.03881	18.35729	0.19738
19.39939	0.46596	19.46457	0.05176	19.18737	0.03881	18.45098	0.17149
19.41993	0.43037	19.56853	0.05176	19.18737	0.03881	18.47408	0.14236
19.44046	0.39477	19.46457	0.05176	19.18737	0.03881	18.49975	0.11971
19.39683	0.37212	19.49922	0.05176	19.18737	0.03881	18.56777	0.11648
19.38785	0.34947	19.56853	0.05176	19.22202	0.03881	18.59729	0.10353

Table F-1 Measurements performed with Solmetric PVA-600 PV Analyzer

Dataset 1		Dataset 2		Dataset 3		Dataset 4	
V	I	V	I	V	I	V	I
19.41352	0.32682	19.63783	0.05176	19.26598	0.04205	18.65751	0.09382
19.40582	0.30740	19.56853	0.05176	19.30737	0.03234	18.67394	0.08088
19.50464	0.29446	19.53388	0.05176	19.37924	0.04528	18.66938	0.07764
19.46229	0.27504	19.45784	0.04852	19.20341	0.03234	18.66482	0.07441
19.49053	0.25886	19.46913	0.05499	19.16876	0.03234	18.65571	0.06794
19.48796	0.25239	19.53843	0.05499	19.30993	0.04528	18.63292	0.05176
19.48283	0.23944	19.49250	0.04852	19.24063	0.04528	18.94935	0.05499
19.54444	0.22003	19.46913	0.05499	19.26598	0.04205	18.66758	0.05176
19.54059	0.21032	19.53843	0.05499	19.30063	0.04205	18.82897	0.06794
19.60989	0.21032	19.60774	0.05499	19.30063	0.04205	18.71590	0.06146
19.53417	0.19414	19.48319	0.04528	19.21272	0.03558	18.94479	0.05176
19.53032	0.18443	19.49924	0.03881	19.22202	0.03881	18.67689	0.04205
19.56369	0.18120	19.46459	0.03881	19.19411	0.02910	18.66759	0.03881
19.52519	0.17149	19.47389	0.04205	19.28846	0.02587	18.77155	0.03881
19.52134	0.16178	19.49924	0.03881	19.29133	0.03881	18.73689	0.03881
19.51877	0.15531	19.49924	0.03881	19.32311	0.02587	18.77155	0.03881
19.62273	0.15531	19.48063	0.03234	19.18450	0.02587	18.77155	0.03881
19.54958	0.14560	19.49924	0.03881	19.21916	0.02587	18.75294	0.03234
19.54829	0.14236	19.58459	0.03234	19.28846	0.02587	18.79015	0.04528
19.54316	0.12942	19.51784	0.04528	19.32598	0.03881	18.73403	0.02587
19.61375	0.13266	19.50854	0.04205	19.31667	0.03558	18.79015	0.04528
19.54059	0.12295	19.55250	0.04528	19.27272	0.03234	18.79689	0.03558
19.54188	0.12618	19.58715	0.04528	19.33528	0.04205	18.85015	0.04205
19.53931	0.11971	19.49924	0.03881	19.23807	0.03234	18.79689	0.03558
19.53931	0.11971	19.57528	0.02910	19.28846	0.02587	18.79689	0.03558
19.53803	0.11648	19.55924	0.03558	19.25381	0.02587	18.83155	0.03558
19.57140	0.11324	19.52459	0.03558	19.25381	0.02587	18.76868	0.02587
19.53418	0.10677	19.50854	0.04205	19.28846	0.02587	18.73403	0.02587
19.56883	0.10677	19.52459	0.03558	19.28846	0.02587	18.83798	0.02587
19.63557	0.10030	19.54993	0.03234	19.28846	0.02587	18.86620	0.03558
19.56883	0.10677	19.54063	0.02910	19.28846	0.02587	18.83798	0.02587
19.63232	0.09706	19.47133	0.02910	19.28846	0.02587	18.83798	0.02587
19.53290	0.10353	19.55924	0.03558	19.28846	0.02587	18.84759	0.02910
19.51925	0.09059	19.54993	0.03234	19.31667	0.03558	18.87550	0.03881
19.60092	0.10030	19.60033	0.02587	19.28846	0.02587	18.80333	0.02587
19.51470	0.08735	19.49637	0.02587	19.28846	0.02587	18.84085	0.03881
19.62321	0.09059	19.57785	0.04205	19.29807	0.02910	18.87550	0.03881
19.51014	0.08412	19.56854	0.03881	19.27169	0.02263	18.83798	0.02587
19.69251	0.09059	19.59645	0.04852	19.25381	0.02587	18.84759	0.02910
19.54024	0.08088	19.57785	0.04205	19.26342	0.02910	18.83798	0.02587
19.69707	0.09382	19.56568	0.02587	19.29807	0.02910	18.83798	0.02587
19.57033	0.07764	19.53102	0.02587	19.37667	0.03234	18.83798	0.02587
19.57033	0.07764	19.46172	0.02587	19.45528	0.03558	18.84759	0.02910
19.54024	0.08088	19.46172	0.02587	19.27169	0.02263	18.83798	0.02587
19.53568	0.07764	19.56854	0.03881	19.28846	0.02587	18.84759	0.02910
19.60954	0.08088	19.56854	0.03881	19.28846	0.02587	18.83798	0.02587
19.63963	0.07764	19.56568	0.02587	19.45528	0.03558	18.86620	0.03558
19.63963	0.07764	19.55924	0.03558	19.29807	0.02910	18.76495	0.00000
19.67884	0.08088	19.56568	0.02587	19.29807	0.02910		
19.57489	0.08088	19.54063	0.02910	19.37667	0.03234		
19.62596	0.06794	19.53102	0.02587	19.32311	0.02587		
19.60043	0.07441	19.51425	0.02263	19.32311	0.02587		
19.63464	0.00000	19.56568	0.02587	19.39353	0.01940		
		19.57292	0.00000	19.26273	0.00000		

Table F-1 continued

	Dataset 1			Dataset 2		
V	I(fitted)	I(proposed)	I(Castaner)	I(fitted)	I(proposed)	I(Castaner)
0.0	7.97672	7.98492	7.99960	5.65004	5.88589	5.93398
0.1	7.97669	7.98492	7.99960	5.65003	5.88589	5.93398
0.2	7.97665	7.98492	7.99960	5.65003	5.88589	5.93398
0.3	7.97662	7.98492	7.99960	5.65002	5.88589	5.93398
0.4	7.97658	7.98492	7.99960	5.65002	5.88589	5.93398
0.5	7.97654	7.98492	7.99960	5.65001	5.88589	5.93398
0.6	7.97650	7.98492	7.99960	5.65001	5.88589	5.93398
0.7	7.97646	7.98492	7.99960	5.65000	5.88589	5.93398
0.8	7.97641	7.98492	7.99960	5.64999	5.88589	5.93398
0.9	7.97637	7.98492	7.99960	5.64999	5.88589	5.93398
1.0	7.97632	7.98492	7.99960	5.64998	5.88589	5.93398
1.1	7.97626	7.98492	7.99960	5.64997	5.88589	5.93398
1.2	7.97621	7.98492	7.99960	5.64996	5.88589	5.93398
1.3	7.97615	7.98492	7.99960	5.64995	5.88589	5.93398
1.4	7.97609	7.98492	7.99960	5.64995	5.88589	5.93398
1.5	7.97603	7.98492	7.99960	5.64994	5.88589	5.93398
1.6	7.97596	7.98492	7.99960	5.64993	5.88589	5.93398
1.7	7.97589	7.98492	7.99960	5.64991	5.88589	5.93398
1.8	7.97582	7.98492	7.99960	5.64990	5.88589	5.93398
1.9	7.97574	7.98492	7.99960	5.64989	5.88589	5.93398
2.0	7.97566	7.98492	7.99960	5.64988	5.88589	5.93398
2.1	7.97557	7.98492	7.99960	5.64986	5.88589	5.93398
2.2	7.97548	7.98492	7.99960	5.64985	5.88589	5.93398
2.3	7.97539	7.98492	7.99960	5.64983	5.88589	5.93398
2.4	7.97529	7.98492	7.99960	5.64982	5.88589	5.93398
2.5	7.97518	7.98492	7.99960	5.64980	5.88589	5.93398
2.6	7.97508	7.98492	7.99960	5.64978	5.88589	5.93398
2.7	7.97496	7.98492	7.99960	5.64976	5.88589	5.93398
2.8	7.97484	7.98492	7.99960	5.64974	5.88589	5.93398
2.9	7.97471	7.98492	7.99960	5.64972	5.88589	5.93398
3.0	7.97458	7.98492	7.99960	5.64969	5.88589	5.93398
3.1	7.97444	7.98492	7.99960	5.64967	5.88589	5.93398
3.2	7.97430	7.98492	7.99960	5.64964	5.88589	5.93398
3.3	7.97414	7.98492	7.99960	5.64961	5.88589	5.93398
3.4	7.97398	7.98492	7.99960	5.64958	5.88589	5.93398
3.5	7.97381	7.98492	7.99960	5.64955	5.88589	5.93398
3.6	7.97363	7.98492	7.99960	5.64952	5.88589	5.93398
3.7	7.97345	7.98492	7.99960	5.64948	5.88589	5.93398
3.8	7.97325	7.98492	7.99960	5.64945	5.88589	5.93398
3.9	7.97304	7.98492	7.99960	5.64940	5.88589	5.93398
4.0	7.97283	7.98492	7.99960	5.64936	5.88589	5.93398
4.1	7.97260	7.98492	7.99960	5.64932	5.88589	5.93398
4.2	7.97236	7.98492	7.99960	5.64927	5.88589	5.93398
4.3	7.97211	7.98492	7.99960	5.64922	5.88589	5.93398
4.4	7.97184	7.98492	7.99960	5.64917	5.88589	5.93398
4.5	7.97157	7.98492	7.99960	5.64911	5.88589	5.93398
4.6	7.97128	7.98492	7.99960	5.64905	5.88589	5.93398
4.7	7.97097	7.98492	7.99960	5.64898	5.88589	5.93398
4.8	7.97065	7.98492	7.99960	5.64892	5.88589	5.93398
4.9	7.97031	7.98492	7.99960	5.64884	5.88589	5.93398
5.0	7.96996	7.98492	7.99960	5.64877	5.88589	5.93398
5.1	7.96959	7.98492	7.99960	5.64869	5.88589	5.93398
5.2	7.96920	7.98492	7.99960	5.64860	5.88589	5.93398
5.3	7.96879	7.98492	7.99960	5.64851	5.88589	5.93398
5.4	7.96836	7.98492	7.99960	5.64841	5.88589	5.93398
5.5	7.96791	7.98492	7.99960	5.64831	5.88589	5.93398
5.6	7.96743	7.98492	7.99960	5.64820	5.88589	5.93398

Table F-2 Raw data of validation simulations for dataset 1 and 2

	Dataset 1			Dataset 2		
V	I(fitted)	I(proposed)	I(Castaner)	I(fitted)	I(proposed)	I(Castaner)
5.7	7.96693	7.98492	7.99960	5.64809	5.88589	5.93398
5.8	7.96641	7.98492	7.99960	5.64796	5.88589	5.93398
5.9	7.96586	7.98492	7.99960	5.64784	5.88589	5.93398
6.0	7.96528	7.98492	7.99960	5.64770	5.88589	5.93398
6.1	7.96468	7.98492	7.99960	5.64755	5.88589	5.93398
6.2	7.96404	7.98492	7.99960	5.64740	5.88589	5.93398
6.3	7.96337	7.98492	7.99960	5.64723	5.88589	5.93398
6.4	7.96267	7.98492	7.99960	5.64706	5.88589	5.93398
6.5	7.96193	7.98492	7.99960	5.64688	5.88589	5.93398
6.6	7.96116	7.98492	7.99960	5.64668	5.88589	5.93398
6.7	7.96035	7.98492	7.99960	5.64647	5.88589	5.93398
6.8	7.95949	7.98492	7.99960	5.64625	5.88589	5.93398
6.9	7.95859	7.98492	7.99960	5.64602	5.88589	5.93398
7.0	7.95765	7.98492	7.99960	5.64577	5.88589	5.93398
7.1	7.95666	7.98492	7.99960	5.64551	5.88589	5.93398
7.2	7.95562	7.98492	7.99960	5.64523	5.88589	5.93398
7.3	7.95453	7.98492	7.99960	5.64494	5.88589	5.93398
7.4	7.95339	7.98492	7.99960	5.64463	5.88589	5.93398
7.5	7.95218	7.98492	7.99960	5.64429	5.88589	5.93398
7.6	7.95092	7.98492	7.99960	5.64394	5.88589	5.93398
7.7	7.94959	7.98492	7.99960	5.64357	5.88589	5.93398
7.8	7.94820	7.98492	7.99960	5.64318	5.88589	5.93398
7.9	7.94673	7.98492	7.99960	5.64276	5.88589	5.93398
8.0	7.94519	7.98492	7.99960	5.64231	5.88589	5.93398
8.1	7.94358	7.98492	7.99960	5.64184	5.88589	5.93398
8.2	7.94188	7.98492	7.99960	5.64134	5.88589	5.93398
8.3	7.94010	7.98492	7.99960	5.64081	5.88589	5.93398
8.4	7.93823	7.98492	7.99960	5.64025	5.88589	5.93398
8.5	7.93627	7.98492	7.99960	5.63965	5.88589	5.93398
8.6	7.93421	7.98492	7.99960	5.63902	5.88589	5.93398
8.7	7.93204	7.98492	7.99960	5.63835	5.88589	5.93398
8.8	7.92976	7.98492	7.99960	5.63764	5.88589	5.93398
8.9	7.92737	7.98492	7.99960	5.63688	5.88589	5.93398
9.0	7.92486	7.98492	7.99959	5.63608	5.88589	5.93398
9.1	7.92223	7.98491	7.99959	5.63524	5.88588	5.93398
9.2	7.91946	7.98491	7.99959	5.63434	5.88588	5.93398
9.3	7.91655	7.98491	7.99959	5.63338	5.88588	5.93398
9.4	7.91350	7.98491	7.99959	5.63237	5.88588	5.93398
9.5	7.91029	7.98490	7.99959	5.63130	5.88588	5.93398
9.6	7.90693	7.98490	7.99958	5.63016	5.88587	5.93398
9.7	7.90339	7.98489	7.99958	5.62896	5.88587	5.93398
9.8	7.89968	7.98489	7.99957	5.62768	5.88586	5.93398
9.9	7.89578	7.98488	7.99957	5.62632	5.88586	5.93398
10.0	7.89168	7.98487	7.99956	5.62488	5.88585	5.93398
10.1	7.88738	7.98486	7.99955	5.62336	5.88584	5.93398
10.2	7.88286	7.98485	7.99954	5.62174	5.88583	5.93398
10.3	7.87812	7.98483	7.99953	5.62003	5.88582	5.93398
10.4	7.87314	7.98481	7.99952	5.61821	5.88580	5.93398
10.5	7.86790	7.98478	7.99950	5.61628	5.88579	5.93398
10.6	7.86241	7.98475	7.99948	5.61423	5.88576	5.93397
10.7	7.85664	7.98472	7.99945	5.61206	5.88574	5.93397
10.8	7.85058	7.98467	7.99942	5.60976	5.88570	5.93397
10.9	7.84421	7.98462	7.99938	5.60732	5.88566	5.93397
11.0	7.83752	7.98455	7.99934	5.60473	5.88561	5.93396
11.1	7.83050	7.98447	7.99928	5.60199	5.88555	5.93396
11.2	7.82313	7.98437	7.99921	5.59908	5.88547	5.93395
11.3	7.81539	7.98425	7.99912	5.59599	5.88538	5.93395

Table F-2 continued

	Dataset 1			Dataset 2		
V	I(fitted)	I(proposed)	I(Castaner)	I(fitted)	I(proposed)	I(Castaner)
11.4	7.80726	7.98410	7.99902	5.59272	5.88527	5.93394
11.5	7.79872	7.98392	7.99890	5.58925	5.88514	5.93393
11.6	7.78975	7.98370	7.99874	5.58557	5.88497	5.93392
11.7	7.78033	7.98344	7.99856	5.58167	5.88477	5.93390
11.8	7.77043	7.98312	7.99833	5.57753	5.88453	5.93388
11.9	7.76004	7.98273	7.99806	5.57314	5.88423	5.93386
12.0	7.74913	7.98225	7.99773	5.56849	5.88387	5.93383
12.1	7.73768	7.98167	7.99732	5.56355	5.88343	5.93380
12.2	7.72564	7.98097	7.99683	5.55832	5.88289	5.93376
12.3	7.71300	7.98011	7.99623	5.55277	5.88224	5.93371
12.4	7.69973	7.97907	7.99551	5.54688	5.88145	5.93365
12.5	7.68579	7.97781	7.99462	5.54064	5.88049	5.93358
12.6	7.67115	7.97627	7.99355	5.53402	5.87932	5.93350
12.7	7.65578	7.97441	7.99225	5.52700	5.87789	5.93339
12.8	7.63964	7.97215	7.99067	5.51956	5.87617	5.93326
12.9	7.62268	7.96942	7.98876	5.51166	5.87407	5.93310
13.0	7.60487	7.96610	7.98644	5.50329	5.87153	5.93291
13.1	7.58617	7.96209	7.98364	5.49441	5.86846	5.93268
13.2	7.56653	7.95725	7.98025	5.48500	5.86475	5.93240
13.3	7.54590	7.95142	7.97615	5.47501	5.86027	5.93205
13.4	7.52424	7.94439	7.97120	5.46442	5.85488	5.93163
13.5	7.50149	7.93595	7.96525	5.45319	5.84840	5.93112
13.6	7.47760	7.92585	7.95809	5.44129	5.84065	5.93050
13.7	7.45251	7.91379	7.94952	5.42866	5.83138	5.92975
13.8	7.42616	7.89944	7.93926	5.41527	5.82036	5.92883
13.9	7.39848	7.88244	7.92704	5.40107	5.80732	5.92772
14.0	7.36942	7.86240	7.91253	5.38601	5.79194	5.92636
14.1	7.33890	7.83889	7.89538	5.37004	5.77391	5.92472
14.2	7.30684	7.81148	7.87521	5.35310	5.75292	5.92272
14.3	7.27318	7.77972	7.85161	5.33514	5.72862	5.92030
14.4	7.23782	7.74320	7.82416	5.31609	5.70072	5.91737
14.5	7.20069	7.70149	7.79246	5.29589	5.66890	5.91382
14.6	7.16170	7.65424	7.75610	5.27447	5.63292	5.90953
14.7	7.12075	7.60114	7.71472	5.25176	5.59255	5.90435
14.8	7.07774	7.54194	7.66797	5.22767	5.54763	5.89812
14.9	7.03257	7.47649	7.61560	5.20213	5.49806	5.89062
15.0	6.98514	7.40467	7.55738	5.17504	5.44379	5.88163
15.1	6.93532	7.32650	7.49320	5.14631	5.38481	5.87088
15.2	6.88300	7.24202	7.42299	5.11584	5.32120	5.85807
15.3	6.82806	7.15135	7.34676	5.08353	5.25306	5.84287
15.4	6.77035	7.05465	7.26457	5.04927	5.18051	5.82490
15.5	6.70975	6.95215	7.17656	5.01294	5.10372	5.80379
15.6	6.64611	6.84407	7.08290	4.97441	5.02288	5.77911
15.7	6.57927	6.73069	6.98380	4.93355	4.93819	5.75045
15.8	6.50908	6.61227	6.87949	4.89022	4.84983	5.71739
15.9	6.43536	6.48909	6.77023	4.84426	4.75804	5.67953
16.0	6.35794	6.36141	6.65626	4.79553	4.66299	5.63650
16.1	6.27664	6.22952	6.53785	4.74386	4.56490	5.58800
16.2	6.19125	6.09365	6.41526	4.68905	4.46393	5.53377
16.3	6.10157	5.95407	6.28873	4.63094	4.36029	5.47362
16.4	6.00740	5.81101	6.15851	4.56931	4.25414	5.40744
16.5	5.90849	5.66468	6.02483	4.50395	4.14564	5.33520
16.6	5.80462	5.51529	5.88790	4.43464	4.03493	5.25692
16.7	5.69553	5.36305	5.74794	4.36114	3.92216	5.17270
16.8	5.58097	5.20812	5.60512	4.28319	3.80746	5.08269
16.9	5.46065	5.05067	5.45964	4.20053	3.69094	4.98707
17.0	5.33430	4.89087	5.31165	4.11288	3.57273	4.88606

Table F-2 continued

	Dataset 1			Dataset 2		
V	I(fitted)	I(proposed)	I(Castaner)	I(fitted)	I(proposed)	I(Castaner)
17.1	5.20160	4.72885	5.16132	4.01992	3.45292	4.77990
17.2	5.06223	4.56475	5.00878	3.92134	3.33161	4.66886
17.3	4.91587	4.39869	4.85418	3.81680	3.20890	4.55319
17.4	4.76217	4.23079	4.69763	3.68669	3.08485	4.43316
17.5	4.54878	4.06116	4.53926	3.51528	2.95956	4.30902
17.6	4.33455	3.88989	4.37916	3.34387	2.83308	4.18102
17.7	4.12032	3.71707	4.21744	3.17246	2.70549	4.04940
17.8	3.90609	3.54279	4.05419	3.00104	2.57685	3.91439
17.9	3.69186	3.36713	3.88949	2.82963	2.44722	3.77620
18.0	3.47763	3.19017	3.72342	2.65822	2.31664	3.63504
18.1	3.26340	3.01196	3.55606	2.48681	2.18517	3.49110
18.2	3.04916	2.83258	3.38748	2.31540	2.05284	3.34454
18.3	2.83493	2.65208	3.21773	2.14398	1.91972	3.19553
18.4	2.62070	2.47052	3.04688	1.97257	1.78582	3.04423
18.5	2.40647	2.28795	2.87498	1.80116	1.65120	2.89078
18.6	2.19224	2.10442	2.70209	1.62975	1.51589	2.73530
18.7	1.97801	1.91998	2.52825	1.45834	1.37991	2.57793
18.8	1.76378	1.73465	2.35350	1.28692	1.24330	2.41876
18.9	1.54955	1.54850	2.17790	1.11551	1.10609	2.25792
19.0	1.33531	1.36155	2.00147	0.94410	0.96831	2.09548
19.1	1.12108	1.17383	1.82426	0.77269	0.82997	1.93154
19.2	0.90685	0.98539	1.64630	0.60128	0.69110	1.76619
19.3	0.69262	0.79625	1.46762	0.42986	0.55173	1.59950
19.4	0.47839	0.60643	1.28825	0.25845	0.41188	1.43154
19.5	0.26416	0.41598	1.10823	0.08704	0.27156	1.26238
19.6	0.04993	0.22491	0.92758	-0.08437	0.13080	1.09209
19.7	-0.16430	0.03325	0.74632	-0.25578	-0.01039	0.92071
19.8	-0.37854	-0.15899	0.56448	-0.42720	-0.15200	0.74831
19.9	-0.59277	-0.35176	0.38209	-0.59861	-0.29400	0.57493
20.0	-0.80700	-0.54507	0.19915	-0.77002	-0.43638	0.40062
20.1	-1.02123	-0.73888	0.01570	-0.94143	-0.57912	0.22542
20.2	-1.23546	-0.93318	-0.16824	-1.11284	-0.72223	0.04939
20.3	-1.44969	-1.12795	-0.35266	-1.28426	-0.86567	-0.12746
20.4	-1.66392	-1.32318	-0.53755	-1.45567	-1.00944	-0.30507
20.5	-1.87816	-1.51884	-0.72287	-1.62708	-1.15353	-0.48342
20.6	-2.09239	-1.71493	-0.90863	-1.79849	-1.29792	-0.66248
20.7	-2.30662	-1.91143	-1.09480	-1.96990	-1.44261	-0.84220
20.8	-2.52085	-2.10832	-1.28137	-2.14132	-1.58759	-1.02258
20.9	-2.73508	-2.30559	-1.46832	-2.31273	-1.73284	-1.20357
21.0	-2.94931	-2.50323	-1.65565	-2.48414	-1.87836	-1.38516

Table F-2 continued

	Dataset 3			Dataset 4		
V	I(fitted)	I(proposed)	I(Castaner)	I(fitted)	I(proposed)	I(Castaner)
0.0	3.70520	3.72540	3.79872	0.83487	0.87320	0.92003
0.1	3.70498	3.72540	3.79872	0.83478	0.87320	0.92003
0.2	3.70477	3.72540	3.79872	0.83468	0.87320	0.92003
0.3	3.70455	3.72540	3.79872	0.83459	0.87320	0.92003
0.4	3.70434	3.72540	3.79872	0.83450	0.87320	0.92003
0.5	3.70412	3.72540	3.79872	0.83441	0.87320	0.92003
0.6	3.70390	3.72540	3.79872	0.83431	0.87320	0.92003
0.7	3.70369	3.72540	3.79872	0.83422	0.87320	0.92003
0.8	3.70347	3.72540	3.79872	0.83413	0.87320	0.92003
0.9	3.70325	3.72540	3.79872	0.83404	0.87320	0.92003
1.0	3.70303	3.72540	3.79872	0.83394	0.87320	0.92003
1.1	3.70282	3.72540	3.79872	0.83385	0.87320	0.92003
1.2	3.70260	3.72540	3.79872	0.83376	0.87320	0.92003
1.3	3.70238	3.72540	3.79872	0.83367	0.87320	0.92003
1.4	3.70216	3.72540	3.79872	0.83357	0.87320	0.92003
1.5	3.70194	3.72540	3.79872	0.83348	0.87320	0.92003
1.6	3.70172	3.72540	3.79872	0.83339	0.87320	0.92003
1.7	3.70150	3.72540	3.79872	0.83330	0.87320	0.92003
1.8	3.70128	3.72540	3.79872	0.83320	0.87320	0.92003
1.9	3.70106	3.72540	3.79872	0.83311	0.87320	0.92003
2.0	3.70083	3.72540	3.79872	0.83302	0.87320	0.92003
2.1	3.70061	3.72540	3.79872	0.83293	0.87320	0.92003
2.2	3.70039	3.72540	3.79872	0.83283	0.87320	0.92003
2.3	3.70016	3.72540	3.79872	0.83274	0.87320	0.92003
2.4	3.69994	3.72540	3.79872	0.83265	0.87320	0.92003
2.5	3.69971	3.72540	3.79872	0.83256	0.87320	0.92003
2.6	3.69949	3.72540	3.79872	0.83246	0.87320	0.92003
2.7	3.69926	3.72540	3.79872	0.83237	0.87320	0.92003
2.8	3.69903	3.72540	3.79872	0.83228	0.87320	0.92003
2.9	3.69880	3.72540	3.79872	0.83218	0.87320	0.92003
3.0	3.69857	3.72540	3.79872	0.83209	0.87320	0.92003
3.1	3.69834	3.72540	3.79872	0.83200	0.87320	0.92003
3.2	3.69811	3.72540	3.79872	0.83191	0.87320	0.92003
3.3	3.69788	3.72540	3.79872	0.83181	0.87320	0.92003
3.4	3.69764	3.72540	3.79872	0.83172	0.87320	0.92003
3.5	3.69741	3.72540	3.79872	0.83163	0.87320	0.92003
3.6	3.69717	3.72540	3.79872	0.83153	0.87320	0.92003
3.7	3.69693	3.72540	3.79872	0.83144	0.87320	0.92003
3.8	3.69669	3.72540	3.79872	0.83135	0.87320	0.92003
3.9	3.69645	3.72540	3.79872	0.83126	0.87320	0.92003
4.0	3.69621	3.72540	3.79872	0.83116	0.87320	0.92003
4.1	3.69597	3.72540	3.79872	0.83107	0.87320	0.92003
4.2	3.69572	3.72540	3.79872	0.83098	0.87320	0.92003
4.3	3.69547	3.72540	3.79872	0.83088	0.87320	0.92003
4.4	3.69522	3.72540	3.79872	0.83079	0.87320	0.92003
4.5	3.69497	3.72540	3.79872	0.83070	0.87320	0.92003
4.6	3.69471	3.72540	3.79872	0.83060	0.87320	0.92003
4.7	3.69445	3.72540	3.79872	0.83051	0.87320	0.92003
4.8	3.69419	3.72540	3.79872	0.83042	0.87320	0.92003
4.9	3.69393	3.72540	3.79872	0.83032	0.87320	0.92003
5.0	3.69367	3.72540	3.79872	0.83023	0.87320	0.92003
5.1	3.69340	3.72540	3.79872	0.83014	0.87320	0.92003
5.2	3.69312	3.72540	3.79872	0.83004	0.87320	0.92003
5.3	3.69285	3.72540	3.79872	0.82995	0.87320	0.92003
5.4	3.69257	3.72540	3.79872	0.82985	0.87320	0.92003
5.5	3.69228	3.72540	3.79872	0.82976	0.87320	0.92003
5.6	3.69199	3.72540	3.79872	0.82966	0.87320	0.92003

Table F-3 Raw data of validation simulations for dataset 3 and 4

	Dataset 3			Dataset 4		
V	I(fitted)	I(proposed)	I(Castaner)	I(fitted)	I(proposed)	I(Castaner)
5.7	3.69170	3.72540	3.79872	0.82957	0.87320	0.92003
5.8	3.69140	3.72540	3.79872	0.82948	0.87320	0.92003
5.9	3.69110	3.72540	3.79872	0.82938	0.87320	0.92003
6.0	3.69079	3.72540	3.79872	0.82929	0.87320	0.92003
6.1	3.69048	3.72540	3.79872	0.82919	0.87320	0.92003
6.2	3.69016	3.72540	3.79872	0.82910	0.87320	0.92003
6.3	3.68984	3.72540	3.79872	0.82900	0.87320	0.92003
6.4	3.68950	3.72540	3.79872	0.82890	0.87320	0.92003
6.5	3.68916	3.72540	3.79872	0.82881	0.87320	0.92003
6.6	3.68882	3.72540	3.79872	0.82871	0.87320	0.92003
6.7	3.68846	3.72540	3.79872	0.82862	0.87320	0.92003
6.8	3.68810	3.72540	3.79872	0.82852	0.87320	0.92003
6.9	3.68772	3.72540	3.79872	0.82842	0.87320	0.92003
7.0	3.68734	3.72540	3.79872	0.82832	0.87320	0.92003
7.1	3.68695	3.72540	3.79872	0.82823	0.87320	0.92003
7.2	3.68654	3.72540	3.79872	0.82813	0.87320	0.92003
7.3	3.68613	3.72540	3.79872	0.82803	0.87320	0.92003
7.4	3.68570	3.72540	3.79872	0.82793	0.87320	0.92003
7.5	3.68526	3.72540	3.79872	0.82783	0.87320	0.92003
7.6	3.68481	3.72540	3.79872	0.82773	0.87320	0.92003
7.7	3.68434	3.72540	3.79872	0.82763	0.87320	0.92003
7.8	3.68386	3.72540	3.79872	0.82753	0.87320	0.92003
7.9	3.68336	3.72540	3.79872	0.82743	0.87320	0.92003
8.0	3.68284	3.72540	3.79872	0.82732	0.87320	0.92003
8.1	3.68230	3.72540	3.79872	0.82722	0.87320	0.92003
8.2	3.68175	3.72539	3.79872	0.82711	0.87320	0.92003
8.3	3.68117	3.72539	3.79872	0.82701	0.87320	0.92003
8.4	3.68058	3.72539	3.79872	0.82690	0.87320	0.92003
8.5	3.67995	3.72539	3.79872	0.82679	0.87320	0.92003
8.6	3.67931	3.72539	3.79872	0.82668	0.87320	0.92003
8.7	3.67864	3.72539	3.79872	0.82657	0.87320	0.92003
8.8	3.67794	3.72539	3.79872	0.82646	0.87320	0.92003
8.9	3.67721	3.72539	3.79872	0.82634	0.87320	0.92003
9.0	3.67645	3.72539	3.79872	0.82623	0.87320	0.92003
9.1	3.67566	3.72539	3.79872	0.82611	0.87320	0.92003
9.2	3.67483	3.72539	3.79872	0.82599	0.87320	0.92003
9.3	3.67397	3.72539	3.79872	0.82586	0.87320	0.92003
9.4	3.67306	3.72539	3.79872	0.82574	0.87320	0.92003
9.5	3.67212	3.72539	3.79872	0.82561	0.87320	0.92003
9.6	3.67113	3.72539	3.79872	0.82548	0.87320	0.92003
9.7	3.67009	3.72538	3.79872	0.82535	0.87320	0.92003
9.8	3.66900	3.72538	3.79872	0.82521	0.87320	0.92003
9.9	3.66786	3.72538	3.79872	0.82507	0.87320	0.92003
10.0	3.66667	3.72537	3.79872	0.82492	0.87320	0.92003
10.1	3.66541	3.72537	3.79872	0.82477	0.87320	0.92003
10.2	3.66410	3.72536	3.79872	0.82462	0.87320	0.92003
10.3	3.66271	3.72536	3.79872	0.82446	0.87320	0.92003
10.4	3.66125	3.72535	3.79872	0.82429	0.87320	0.92003
10.5	3.65972	3.72534	3.79872	0.82412	0.87320	0.92003
10.6	3.65811	3.72533	3.79872	0.82394	0.87320	0.92003
10.7	3.65642	3.72531	3.79872	0.82375	0.87320	0.92003
10.8	3.65463	3.72529	3.79872	0.82356	0.87320	0.92003
10.9	3.65275	3.72527	3.79872	0.82336	0.87319	0.92003
11.0	3.65077	3.72524	3.79872	0.82315	0.87319	0.92003
11.1	3.64868	3.72521	3.79872	0.82292	0.87319	0.92003
11.2	3.64648	3.72517	3.79872	0.82269	0.87319	0.92003
11.3	3.64415	3.72511	3.79872	0.82245	0.87318	0.92003

Table F-3 continued

	Dataset 3			Dataset 4		
V	I(fitted)	I(proposed)	I(Castaner)	I(fitted)	I(proposed)	I(Castaner)
11.4	3.64170	3.72505	3.79872	0.82219	0.87318	0.92003
11.5	3.63911	3.72498	3.79872	0.82192	0.87317	0.92003
11.6	3.63638	3.72488	3.79872	0.82163	0.87317	0.92003
11.7	3.63350	3.72477	3.79872	0.82133	0.87316	0.92003
11.8	3.63045	3.72463	3.79872	0.82101	0.87315	0.92003
11.9	3.62724	3.72446	3.79872	0.82067	0.87313	0.92003
12.0	3.62384	3.72426	3.79871	0.82031	0.87312	0.92003
12.1	3.62024	3.72401	3.79871	0.81992	0.87310	0.92003
12.2	3.61645	3.72370	3.79871	0.81951	0.87308	0.92003
12.3	3.61243	3.72333	3.79871	0.81908	0.87305	0.92003
12.4	3.60819	3.72288	3.79871	0.81861	0.87301	0.92003
12.5	3.60370	3.72232	3.79870	0.81812	0.87296	0.92003
12.6	3.59895	3.72165	3.79870	0.81759	0.87291	0.92003
12.7	3.59392	3.72083	3.79869	0.81702	0.87284	0.92003
12.8	3.58860	3.71983	3.79869	0.81641	0.87276	0.92003
12.9	3.58298	3.71862	3.79868	0.81576	0.87265	0.92003
13.0	3.57702	3.71715	3.79867	0.81506	0.87253	0.92003
13.1	3.57072	3.71536	3.79866	0.81431	0.87237	0.92003
13.2	3.56405	3.71319	3.79865	0.81351	0.87218	0.92003
13.3	3.55698	3.71057	3.79863	0.81264	0.87195	0.92003
13.4	3.54950	3.70741	3.79861	0.81171	0.87166	0.92003
13.5	3.54158	3.70360	3.79859	0.81070	0.87130	0.92003
13.6	3.53319	3.69902	3.79856	0.80962	0.87087	0.92003
13.7	3.52430	3.69353	3.79852	0.80846	0.87034	0.92003
13.8	3.51489	3.68699	3.79848	0.80720	0.86970	0.92003
13.9	3.50492	3.67922	3.79842	0.80585	0.86892	0.92003
14.0	3.49436	3.67002	3.79836	0.80439	0.86797	0.92003
14.1	3.48317	3.65921	3.79828	0.80281	0.86681	0.92003
14.2	3.47131	3.64658	3.79818	0.80110	0.86543	0.92003
14.3	3.45875	3.63190	3.79806	0.79926	0.86376	0.92003
14.4	3.44544	3.61498	3.79792	0.79727	0.86178	0.92003
14.5	3.43133	3.59563	3.79774	0.79512	0.85942	0.92003
14.6	3.41638	3.57366	3.79753	0.79280	0.85664	0.92002
14.7	3.40053	3.54894	3.79726	0.79028	0.85338	0.92002
14.8	3.38373	3.52135	3.79694	0.78756	0.84959	0.92002
14.9	3.36593	3.49081	3.79655	0.78461	0.84523	0.92002
15.0	3.34706	3.45728	3.79608	0.78143	0.84024	0.92002
15.1	3.32706	3.42076	3.79550	0.77798	0.83460	0.92002
15.2	3.30586	3.38129	3.79479	0.77424	0.82828	0.92002
15.3	3.28338	3.33891	3.79393	0.77020	0.82125	0.92002
15.4	3.25955	3.29372	3.79288	0.76582	0.81350	0.92002
15.5	3.23429	3.24581	3.79160	0.76107	0.80504	0.92002
15.6	3.20750	3.19531	3.79005	0.75593	0.79588	0.92002
15.7	3.17911	3.14234	3.78816	0.75036	0.78603	0.92001
15.8	3.14900	3.08702	3.78586	0.74433	0.77552	0.92001
15.9	3.11707	3.02950	3.78307	0.73779	0.76436	0.92001
16.0	3.08323	2.96989	3.77968	0.73070	0.75260	0.92001
16.1	3.04734	2.90834	3.77558	0.72302	0.74026	0.92000
16.2	3.00928	2.84495	3.77062	0.71469	0.72738	0.91999
16.3	2.96893	2.77984	3.76463	0.70566	0.71399	0.91999
16.4	2.92613	2.71313	3.75742	0.69588	0.70012	0.91998
16.5	2.88076	2.64492	3.74874	0.68527	0.68580	0.91997
16.6	2.83264	2.57531	3.73834	0.67376	0.67107	0.91995
16.7	2.78161	2.50437	3.72592	0.66129	0.65594	0.91994
16.8	2.72750	2.43221	3.71114	0.64776	0.64045	0.91992
16.9	2.67012	2.35889	3.69363	0.63310	0.62462	0.91989
17.0	2.60926	2.28449	3.67300	0.61719	0.60848	0.91986

Table F-3 continued

	Dataset 3			Dataset 4		
V	I(fitted)	I(proposed)	I(Castaner)	I(fitted)	I(proposed)	I(Castaner)
17.1	2.54472	2.20908	3.64883	0.59994	0.59203	0.91982
17.2	2.47628	2.13271	3.62069	0.58123	0.57532	0.91977
17.3	2.40369	2.05545	3.58816	0.56094	0.55834	0.91971
17.4	2.32671	1.97735	3.55081	0.53894	0.54112	0.91964
17.5	2.24507	1.89845	3.50829	0.51507	0.52368	0.91955
17.6	2.15848	1.81880	3.46026	0.48918	0.50602	0.91944
17.7	2.06665	1.73845	3.40645	0.46109	0.48817	0.91931
17.8	1.96926	1.65743	3.34668	0.43063	0.47013	0.91914
17.9	1.86597	1.57578	3.28082	0.39759	0.45191	0.91893
18.0	1.75641	1.49354	3.20884	0.36175	0.43353	0.91868
18.1	1.64022	1.41073	3.13075	0.32287	0.41499	0.91837
18.2	1.51699	1.32738	3.04666	0.28069	0.39631	0.91799
18.3	1.38628	1.24352	2.95671	0.23493	0.37749	0.91752
18.4	1.24766	1.15918	2.86109	0.18530	0.35853	0.91694
18.5	1.10063	1.07438	2.76003	0.13145	0.33945	0.91623
18.6	0.94468	0.98914	2.65378	0.07304	0.32026	0.91535
18.7	0.77928	0.90349	2.54260	0.00967	0.30095	0.91427
18.8	0.60384	0.81743	2.42675	-0.05908	0.28153	0.91295
18.9	0.43755	0.73100	2.30650	-0.13367	0.26202	0.91132
19.0	0.32974	0.64420	2.18212	-0.21458	0.24241	0.90933
19.1	0.22194	0.55705	2.05385	-0.30237	0.22270	0.90689
19.2	0.11414	0.46958	1.92195	-0.39761	0.20292	0.90389
19.3	0.00633	0.38178	1.78664	-0.50093	0.18304	0.90023
19.4	-0.10147	0.29368	1.64814	-0.61303	0.16309	0.89575
19.5	-0.20928	0.20529	1.50665	-0.73465	0.14306	0.89030
19.6	-0.31708	0.11662	1.36237	-0.86660	0.12296	0.88365
19.7	-0.42489	0.02768	1.21548	-1.00976	0.10279	0.87559
19.8	-0.53269	-0.06152	1.06614	-1.16507	0.08256	0.86584
19.9	-0.64050	-0.15097	0.91450	-1.33358	0.06226	0.85407
20.0	-0.74830	-0.24066	0.76070	-1.51640	0.04190	0.83994
20.1	-0.85611	-0.33058	0.60489	-1.71475	0.02148	0.82304
20.2	-0.96391	-0.42073	0.44717	-1.92995	0.00100	0.80296
20.3	-1.07172	-0.51108	0.28767	-2.16344	-0.01953	0.77924
20.4	-1.17952	-0.60164	0.12648	-2.41676	-0.04011	0.75140
20.5	-1.28733	-0.69241	-0.03628	-2.69161	-0.06074	0.71898
20.6	-1.39513	-0.78336	-0.20055	-2.98980	-0.08143	0.68153
20.7	-1.50294	-0.87450	-0.36622	-3.31334	-0.10215	0.63865
20.8	-1.61074	-0.96582	-0.53323	-3.66436	-0.12293	0.58997
20.9	-1.71854	-1.05732	-0.70151	-4.04521	-0.14374	0.53521
21.0	-1.82635	-1.14898	-0.87098	-4.45842	-0.16460	0.47418

Table F-3 continued